University of Southern Queensland
Faculty of Health, Engineering & Sciences

Effect of Distributed Photovoltaic Embedded Generation on the Electricity Distribution Network

A dissertation submitted by

Karen Hourigan

In fulfilment of the requirements of

ENG4111/ ENG4112 Research Project

Towards the degree of

Bachelor of Engineering Honours

Electrical and Electronic

Submitted: October 2016

Abstract

Local consumer conscience and rising electricity costs are not the only incentives driving the increases in penetration of distributed or rooftop photovoltaic (PV) embedded generation (EG). Worldwide environmental conscience in the form of government incentives have had significant effects on past and present levels and will continue to affect future increases in rooftop PV EG. To this effect, the purpose of this project was twofold - to investigate both the effects of current levels of rooftop PV EG on the electricity distribution network and to investigate the effects of future predicted levels of PV EG.

The results of before and after studies at both a local LV level where the PV EG systems were installed, and on HV feeders that demonstrated a high penetration of PV EG confirmed that the current levels of rooftop PV EG have had significant effects on the electricity distribution network, especially with respect to decreases in feeder loadings during the middle of the day. Power flow modelling of the existing network yielded results that demonstrated increased effects on the electricity distribution network. It also identified possible future effects with respect to voltage rise as well as reverse power flow.

Several options were discussed to alleviate or lessen the effects of increased levels of PV EG, the main existing method being export limitations being imposed by the electricity distributor. Another method that was investigated was introducing a reactive power component to PV EG, though this proved to cause more problems than possible solutions with respect to the feeder that was modelled, though it cannot be ruled out with regards to larger more centralised PV EG systems or longer radial feeders.

Another possible solution that was suggested was intentional islanding or establishing a micro grid under certain conditions. This was a theoretical study only and was not modelled within the bounds of the current project.

Current regulatory standards were investigated as part of the literature review, with several suggestions made on possible improvements for the future, including making allowances for islanding.

It was found, that while current and predicted future levels of rooftop PV EG, have and will continue to cause problems on the electricity distribution network, not all effects of PV EG on the network are negative with some, such as being able to defer network augmentation and equalising voltage on a feeder, found to be quite advantageous.

It will be necessary to further investigate regulatory changes, both nationally and locally, to better allow for the integration of the increased levels of PV EG that are forecast.

University of Southern Queensland

Faculty of Health, Engineering and Sciences

ENG4111/ENG4112 Research Project

Limitations of Use

The Council of the University of Southern Queensland, its Faculty of Health, Engineering & Sciences, and the staff of the University of Southern Queensland, do not accept any responsibility for the truth, accuracy or completeness of material contained within or associated with this dissertation.

Persons using all or any part of this material do so at their own risk, and not at the risk of the Council of the University of Southern Queensland, its Faculty of Health, Engineering & Sciences or the staff of the University of Southern Queensland.

This dissertation reports an educational exercise and has no purpose or validity beyond this exercise. The sole purpose of the course pair entitled "Research Project" is to contribute to the overall education within the student's chosen degree program. This document, the associated hardware, software, drawings, and other material set out in the associated appendices should not be used for any other purpose: if they are so used, it is entirely at the risk of the user.

University of Southern Queensland

Faculty of Health, Engineering and Sciences

ENG4111/ENG4112 Research Project

Certification of Dissertation

I certify that the ideas, designs and experimental work, results, analyses and conclusions set out in this dissertation are entirely my own effort, except where otherwise indicated and acknowledged.

I further certify that the work is original and has not been previously submitted for assessment in any other course or institution, except where specifically stated.

Karen Hourigan

0061030322

10th October 2016

Acknowledgements

I would like to acknowledge and thank the following people:

- Associate Professor Tony Ahfock – USQ supervisor for the project, for his advice and timely feedback;
- Mr. Matthew Jolliffe – Ausgrid Distribution Planning for providing modelling software and guidance;
- Mr. John Menegus – Ausgrid Distribution Planning for providing critical modelling data;
- My partner Rick – for supporting me through the last 5 years of full time work and part time study.

Glossary of Terms

AEMO – Australian Energy Market Operator

AS – Australian Standard

ASPEN – Advanced Systems for Power Engineering Inc. (trade name)

AS/ NZS – Australian/ New Zealand Standard

BoM – Bureau of Meteorology

CEC – Clean Energy Council

CSIRO – Commonwealth Scientific and Industrial Research Organisation

CT – Current Transformer

DM&C – Distribution Monitoring and Control

EG – Embedded Generation

ENA – Electricity Networks Association

HAC – Hazard Assessment Checklist

HV – High Voltage

LID – Line Impedance Data

LIS – Load Information System

LV – Low Voltage

NLTC – No Load Tap Changer

NMI – National Metering Identifier

OLTC – On Load Tap Changer

P – real power

PF – Power Flow

PV – Photovoltaic

Q – reactive power

S&IRNSW – Service and Installation Rules of New South Wales

SBS – Solar Bonus Scheme

SCADA – Supervisory Control and Data Acquisition

SWMS – Safe Work Method Statement

Tx – Transformer

UNFCCC – United Nations Framework Convention for Climate Change

pf – power factor

Table of Contents

List of Figures

List of Tables

Chapter 1

1 Introduction

1.1 Project Overview

There has been an exponential increase in the last seven years of private embedded generation (EG), mainly in the form of photovoltaic (PV) arrays.
With the cessation of the NSW governments Solar Bonus Scheme (SBS) in 2011, the number of new small scale PV installations has predictably decreased, though with rising electricity costs the number of larger systems being installed on domestic premises and much larger systems being installed on commercial premises has increased. With global focus on climate change it is predicted that the installation of renewables will continue to thrive meaning the effects on the traditional electricity distribution network will become much more apparent.
Using empirical data this project seeks to analyse the effects of the current level of penetration of EG has had on the network with regards to voltage rise, reverse power flow, decrease in consumer demand on the grid and network load predictions.
Through modelling of actual electricity distribution network feeders, it then proposes to investigate the ongoing effects to the network if the predicted increase in private EG continues and analyse any issues that are identified.

1.2 Project Aims

The main aim of this project is to investigate the effects of current and future levels of distributed or rooftop PV EG on the electricity distribution network.

It will seek to investigate and determine:

- the effects on load flow within the network;
- possible quality of supply issues;
- solutions to any adverse effects that are identified.

1.3 Project Objectives

The specific objectives of this project are:

1. Investigate effects of current levels of PV EG on the distribution network;

2. Prove a correlation exists between load flows on small scale rooftop PV EG connected to the low voltage (LV) network and their respective high voltage (HV) 11kV feeders using empirical data;

3. Model the distribution network and compare this to the empirical data, validating the theoretical model;

4. Research current and historical data to predict future levels of PV EG penetration;

5. Modify the model of the distribution network developed as part of achieving objective 2 to accommodate the new levels of PV EG established in objective 3;

6. Investigate effects of future levels of PV EG on the distribution network with regards to load flow, voltage rise and decreased demand;

7. Investigate when the distribution network will likely reach ‘saturation’ with regards to generation into a zone substation;

8. Investigate current standards for the connection of PV EG to the distribution network;

9. Investigate and suggest possible solutions to any adverse effects on the distribution network identified through modelling by increased levels of PV EG.

Chapter 2

2 Literature Review

2.1 History

2.1.1 Evolution of the Electricity Distribution Network

The electricity distribution network we are familiar with today has been designed around a model consisting of centralised generation with a ‘top-down’ uni-directional power flow (Bayliss & Hardy 2012).

Early days of electricity generation saw a system that was less centralised, with larger numbers of localised generation plants, each supplying its own distribution network, the majority of these plants being decommissioned when the ‘generation–transmission–distribution’ type network was established (Jenkins 2000).

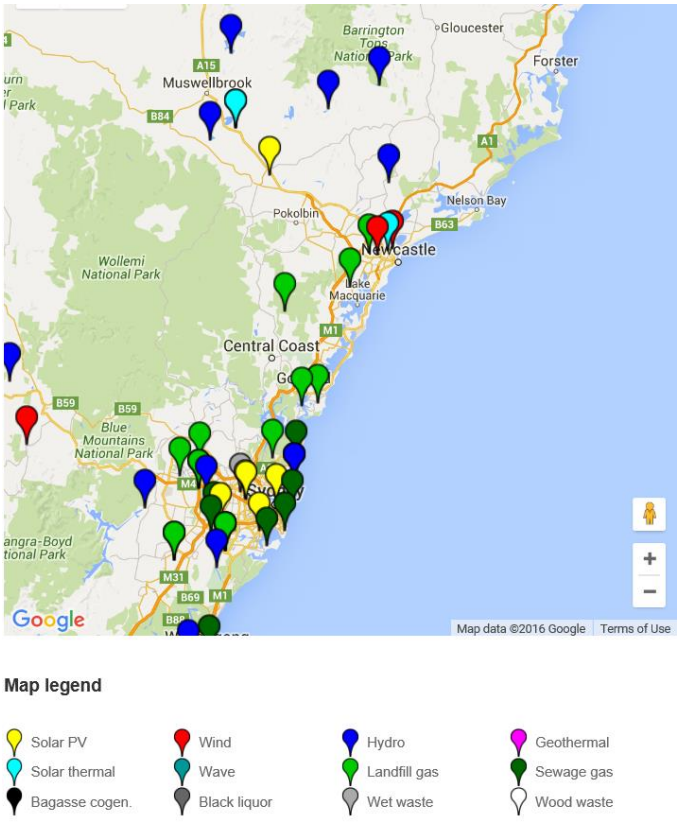

Figure 1: Renewable Energy Map showing Ausgrid network area - EG >100kW (CEC 2016)

There has been some movement over the last few decades to re-establish some privately owned power generators that are connected into the existing electricity network at the transmission level. Focussing on the network area of New South Wales electricity distributor Ausgrid, these are comprised mainly of hydro, solar thermal, landfill gas, sewage gas and wind schemes (CEC 2016) as well as one coal fired plant (RedbankEnergy 2006).
The possible issues that may arise with the connection of these large embedded generators have been well researched (Jenkins 2000) and utility companies have established guidelines as to their connection, co-generation and maintenance requirements (Ausgrid 2009).
In more recent years however, there has been a marked increase in the connection of decentralised small scale EG to the low voltage (LV) side of the network, with Australia now having the highest penetration rates of rooftop solar PV EG in the world (ENA, C. a. 2015), the effects of which have not been as thoroughly realised.

2.1.2 The Rise of Small Scale Distributed or Rooftop PV EG in Australia

Compared to other countries, Australia has not traditionally been a leader in the installation of renewable energy technologies.
At the beginning of 2009 Australia had a total PV generation capacity of just 37250kW or 0.03725GW (APVI 2016), compared with global leader Germany at 9.87GW (REN21 2010).

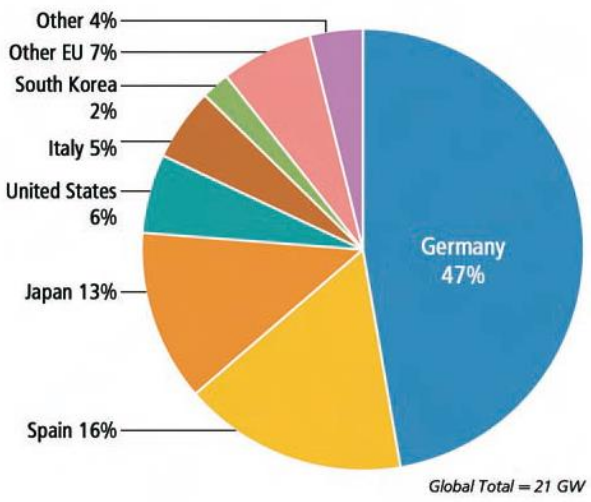

Figure 2: Solar PV Existing Capacity, Top Six Countries, 2009 (REN21 2010)

In 1992 nearly 200 developed industrialised countries, including Australia, joined the United Nations Framework Convention for Climate Change (UNFCCC) in an attempt, as a global community, to reduce the effects of climate change. The first agreement was reached in 1997 and took the form of the Kyoto Protocol, which was a legally binding agreement by the

constituent countries to reduce greenhouse emissions by 5.2% of those measured in 1990, with the first commitment period starting in 2008 (UNFCCC 2016).

There have been several energy saving initiatives developed by the New South Wales Government since then to encourage an increase in the installation of renewable energy sources by residential customers, including rebates for the installation of solar and heat pump hot water systems. The largest scheme to date has been the Solar Bonus Scheme (SBS) which opened on the 1st January 2010 and closed on the 28th April 2011. The SBS encouraged the installation of solar as well as wind generation, by offering generous renewable energy certificates (RECs) that significantly reduced the price of solar installations. This saw the increase of EG in NSW increase exponentially in a very small amount of time, leaving standards and network distributors ability to cope with the sudden increase in connections in its wake.

Prior to the SBS being implemented there was approximately 7.5MWh of solar generation connected to Ausgrid's LV distribution network. By the time the SBS scheme closed sixteen months later this figure had risen to 76MWh (Simpson 2011).

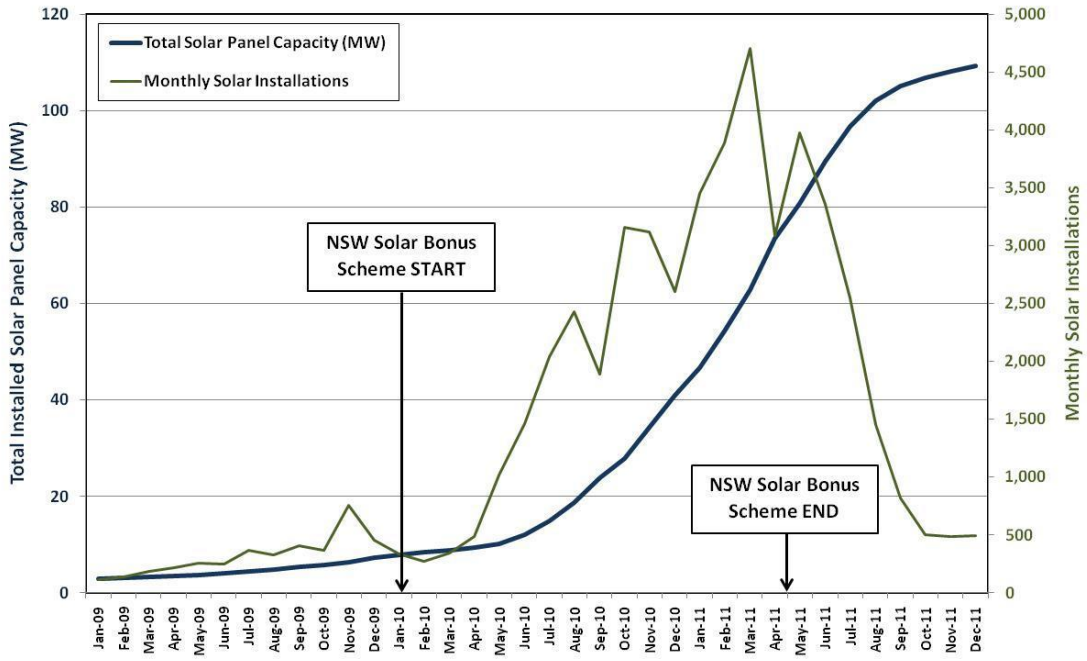

Figure 3: Ausgrid Solar Panel Capacity and Monthly Installs - 2009 to 2011 (Simpson 2011)

At the beginning of 2015, Australia's total PV generation capacity had risen to 4.1GW (APVI 2016), seeing it become the ninth highest country in the world for total PV generation, but first in the world per capita (ENA, C. a. 2015).

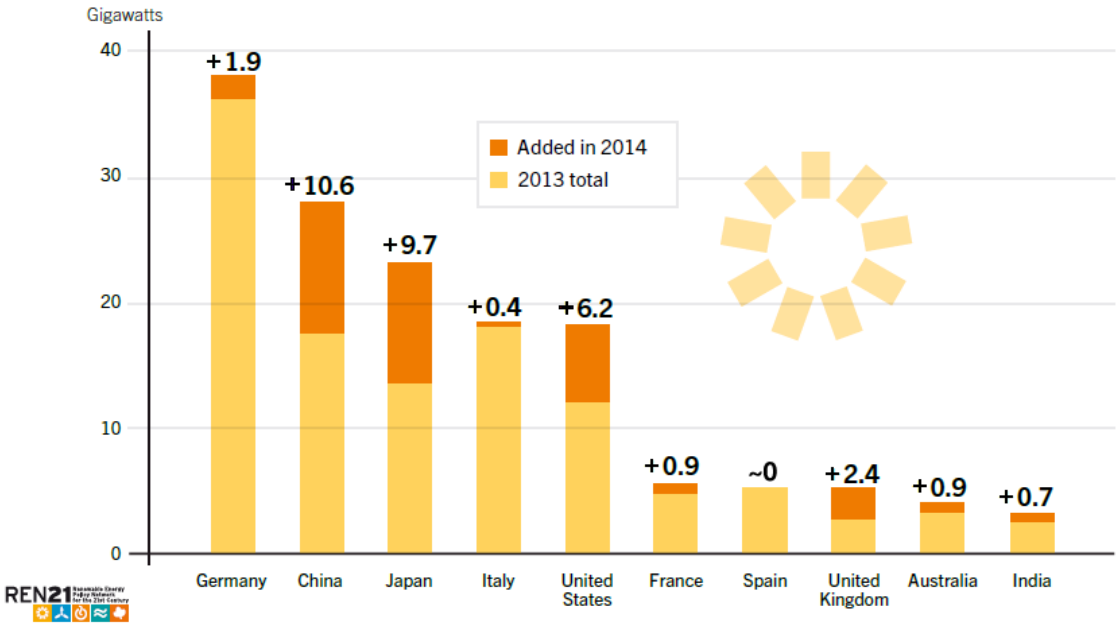

Figure 4: Solar PV global capacity and additions top ten countries 2014 (REN21 2015)

The next agreement of the UNFCCC to be reached was the Paris agreement, adopted on the 12th December 2015. This agreement saw member countries agree to restrict global warming to within 2% of pre-industrialisation temperatures (UNFCCC 2016) and to reduce greenhouse gas emissions by 26% to 28% below 2005 levels by 2030. It is suggested that a large part of the requirement for this will be met by the installation of renewables (AEMO 2015). In this case it is a reasonable assumption that a scheme along the lines of the SBS could once again be implemented by government to achieve this target.

There has been a steady rate of installation of EG since the end of the SBS, with the number of installations being connected per month not being as high, but the size of the connected generation at each of these sites increasing from an average of approximately 1.5kW per site at the start of 2010, to an average of approximately 2.5kW by the end of the SBS in April 2011, to an average of approximately 5.6kW at the end of 2015 (APVI 2016).

2.2 Charting the Future of PV EG in Australia

2.2.1 Electricity Network Transformation Roadmap

The Electricity Network Transformation Roadmap is a joint venture between the CSIRO and Energy Networks Australia (ENA), the purpose of which is to identify viable options for the energy industry reform required to integrate traditional distribution networks with the increasing level of customer owned EG.

It has several sections that deal with different facets of proposed reforms. Chapter 3 addresses the technical challenges as well as the possible benefits that could be gained from increased levels of EG (ENA, C. a. 2015).

In ENA, C. a. (2015), one of the four possible future pathways that have been developed is the rise of the 'prosumer', predicting a future network where the traditionally passive consumer is just as much a producer of electricity at localised levels as they are a consumer.

2.2.2 National Transmission Network Development Plan

The National Transmission Network Development Plan developed by the Australian Energy Market Operator (AEMO), is a plan for the long-term development of the national transmission grid. This report also addresses the challenges of successfully managing power systems with increased levels of EG. The main problems identified are less dispatchable generation, leading to less controllable generation, inertia and frequency control requirements and voltage stability during faults (AEMO 2015).

AEMO (2015) predicts that the rapid growth of rooftop PV installed in Australia that has been seen since 2010 is expected to increase with an additional 9,600MW to be installed in the next decade with the target for large-scale renewable generation set at 33,000GWh per year by 2020.

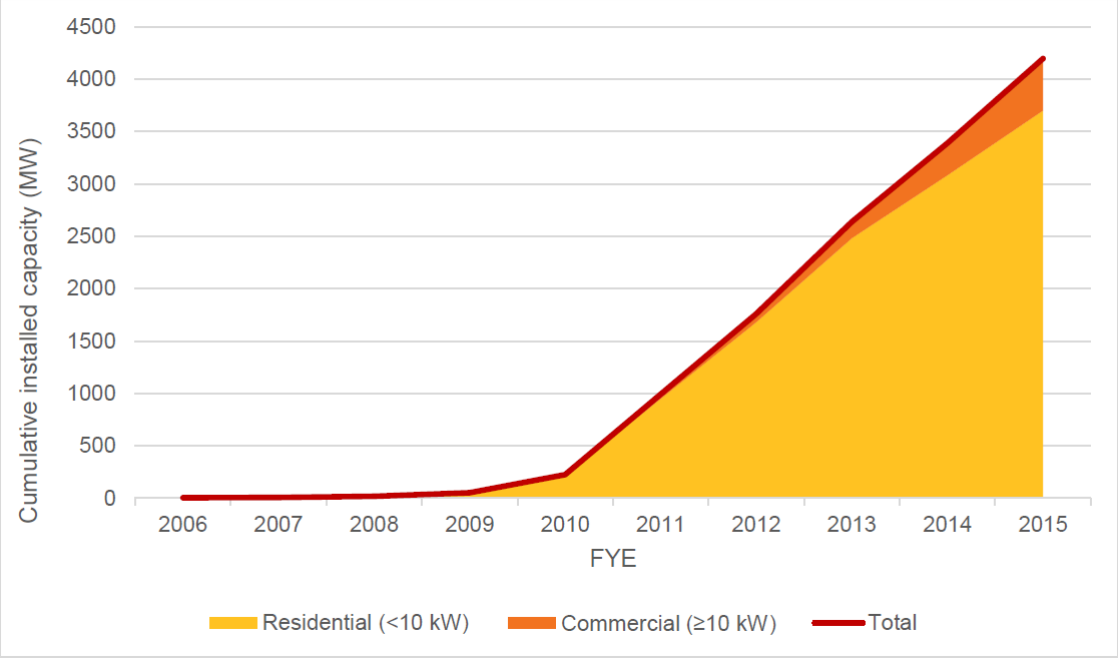

Figure 5: Rooftop PV EG uptake across the National Electricity Market (AEMO 2015)

2.3 Methods to Predict the Future Level of PV EG Penetration

Network planning is traditionally based on projected consumption using historical empirical data (Kolenc et al. 2015) as well as predicted load growth (Ausgrid 2015a).

Due to the stochastic nature of EG installations, it is not such simple task to accurately model the future increase in EG connections, especially where these connections are likely to take place (Kolenc et al. 2015). There are many unpredictable factors that must be taken into consideration such as electricity retail prices, cost of EG systems, changes to regulatory requirements and even the environmental conscience of consumers.

Kolenc et al. (2015) suggest that the statistical Monte Carlo simulation (MCS) is the optimal way in which to predict this as it is used to model systems in which analytical solutions are not viable.

Since the MCS is a probabilistic approach to uncertainty modelling it follows a probability distribution function (PDF). If the PDF is not known or the parameters are not repeatable a possibilistic method should be used (Soroudi et al. 2011).

There have been studies to predict the future increase in EG Australia wide (AEMO 2015), but it has not been achieved for state or distribution level. As EG incentive schemes have thus far been state based and not nationally based this is an important distinction to make for future prediction of networks within NSW. Also, as the geographical area and network configuration of the individual distribution networks also vary greatly, figures that relate more directly to the individual network distributor would be very useful.

2.4 Standards Relating to the Connection of PV EG

There are multiple standards that relate to the connection of PV EG. These are administered at three levels: Australian, state and local. In all cases, these standards were in place years before the SBS scheme started and were not revised, in some cases, until years after it closed.

2.4.1 Australian Standards

i. AS/NZS 5033: 2014 Installation and safety requirements for photovoltaic arrays. (StandardsAustralia 2014, p. 5)

   This standard was updated in 2014, but the previous version that was current at the time of SBS was issued in 2005. This saw a large number of PV systems installed in the intervening years whose technologies were not adequately covered by the standard at the time. Regular amendments to this standard is required to keep up with emerging technologies.

ii. AS/NZS 4777.1: 2005 Grid connection of energy systems via inverters – installation requirements.

This standard specifies the minimum electrical installation requirements for inverter energy systems up to 30kW total generation (StandardsAustralia 2005). The entire document is only 15 pages long, it has not been updated since 2005 and is severely lacking in content with regards to new technologies that have been in widespread use for the last decade.

iii. AS/NZS 4777.2:2015 Grid connection of energy systems via inverters – inverter requirements.

> "This Standard specifies requirements and tests for low voltage inverters for the injection of electric power through an electrical installation into the grid at low voltage." (StandardsAustralia 2015, p. 5)

This is an amalgamation of two previous standards:

1. AS/NZS 4777.2:2005 Grid connection of energy systems via inverters – inverter requirements

2. AS/NZS 4777.3:2005 Grid connection of energy systems via inverters – Grid protection requirements

These previous versions of this standard did not adequately address the requirements of new inverters being introduced, with much of this approval process falling back onto the Clean Energy Council (CEC). To demonstrate the lack of information in the previous versions of these standards that were current until 9th October 2015, AS/NZS 4777.2:2005 was 13 pages long, AS/NZS 4777.3:2005 was 16 pages long and AS/NZS 4777.2:2015 is 75 pages long.

iv. AS/NZS 3000:2007 Wiring Rules.

This standard states minimum requirements for design and connection of electrical installations with some specific clauses regarding PV EG, but it mainly refers to the standards listed above. There have been some updates to this standard relating to Section 7.3 Electricity Generation Systems to add PV EG (StandardsAustralia 2007).

2.4.2 New South Wales State Standards

i. Service and Installation Rules of New South Wales – August 2012

> "The Service and Installation Rules of New South Wales is the recognised industry code outlining the requirements of electrical distributors when connecting a customer to the distribution systems of New South Wales." (S&IRNSW 2012).

Section 8 - Alternative Sources of Supply - has subsection 8.6 that is now entirely in reference to Small Scale Parallel Customer Generation (via Inverters). In previous versions of this standard there was some reference to inverter systems, but there was not a great deal of guidance or restriction as to how they were connected to the distribution system. This shortfall during the SBS, in conjunction with similar shortfalls in local distributor connection requirements has led to many installations, some up to 10kW single phase rooftop PV systems in domestic situations, being connected to the detriment of the distribution system, especially with regards to load imbalance on the LV network (Simpson 2011).

2.4.3 Ausgrid Local Distribution Standards

i. NIS418 Embedded Generation

> "This standard covers the required outcomes for connection and management of all types and sizes of embedded generation connected or proposing to connect to Ausgrid's network." (Ausgrid 2015b)

This is an interim standard which now starts to address that smaller more distributed PV EG can present an issue to the distribution network as it states that it refers to all sizes of PV EG, however the emphasis is still on larger centrally connected generation. Aspects of the content will be discussed further in the next section.

ii. ES11 Requirements for Connection of Embedded Generators

> "This publication contains essential information and requirements relevant to applicants (Generators) proposing to connect or alter a connection of an embedded generating system to Ausgrid's network for parallel operation." (Ausgrid 2011)

There are a number of Ausgrid standards and technical/ work instructions that overlap, and the ones listed here share some common areas. This standard does outline the required technical investigations required, but does not provide a great deal of detailed guidance.
This standard has been withdrawn and is currently under review, with this document for internal reference only. There is no predicted date for release of the new version.

2.5 Connection of PV EG from the Electricity Distributors Point of View (Classical POV)

The main considerations of the electricity distributor when assessing applications for connection to the grid at present are to protect the safety and integrity of the network and to ensure that any PV EG does not reduce the quality of supply offered to other customers (Jenkins 2000).
To achieve this the distributor carries out a number technical investigations when it receives an application for PV EG to connect to the network.
These include:

1. capacity of the network to convey the generation output;
2. voltage regulation;
3. anti-islanding measures;
4. contribution to fault levels and fault detection under reverse power flow;
5. synchronising, isolation, system stability and safety;
6. stand-by supply;
7. quality of supply.

From the current standards it is obvious that systems of less than 30kW total generation are still not considered to materially contribute to the issues listed above as it is recommended that the general requirements of the Service and Installation Rules of NSW be followed, rather than a detailed study such as the one above be conducted (Ausgrid 2009). However the interim standard Ausgrid (2015b, p. 8) does acknowledge that

> "As EG connections within the Distribution Network (or lower) proliferate, the aggregated fault contribution from embedded sources could have a material impact on Fault Level at 11kV busbars – or even higher up into the Sub-transmission network."

This view does not seem as though it will be upheld however as Ausgrid announced in a media release on the 27th July 2016, that it will not assess any application of up to 30kW/ 3 phase for PV EG and/ or battery storage systems (Ausgrid 2016).

2.6 Problems Arising from Connection of PV EG

2.6.1 Technical Issues

There are a number of well-documented problems that can arise due to connection of PV EG on the electricity distribution network (Vovos et al. 2007).
These include:

1. Voltage changes on the network.

> "Every distribution utility has an obligation to supply its customers at a voltage within specified limits" (Jenkins 2000)

High concentrations of PV EG can cause significant voltage rise on the distribution network. Voltage rise is the result of reverse load flow from PV EG source back to the network. It is reliant on several main factors (Nourbakhsh et al. 2013):

i. System impedance;
ii. Generator location;
iii. Generator characteristic;
iv. System load.

S&IRNSW (2012) sets out requirements for voltage rise limitations for EG connections in NSW.
Through steady state and dynamic analysis, Eftekharnejad et al. (2013) found that increasing PV penetration levels up to 20% produced over voltages at transmission level buses. It was also observed that greater voltage dips were experienced in systems with higher levels of PV penetration.

2. Increase in network fault levels.

   In Jenkins (2000), it is stated that most traditional EG uses rotating machinery. Studies have been completed on this type of EG with regards to its contributions to fault levels on the network and methods have been developed to limit the effects, such as increasing impedance between the generator and network.
   Caamaño-Martín et al. (2008) states that the contribution to fault levels of PV grid-connected systems has been largely ignored, deemed to not be a significant contribution to cause concern. However, where high levels of PV EG exist in certain network configurations, such as long radial feeders with high impedance, the PV EG systems may not be able to detect the fault and could end up feeding the fault causing problems with protection.
   As noted earlier (Ausgrid 2015b), electricity distributors are now starting to realise the potential effects of distributed PV EG on fault levels within the network, with future amendments to this standard to consider fault level contribution to the 11kV network of PV EG connected at distribution and LV levels.

3. Reverse power flow, protection, unintentional islanding

   In Horowitz and Phadke (2014) it is shown how back feed of current may cause nuisance tripping of protection relays in certain network configurations if the current contribution from EG exceeds the trip setting of the feeder over current relays. It also goes on to state how there is then the possibility of unintentional islanding if the EG closely matches the feeder load. This could then also lead to problems when the network tries to close back onto the tripped feeder due to frequency and phase angle drift whilst islanded.
   There have always been very strong constraints governing the requirements for anti-islanding (StandardsAustralia 2015) and even stronger requirements placed on large-scale PV EG systems (Ausgrid 2013). Despite these measures, the increase in installation of PV EG in recent years has strongly increased the possibility that unintentional islanding could occur (Caamaño-Martín et al. 2008).

2.6.2 Previous Work in Investigating Problems

Voltage rise on the network caused by high levels of PV EG is a significant issue particularly on rural, radial feeders. This then places more emphasis on the need for effective voltage regulation (Namin & Agelidis 2013).

Vovos et al. (2007) explores the effectiveness of both centralised voltage control and distributed voltage and reactive power control of PV EG. This study found the two to be comparable in terms of allowing higher penetration of PV EG, though this had to be paired with on load tap changers (OLTC) which are not widely used at the distribution level of the electricity supply network. This would be an economic shortfall for this method as the cost to upgrade distribution Txs to accommodate an OLTC from off-load or no-load tap changer (NLTC) would be prohibitive.

Liu et al. (2012) suggests a co-ordinated approach to voltage regulation utilising a combination of OLTC and step voltage regulators (SVR) to control distributed energy storage systems (ESS). This method purports to lessen stress on the OLTC by requiring less operations due to the distributed ESS being controlled by the OLTC or SVR to charge or discharge storage batteries depending on the load requirements of the feeder. At times of low load, the ESS will charge instead of causing reverse power flow onto the grid. At times of high load, the ESS will discharge effectively 'shaving' the peak load. Ausgrid has completed a practical study of this on one of its rural radial feeders using units known as 'Red-Flow' which comprised a battery storage system that would charge during the night when lower electricity usage tariffs were available, then would discharge during peak tariff times.

Nourbakhsh et al. (2013) proposed an approach to voltage rise mitigation by utilising existing NLTCs. The paper stated that following simulation and practical trials that changing the tap setting at the distribution Txs to lower the nominal LV output that this would effectively mitigate voltage rise on the distribution network. There could be considerable issues with this where there are high impedance LV distribution feeders, due to either length of feeder or small size of cable, as the voltage drop at the ends of these feeders at times when there is little or no PV EG input into the network would be considerable and possibly cause more problems than the voltage rise it was seeking to abate. This would also present a problem on single installation Txs located on large rural properties where there are similar private LV feeders installed.

Reverse power flow can cause a myriad of problems including the voltage rise issue discussed previously. It can also have effects on power systems protection (Horowitz & Phadke 2014) as well as the distribution assets themselves.

Using network modelling Cipcigan and Taylor (2007) found that some primary Txs would exceed their reverse power flow capability if every customer connected to it installed a PV EG of a capacity as small as 1kW. Considering current Ausgrid requirements allow for immediate approval of systems up to and including 5kW/ phase located in urban areas and 3kW/ phase in

rural areas, this has the potential to cause significant issues. In the near future, Ausgrid is planning to increase this to 10kW/ phase.

Caamaño-Martín et al. (2008) states that under certain conditions on high impedance radial feeder's high penetrations of PV can effect overcurrent relay operation. There could be several reasons for this.

As stated in Horowitz and Phadke (2014), prospective fault current at the end of a long radial feeder may be quite low. In the case of an overcurrent protection relay, it would need to be set to be able to detect the 'worst case scenario' which would be a fault at the end of the feeder. If there was high level of PV EG installed towards the origin of this feeder, it would be feasible that at times of low loading there would be the potential of reverse power flow onto the feeder. If the magnitude of this reverse power flow was greater than that of the prospective fault current at the end of the feeder, this could cause nuisance tripping of the protection relay. Conversely if there was a large enough system located near the end of the feeder, it could generate enough reverse power flow for the protection relay to incorrectly see it as a fault and again nuisance trip.

Tripping of the feeder protection could also give rise to another fault condition in unintentional islanding. Caamaño-Martín et al. (2008) proposed that under certain conditions, a 'feeder trip' could cause unintentional islanding despite anti-islanding protection being built into approved inverters. Inverter requirements for anti-islanding as set out in StandardsAustralia (2015) rely on over/ under voltage and over/ under frequency. This type of passive islanding detection method has a large non-detection zone which could ultimately lead to instances of unintentional islanding especially where constant power controlled inverters are connected to feeders with mainly constant impedance loads (Zeineldin & Kirtley 2008).

It must be noted that not all effects of PV EG on the electricity distribution network are negative (Caamaño-Martín et al. 2008). It has been shown that under certain conditions increased levels of PV EG can lessen energy distribution losses in the network (Quezada et al. 2006). It can also lessen stresses on OLTC if managed in conjunction with ESS (Liu et al. 2012).
One main area of interest of using PV EG to advantage is intentional islanding and the resultant micro grids (Balaguer et al. 2011). As part of ENA (2015), the ENA and CSIRO are investigating the feasibility of micro grids as one of the possible solutions to the increase in PV EG.

2.7 System Studies

Two of the types of system studies used in electricity distribution network analysis are (Bayliss & Hardy 2012):

- Power flow modelling
- Fault analysis

2.7.1 Power Flow Modelling

Power flow (PF) or load flow modelling is used to simulate an electricity network. It is used to demonstrate how a network will perform under certain conditions identifying real and reactive power flows, voltage profiles, power factor and any overloads in the network (Bayliss & Hardy 2012).

The four quantities associated with PF modelling are active power (P) and reactive power (Q) of all loads on the section of network being studied, voltage magnitude (|V|) and voltage angle (δ). P and Q are usually the known quantities, with the PF model solving for |V| and δ.
Since there are two unknowns, two algebraic equations are required and a numerical iterative method is then used to solve for the unknown quantities (Powell 2005).

There are a number of iterative methods that can be used to solve the PF problem, including Jacobi Method, Gauss–Seidel Method, Z-Matrix Method, Newton-Raphson Method and Fast Decoupled Method. They all utilise their own specifically derived algebraic equations and they all have their own advantages and disadvantages depending on what type of system they are being used to analyse and the software that is being used to complete the analysis (Powell 2005). One method that is commonly used in commercial software is the Fast-Decoupled Method as it is much faster than other methods.

When there are generators embedded within the electricity distribution network, their effects must be considered in the PF model. Where such EG is in the form of a rotating generator, the P and |V| values are set and the Q and δ values vary. In the case of connected PV EG it can be considered as a negative load, and just as any other load on the network the P and Q values are set and the |V| and δ values vary (Powell 2005).

2.7.2 Fault Analysis

Fault analysis is the method used to obtain the prospective fault currents on all sections of the network. Faults can be in the form of symmetrical three phase faults or asymmetrical phase to ground faults, they can also be high or low impedance faults.

The determination of the prospective fault currents can then be utilised for several applications including:

- correct rating of system components, such as breaking capacity of reclosers and intellirupters;
- correct setting of protection relays to ensure minimum fault levels are detected;
- any changes to the system that might be required to reduce fault levels

(Bayliss & Hardy 2012).

2.8 Conclusions

Continued growth in the renewable energy sector is inevitable and is being actively encouraged by government partially due to their being a party to the UNFCCC.
In NSW, with the exception of the SBS, growth has been reasonably consistent with decreasing numbers of installations coupled with increasing capacity of the installation combining to keep increases in generation capacity consistent.

With the current level of penetration of PV EG, there are already demonstrable effects on the electricity distribution network, though it has also been proven that not all effects of PV EG on the network are negative.

Studies into increased levels have also proven that at 20% penetration there are over voltage effects at transmission level busbars. With renewable energy targets heading towards 20% of power generation from renewables by 2020 to be able to meet the governments commitments to climate change, this poses a very real problem for distribution network operators.

Chapter 3

3 Methodology

This chapter describes the processes that were required to achieve the project objectives as stated in the introduction, section 1.3.

3.1 Gathering Empirical Data

In order to investigate effects if current levels of PV EG both at a localised level and at a feeder level, it was necessary to gather 'real' data from both manually logged and automatically logged sources.
This data was also required to be able to validate feeder models that were constructed for power flow investigations, used to determine the effects of future predicted levels of PV EG.

3.1.1 Manually Logged Data on Individual Installations

Manual data loggers were installed on three LV direct distributors that feed individual installations with larger PV EG systems.
These particular installations were chosen for several reasons:

- The PV systems were in excess of 50kW, two of the three being 100kW;
- All systems had been installed within the last 2 years;
- All installations were fed from a dedicated direct distributor from a kiosk Tx;
- Manual logging data was available on all three installations prior to the PV systems being installed;
- They represented a range of differing customer installations (a school, a social club and an office building).

The data loggers were left in place for 21 days, taking measurements every 30 seconds for the duration. The loggers were then downloaded, the data being exported from the logger software to a .csv file. This was imported into Matlab and analysed to ascertain the loads the installations were using. From this, any reverse power flows from the installations back into the grid were also identified.

The dates when all three systems were installed were determined and manual logging data for the direct distributors for the same installations prior to the PV EG being installed was obtained. This was also imported into Matlab and the two sets of data were compared to determine the effects of the PV EG systems on these installations.

3.1.2 Auto Logged Data on Distribution Txs and HV Feeders

Automatically logged data in the form of Supervisory Control and Data Acquisition (SCADA), is available on all of Ausgrid's zone substations, thus the substation bus load and voltage data for the HV feeders was obtainable. Using an Excel 'plug-in' called PI-DataLink it was possible to import the feeder data for the exact time period the manual loggers were installed. It was also possible to specify that the load data imported was in 30 second intervals to exactly match the manually logged data.

SCADA data was obtained for the same HV feeders prior to the PV EG being installed, at exactly the same time of year so that the loading of the feeder was similar. This data was obtained for all feeders under investigation from 2009 until 2016.

Using PI-Datalink, Distribution Monitoring and Control (DM&C) data was obtained for 7 distribution Txs on the feeder that was modelled for power flow. This data was required in order to validate the power flow model by comparing the theoretical results from the model to the actual results measured at the origin of the feeder and at each distribution Tx.

3.2 Modelling Network Feeders

Two HV feeders were modelled using a commercially available software suite called ASPEN. First was an initial 'test' feeder, second was the feeder used to demonstrate power flow.

3.2.1 Constructing the Models

The feeder that ultimately became the 'test' feeder was originally chosen as the power flow feeder for several reasons:

- It was a smaller feeder with a lesser number of Txs and connected customers, but with a high penetration of rooftop PV EG;
- A smaller feeder was easier to model in order to become familiar with the modelling software;
- The exact method of allocating load to each Tx had not been determined, so a smaller model was easier to navigate when investigating different methods.

After initial testing of the model, it was decided that although it suited as a test model, and the feeder used to demonstrate effects of current levels of PV EG, it could not be used as the power flow model as there were insufficient points around the feeder from which to source 'real' data

to validate the model comprehensively enough to use it to investigate effects of future predicted level of PV EG.

Two methods were used to construct the test model, the models compared and the better method chosen to model the power flow feeder.

3.2.1.1 Manual Construction

To manually construct the model the following process was followed:

- Determine the structure of the feeder with regards to shackle poles, tee-off points and changes in cable types;
- Determine types and lengths of each section of cable;
- Manually place all buses, cables, loads and generators.

3.2.1.2 Automatic Construction

Automatic construction of the feeder was possible using an Ausgrid database called LID (Line Impedance Data), and a converter program called LID2ASPEN that converts the output of LID to a usable format in the ASPEN modelling software.
Either using GPS coordinates or network system diagram layout, the zone bus, each load (Tx) bus and multiple tap buses are placed on the diagram with the line impedance of the cables interconnecting them imported from the LID database. A tap bus is placed at every point there is a shackle pole or tee-off pole on the feeder.
This resulted in many extra buses that made the model difficult to follow and were not required for the analysis. Removal of the unnecessary tap buses and manual placement of the remaining buses was required to ensure a decipherable model.

3.2.1.3 Comparison of Manual and Automatic Models

The two models were then run and compared to each other as well as to a third model that was used for distribution planning purposes. The total feeder load results of all models were then compared to the empirical data for that feeder. All models proved to be reasonably accurate with reference to the total feeder load measured at the zone substation.
The automatic LID based model was chosen as for the larger feeder that was modelled for power flow it was a much faster method.

3.2.2 Allocating Load to the Tx Buses

3.2.2.1 Tx kVA Rating Method

The method used to allocate load to Txs in all of the models above was based on the kVA rating of the Tx. This method proved sufficient to construct a model that would provide an accurate total feeder load, but there was the possibility it would not give an accurate representation of the feeder at other points, as in a 'real world' situation it is very unlikely that the magnitude of the load on a Tx would be proportional to its size, as existing Txs on distribution networks are often close to operating capacity, where new or replacement Txs are often sized for future growth and are often underutilised.

The test feeder was an older feeder that did not have any monitoring equipment at the distribution Tx level, so the model, when compared to total feeder load from previous years seemed accurate.

The feeder data from this year had been discounted as it showed a marked decrease in magnitude from previous years at all times of the day which could not be accounted for by increased PV EG on the feeder, though on consultation with the feeder system diagram there had been no alterations to feeder open points.

On actual physical inspection however, there had been a change of open point due to a burnt out HV tapping, prior to the data period for this year, , which had caused 10 out of 38 Txs to be shifted to an adjacent feeder.

An air break switch (ABS) was then placed at that point on the model and was then 'opened off' to investigate whether the shedding of the same 10 Txs in the model had the same effect on total feeder load as the change of open point did on the actual feeder. This served to demonstrate the inaccuracies of this model when using the kVA rating method of allocating load. This presented the challenge of finding a way to accurately allocate load to Txs on a network that did not have data monitoring at each Tx.

3.2.2.2 LIS

The Load Information System (LIS) is a database that is still in development within Ausgrid, and is not yet available for system planning.

It is a database containing metering data from all installations within Ausgrids network.

As an exercise to assist in developing the database further, LIS data for all the feeders that were modelled was made available for the purposes of this project.

LIS data for the 7 Txs that had DM&C equipment connected to them was compared to the data retrieved from the DM&C units to validate the use of the LIS data.

Most Txs on the feeders had LIS data allocated to them, but many did not. In these cases it was necessary to obtain the national meter identifier (NMI) numbers (unique identifier numbers allocated to every metered installation in Australia), for each installation connected to the Tx and request the data for each individual installation separately. This returned one large spreadsheet containing 29 days of data (for every day in February 2016), separated into 48 half hour interval blocks for every installation.

This data was imported into Matlab, sorted and allocated to the Tx that supplied the installation, which was then allocated to the correct feeder. At the end of this process all Txs on both feeders had LIS load data allocated to them.

The maximum total feeder load for February was established, with the matching Tx loadings extracted from the data and exported into an excel spreadsheet. These load figures were then loaded into the model for every Tx on the feeder and the model run again.

The results for feeder current obtained from the 'full model' containing all 38 Txs was compared to the averaged maximum measured load data for the feeder for February from 2009 to 2015 and was found to be reasonably accurate. The ABS was then opened to simulate the physical open point in the network and shed the same 10 Txs. The feeder load result obtained from the model closely matched the measured maximum load data from February 2016.

Due to the results presented here, it was decided to use the LIS data to allocate Tx loads.

3.2.3 Further Validation of the Power Flow Model

As stated previously, proving the models at the origin of the feeder only is not sufficient to properly validate the models.

The P and Q load values were known at each point and the load buses were designated PQ buses which have the P and Q values set so that the voltage magnitude and voltage angle are free to vary and as such form the solution of the model.

Using the voltage values of the DM&C and SCADA data that was gathered previously the model was proven at multiple points around the feeder with the theoretical values provided by the model being compared to the measured values.

The DM&C and SCADA equipment does not measure voltage angle, and so no comparison was available for the voltage angles provided by the model.

3.3 Investigating Effects of Future Levels of Photovoltaic Embedded Generation through Power Flow Modelling

Research completed as part of the literature review revealed the predicted level of growth for rooftop PV EG.

Using this as a basis, PV EG was incrementally added at various Tx buses around the modelled feeder.

Research also revealed that although current Ausgrid standards require any PV EG system above 5kW/ phase to be load assessed, in the near future that figure will be increased to 10kW/ phase.

From this, the following was determined:

- the effect of adding the predicted future level of PV EG to the network;
- how much additional PV EG was required before the power flow on the feeder was reversed to the point of generating back into the zone substation;
- the effect of adding up to 2 x the predicted future level of PV EG connected to every distribution Tx.

3.4 Investigation of Possible Solutions to Adverse Effects of Photovoltaic Embedded Generation

Several options for damping the effects of PV EG on the electricity distribution network were investigated:

- PV EG export limitations. This was theoretical only and involved no modelling;
- Addition of a reactive power component to PV EG. This was achieved using the power flow model outlined in section 3.3, and altering the power factor of the PV EG from unity to 0.85;
- Intentional islanding. This was also theoretical only and involved no modelling.

3.5 Connection requirements

In completing the literature review, it was determined when standards changed to reflect more thought in planning process particularly in regards to:

- Service &Installation Rules of NSW;
- AS 5033 PV installations;
- AS 4777 series;
- Internal Ausgrid documents.

Some suggestions were made into how to further improve some of these documents, including:

- Allowing islanding;
- Not increasing assessment limits to 10kW/ phase.

Chapter 4

4 Effects of Current Levels of PV EG

4.1 Overview

Several avenues have been explored in order to investigate the effects of the current levels of PV EG:

- Manual logging equipment was installed on three separate installations with PV EG connected in order to perform a 'before and after' comparison of load profiles of individual installations;
- The load profiles of these individual installations were compared with those of the HV feeders that supply them with the aim of demonstrating that individual PV EG installations have the ability to influence the feeders they are connected to;
- Historic load data on several feeders was procured to investigate any changes in feeder loading in recent years. This data was used to demonstrate whether any decreases in loading could be attributed to PV EG.

4.2 'Before and After' Comparison on Individual PV Installations

Manual data loggers were installed on three installations containing large rooftop PV system for a period of 21 days over April/ May 2016.
These specific installations were chosen for the following reasons:

- They were supplied by a dedicated circuit from a kiosk Tx;
- They had logging data available for a period prior to the PV EG being installed, which was required for the before/ after comparison;
- They represented a variety of installation types (a school, a social club, an office building).

The data from this logging period was compared to data obtained from a logging period prior to the PV EG being installed to investigate the effects the PV systems have had on each installation.
Figure 6 on the next page shows the LV board of the Tx that supplies installation 1. The top corner of the data logger can be seen in the bottom centre of the photo, with the voltage leads being connected to the test block located at the top left hand side of the LV board.

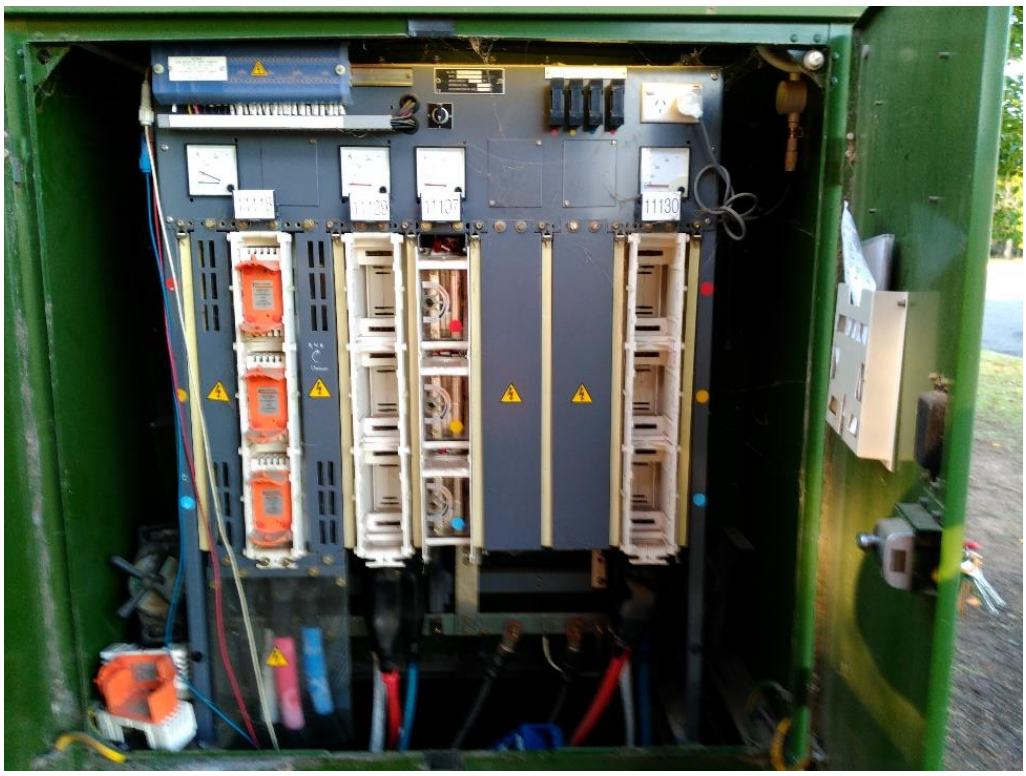

Figure 6: LV board of Tx with manual data logger connected

4.2.1 Installation 1 - School

Installation 1 was a school with a 100kW rooftop PV EG system installed.

The graphs in figure 7 below show the load profile of the installation before and after the PV EG was installed.

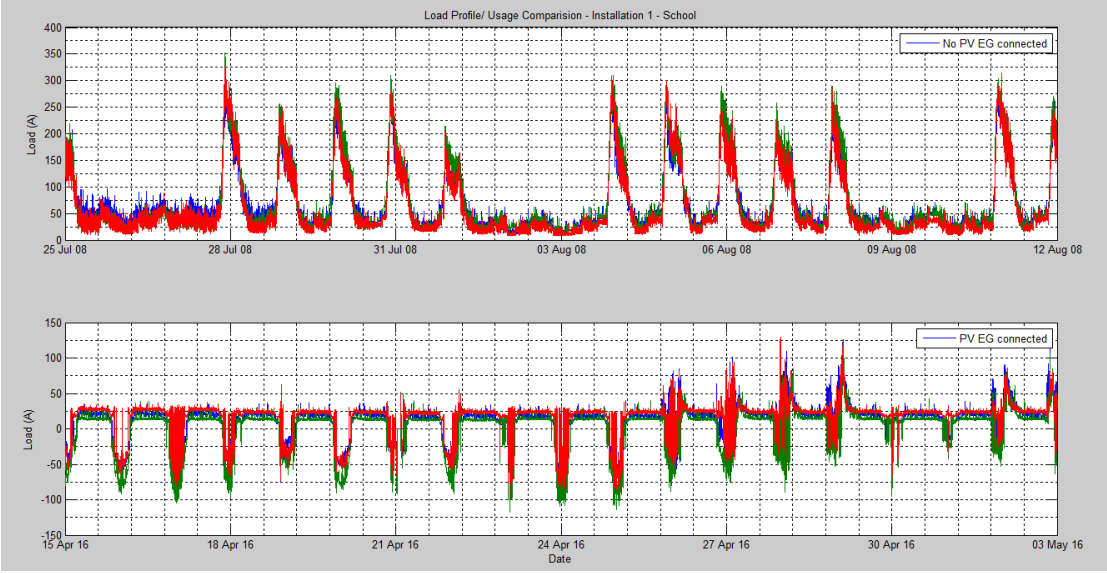

Figure 7: Load Profile Comparison – School[1]

[1] Refer Appendix D1 for Matlab code

On comparison of the data from the logging periods before and after the PV EG was installed it was apparent that:

- During the minimum load period, which is outside PV generation times, the loading had not altered significantly, the demand being approximately 15 – 35A. This was a sound indication that there had been no other significant changes to the installation;
- The first section of the data logging period from April this year was conducted during school holidays. During this period, and on weekends, it was apparent how much power was generated back onto the grid by this one installation alone. Another important factor with this specific installation, or installation type, is the fact that it has minimal load usage for 6 – 8 weeks over the peak PV generating period of the year when the school is closed for the December/ January school holidays. This data logging period was in April, which has much lower PV generation potential than December/ January. This is demonstrated in Figure 8, which shows the daily solar exposure data (MJ/ m^2) for 2015, taken from the Bureau of Meteorology (BoM) for the weather station in the same town;
- When school returned, the maximum demand was between 80 – 125A. Prior to the PV EG being installed it was consistently between 250 – 300A. This is a decrease of approximately 170 amps. Since the maximum output of a 100kW PV system is approximately 140 amps, the higher load in the data sample prior to PV EG being installed could be due to the period being in July as winter loading is generally higher than Autumnal loading due to increased heating demands.

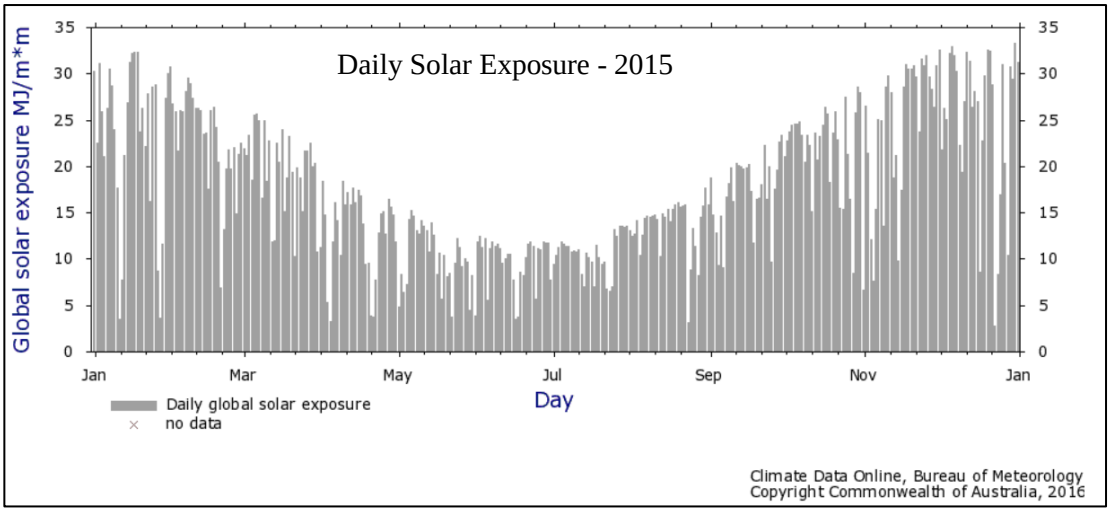

Figure 8: Daily Solar Exposure – 2015

4.2.2 Installation 2 – Social Club

Installation 2 was a social club with a 100kW rooftop PV system installed.

The graphs in figure 9 below show the load profile before and after the PV EG was installed.

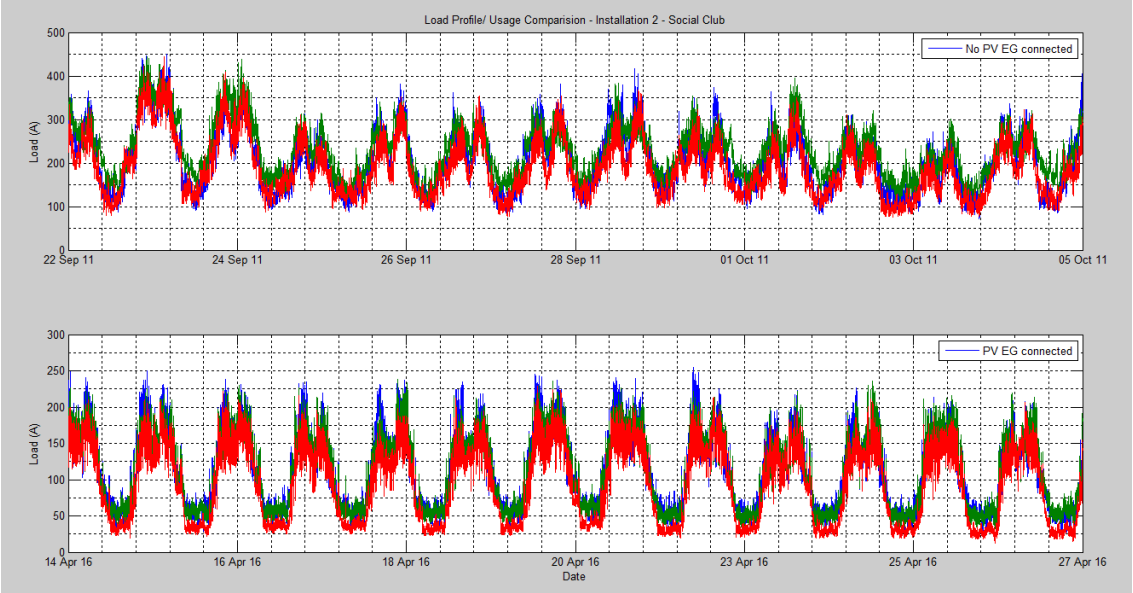

Figure 9: Load Profile Comparison - Social Club[2]

When comparing the data from the two logging periods it was apparent that:

- During the minimum load period, which is outside PV generation times, the loading has decreased by approximately 75A, from 100A down to 25A. This indicated that there had been some changes to loading, other than that caused by the addition of the PV EG system;
- When considering peak demand, it can be seen that it had decreased by approximately 175A, from 400A to 225A. Factoring in other alterations within the installation that caused the base loading to decrease by 75A, this indicates there is a peak demand decrease of 100A due to the PV EG. This is consistent with the generating capacity of a 100kW PV system in Autumn.

[2] Refer Appendix D2 for Matlab code

4.2.3 Installation 3 – Office Building

Installation 3 was an office building with a 50kW rooftop PV system installed.
The graphs in figure 10 below show the load profile before and after the PV EG was installed.

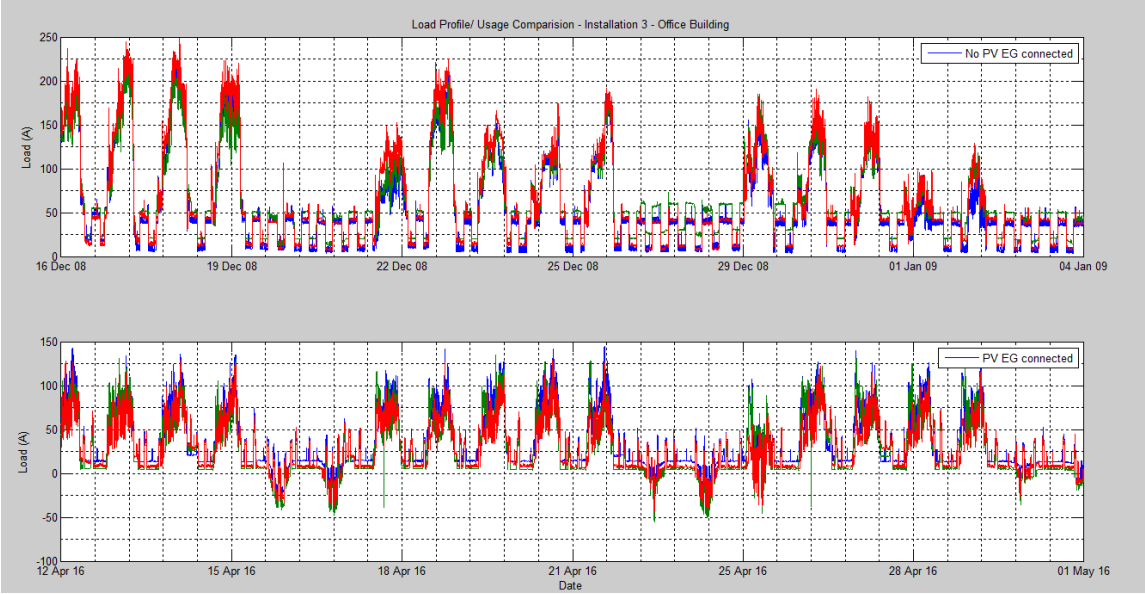

Figure 10: Load Profile Comparison - Office Building[3]

When comparing the data from the two logging periods it was apparent that:

- The latter two thirds of the data logging period from the pre PV EG data set was during the Christmas/ New Year break and did not provide an accurate representation of the installation loading, therefore analysis of this installation will be performed on the first week of data for each period only;
- During the minimum load period, which is outside PV generation times, the loading has not altered significantly, the demand between approximately 10 – 50A. This is a good indication that there had been no other changes to the installation that could be giving a false indication that the PV EG had more of an effect on the installation than it actually did. It also indicated that this load consisted primarily of air conditioning that was cycling on and off at regular time intervals;
- The first period of logged data that represents the installation prior to the PV EG being connected was in peak summer period when air conditioning load can be significantly higher. The fact the air conditioning cycled on and off at regular intervals was significant to the comparison of the two samples of logged data as it indicated that the air conditioning load, while it would have increased the maximum demand of the

[3] Refer Appendix D3 for Matlab code

installation would not have impacted the loading as much as temperature controlled cooling;

- It can be seen on weekends, how much power was generated back onto the grid by this one installation alone. The office building operates Monday to Friday only, so excess power is generated onto the grid every weekend;
- Considering the first 4 days of data only, the maximum demand prior to the PV EG being connected was between 225 – 250A. After the PV EG was installed it was consistently between 125 – 140A. This is a decrease of approximately 85A. Since the maximum output of a 50kW PV system is approximately 70 amps, the higher load in the data sample prior to PV EG being installed could be due to the period being in December. Summer loading is generally higher than Autumnal loading due to increased cooling demands.

4.2.4 Conclusions

It has been demonstrated by all three installations that the addition of PV EG can significantly impact not only the load demands of an installation, but the load profile of the installation it is connected to, at times having the potential for large amounts of power to be generated back onto the distribution network.

This was particularly demonstrated by the load profile of the school. A number of these types of installation connected either to the same feeder, or to adjacent feeders that are supplied by the same zone substation would have significant impacts on the distribution network.

4.3 Comparison of Load Profiles of Individual Installations with Feeder Load Profile

This section investigates the relationship between the installations examined in the previous section and the feeders that supply them, by comparing the load profile of each installation with that of its respective feeder.

4.3.1 Installation 1 - School

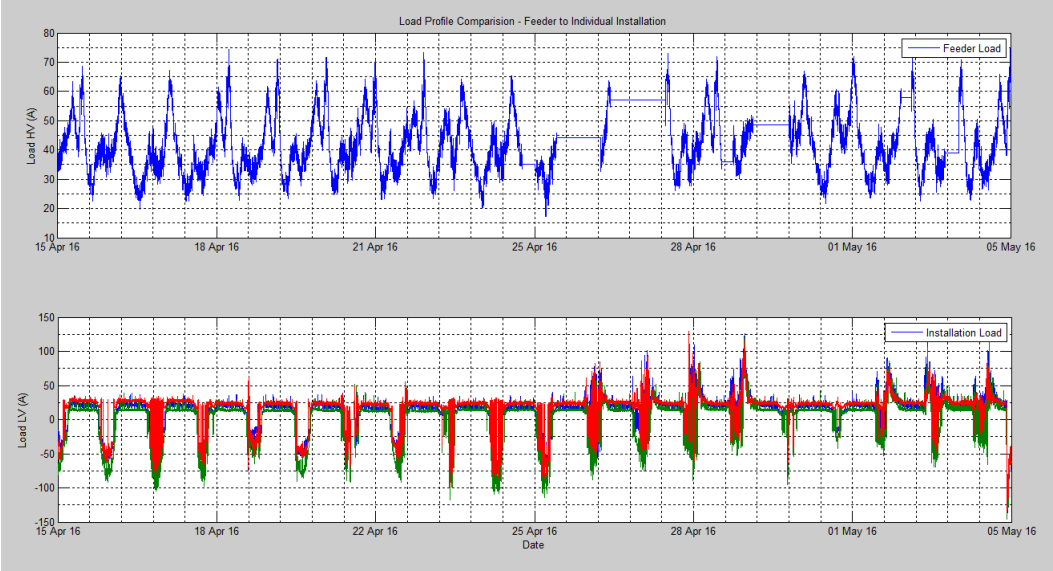

Figure 11: Load Profile Comparison - Feeder to Individual Installation – School[4]

On examination of the load profile of the school, reverse power flow from the installation back onto the grid could be seen. When school returned and the load of the installation increased, as expected the magnitude of the reverse power flow decreased.

Comparison of the load profile of the school with that of the HV feeder that supplies it, showed that there was no corresponding increase in feeder load during that same period. On average the daytime minimum demand of the feeder was not demonstrably lower under the higher reverse power flow conditions from the school.

[4] Refer Appendix D4for Matlab code

4.3.2 Installation 2 – Social Club

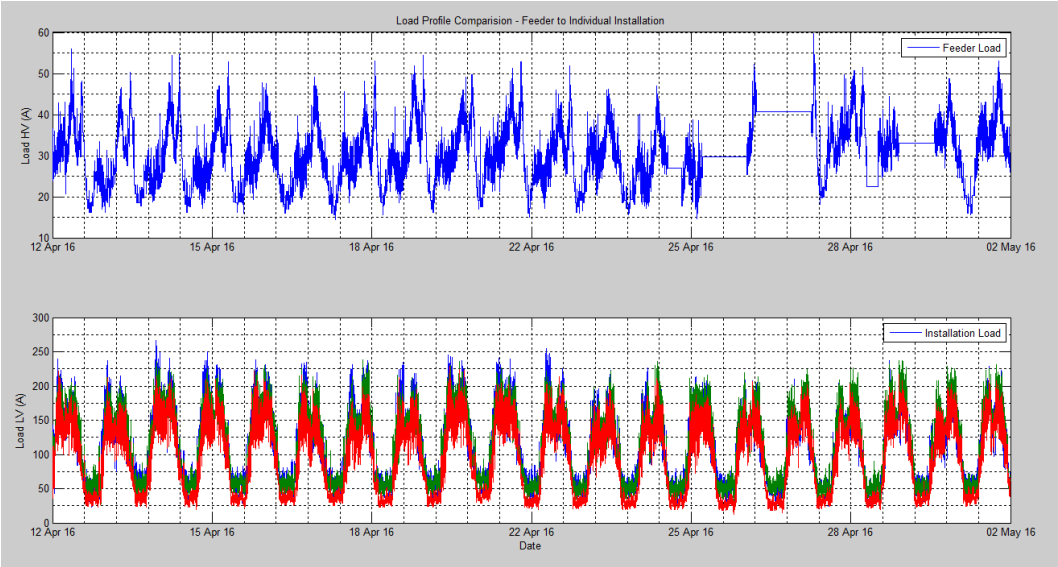

Figure 12: Load Profile Comparison - Feeder to Individual Installation – Social Club[5]

On examination of the load profile of the social club it was found to be relatively consistent every day of the week with no significant change in loading from weekday to weekend. This made comparison with the load profile of the feeder that supplies it more difficult as there were no marked changes in the installation profile to compare with the feeder.

Over the logging period, there were several installation peak loads that were higher than other days to the magnitude of approximately 25A. When taking into consideration the tap setting of the Tx this would mean an increase in feeder load of approximately 1A which is not discernible when the feeder load at the same instant was 30-35A.

[5] Refer Appendix D5 for Matlab code used to produce this figure

4.3.3 Installation 3 – Office Building

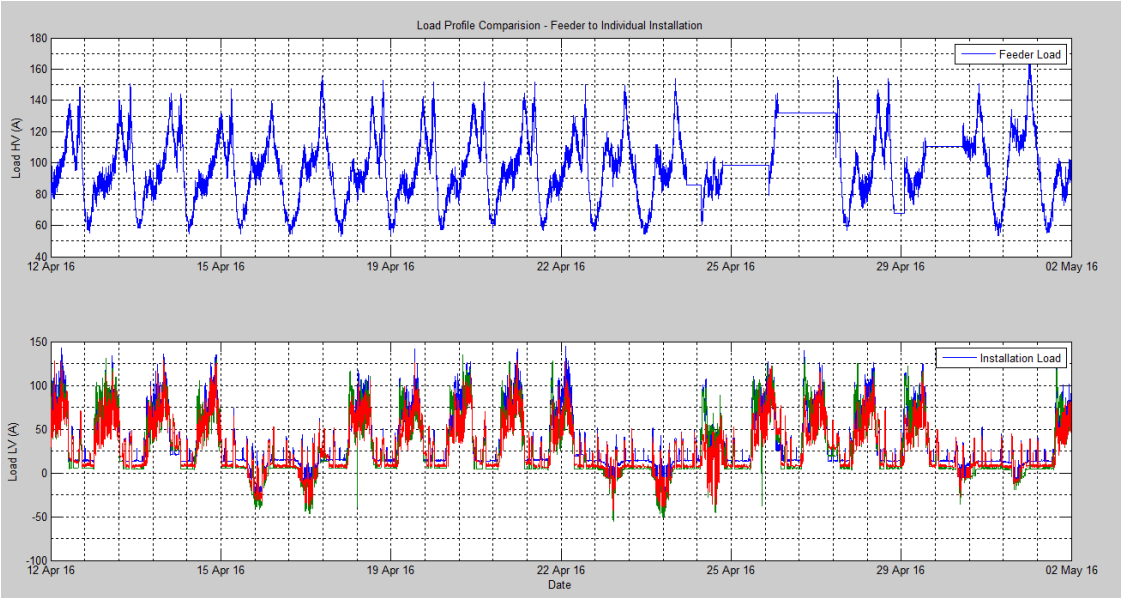

Figure 13: Load Profile Comparison - Feeder to Individual Installation – Office Building[6]

On comparison of the installation load profile with that of the feeder that supplies it, it was found that the daytime low loading condition that was evident in the installation data was reflected in that of the feeder data.

It could be seen that the PV EG connected to the office building generated a significant amount of power back onto the electricity grid on weekends. When comparing this same period on the feeder loading, the trough in the load profile was still evident, but the magnitude of the loading had increased, not decreased as it had in the installation.

This feeder supplies a primarily domestic load which accounts for the increased loading on the weekend.

4.3.4 Conclusions

While the profile of each feeder was found to generally match the 'daily low demand' trend of the installations, none of the feeders demonstrated a close correlation to the individual PV installations they supply. The evident trough that exists on each feeder at the minimum daytime loading time is more likely to be attributed to the combined generation capacity of all of the distributed PV EG systems connected to it rather than any single installation.

This is discussed further in the next section.

[6] Refer Appendix D6 for Matlab code

4.4 Change in Loading on High Voltage Feeder

Since the start of the NSW government Solar Bonus Scheme in 2009, there has been a marked increase in the level of 'rooftop' PV EG. As was demonstrated in section 4.1, this can cause significant changes to an installations load profile and maximum demand.
Figure 14 on the next page shows the demand on a particular 11kV feeder for the period from 19th - 28th April 2009, as well as the demand on the same feeder for the same period in 2015. This was one of the smallest feeders in the network with only 711 customers, but with the highest level of PV EG penetration, with a total connected generation of 486kW, which is an average of 0.684kW per customer. The largest single PV EG system on this feeder was 45kW, with the remaining 441kW distributed around the feeder.

There are 5 main loading times on the feeder as shown on figure 14:

1. Traditional lowest loading period – early hours of the morning;
2. Morning peak – approximately 6:30 – 7:30am;
3. Daytime lowest loading period;
4. Evening peak time – approximately 6 – 7pm;
5. Peak load due to off-peak water heating – approximately 11 – 12pm.

Data for the daily solar exposure for the same period was obtained from the BoM, sourced from the weather station in the same town this feeder supplies. It is shown in figure 15 on the next page.

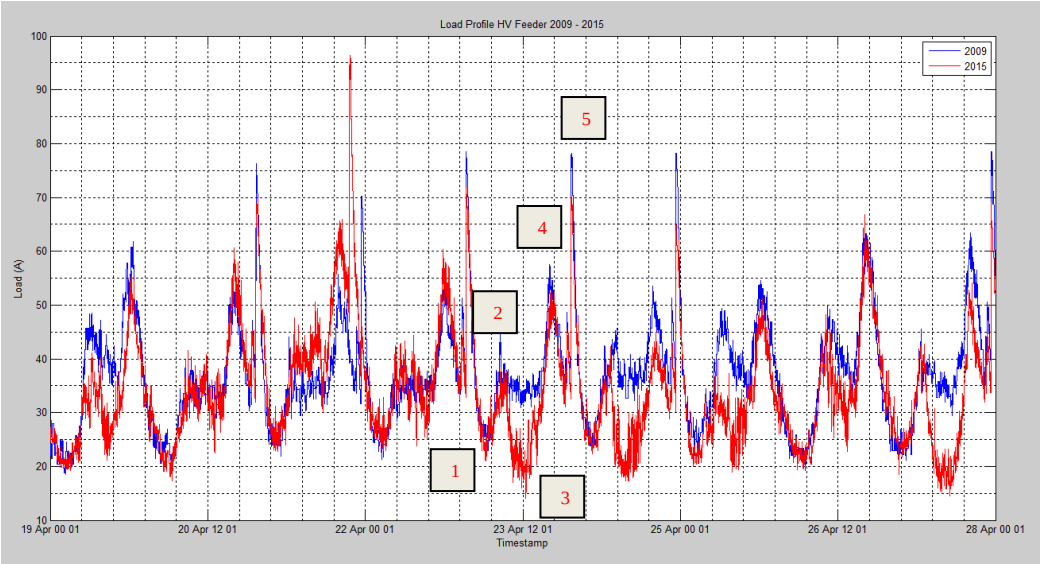

Figure 14: Feeder Load Comparison 2009 / 2015[7]

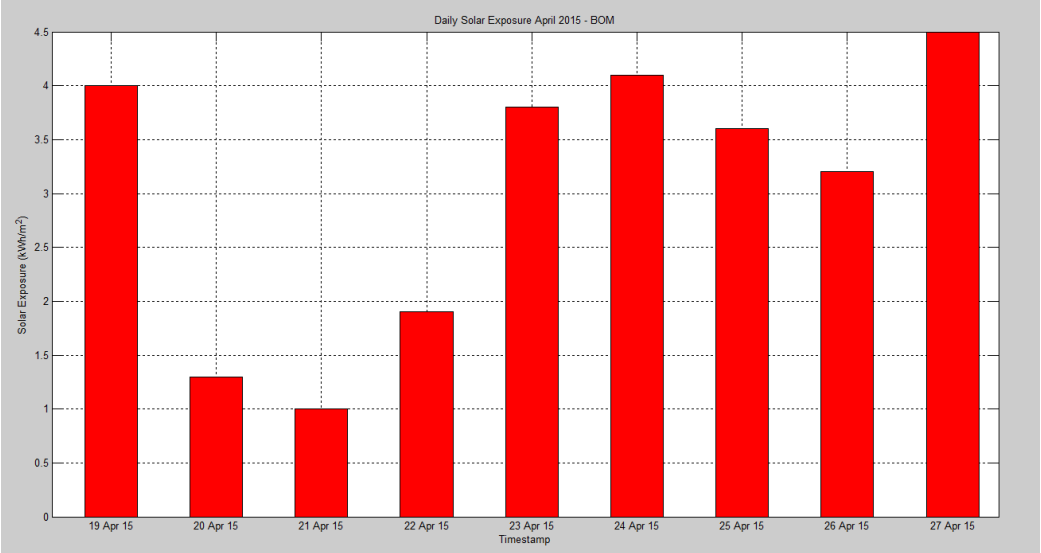

Figure 15: BOM Data - Daily Solar Exposure April 2015[8]

Several observations can be made from the comparison of figures 14 and 15:

- The magnitude of the early morning low loading period has changed little from 2009 – 2015;
- The magnitude of the morning peak load has changed slightly;
- The evening peak changed from day to day, but overall remained similar;
- The off-peak loading has decreased by 5 – 10A. This is consistent with the number of installations on PV EG as the new off-peak meters do not rely on frequency injection from the zone substation, but operate on internal timeclocks that are individually set;

[7] Refer Appendix D7 for Matlab code
[8] Refer Appendix D7 for Matlab code

- The greatest change has occurred in the daytime lowest loading period, which decreased by up to 17A depending on weather conditions;
- It can be seen by comparison of figures 14 and 15 that there is a direct correlation between the decrease in the daytime loading on the feeder and the daily solar exposure levels. The higher the solar exposure level, the lower the load on the feeder as PV generation is higher.

4.5 Conclusions

Current levels of PV EG have had significant effects on loading, not only on the individual installations they are connected to, but on the HV feeders that supply them. While it could not be proven that any individual installation had a significant effect on the feeder that supplied it, it was demonstrated that the combined capacity of distributed rooftop PV EG systems located around a feeder does have a significant effect.

Chapter 5

5 Effects of Future Predicted Levels of PV EG Using Power Flow Modelling

5.1 Background

The fundamental equations that form the basis for all PF equations are:

$$I_k = \sum_{j=1}^{n} Y_{kj} V_j \qquad ①$$

$$I_k = \frac{V_k^*}{S^*} \qquad ②$$

Where:

- I_k is current at bus k
- k is current bus under consideration
- j is bus number (buses adjacent to bus k)
- n is number of buses adjacent to bus k
- Y_{kj} is admittance of the line between bus k and bus j
- V_j is complex voltage at bus j
- V_k^* is complex conjugate of complex voltage at bus k
- S^* is complex conjugate of complex apparent power S

One popular iterative method used to solve PF equations is the Newton–Raphson Method as it is very robust when applied to non-linear systems such as electricity distribution networks. This method uses a set of non-linear equations in the form $y_n = f_n(x_n)$, which it then expands around a starting point using a Taylor Series expansion.

For n buses, there are 2n equations with 4n unknowns.

In matrix form:

$$\begin{bmatrix} y_1 \\ \vdots \\ y_n \end{bmatrix} = \begin{bmatrix} f_1[x_1(0) & \cdots & x_n(0)] \\ \vdots & & \vdots \\ f_n[x_n(0) & \cdots & x_n(0)] \end{bmatrix} \begin{bmatrix} \frac{\partial f_1}{\partial x_1} & \cdots & \frac{\partial f_1}{\partial x_n} \\ \vdots & & \vdots \\ \frac{\partial f_n}{\partial x_1} & \cdots & \frac{\partial f_n}{\partial x_n} \end{bmatrix} \begin{bmatrix} x_1 - x_1(0) \\ \vdots \\ x_n - x_n(0) \end{bmatrix} \qquad ③$$

The matrix of partial derivatives is called the Jacobean matrix (J).

This can be written as:

$$y = f[x(0)] + J(0)[x - x(0)] \qquad ④$$

With:

$$x = x(0) + J(0)^{-1}[y - f\{x(0)\}] \qquad ⑤$$

In recursive form, iteration count i,

$$x_{i+1} = x_i + J_i^{-1}[y - f(x_i)] \qquad ⑥$$

When using polar coordinates this can be written as:

$$\begin{bmatrix}\Delta P \\ \Delta Q\end{bmatrix} = \begin{bmatrix}J_1 & J_2 \\ J_3 & J_4\end{bmatrix}\begin{bmatrix}\Delta\delta \\ \Delta V\end{bmatrix} \qquad ⑦$$

This is more efficient for programming purposes written as:

$$\begin{bmatrix}\Delta P \\ \Delta Q\end{bmatrix} = \begin{bmatrix}J_1 & J_2 \\ J_3 & J_4\end{bmatrix}\begin{bmatrix}\Delta\delta \\ \frac{\Delta|V|}{|V|}\end{bmatrix} \qquad ⑧$$

Hence

$$\begin{bmatrix}\Delta\delta \\ \frac{\Delta|V|}{|V|}\end{bmatrix} = \begin{bmatrix}J_1 & J_2 \\ J_3 & J_4\end{bmatrix}^{-1}\begin{bmatrix}\Delta P \\ \Delta Q\end{bmatrix} \qquad ⑨$$

With reference to the simple two bus system 1-line diagram below (Jenkins 2000):

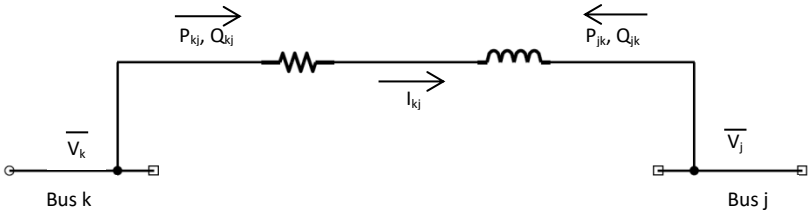

Figure 16: Simple 2 bus 1-Line Diagram

The equations required to solve the Newton-Raphson Method using Polar Coordinates are (Powell 2005):

$$P_k = |V_k| \sum_{\substack{j=1 \\ j \neq k}}^{n} |Y_{kj}| \cdot |V_j| \cos(\delta_k - \delta_j - \theta_{kj}) + |V_k|^2 |Y_{kk}| \cos(\theta_{kk}) \qquad ⑩$$

$$Q_k = |V_k| \sum_{\substack{j=1 \\ j \neq k}}^{n} |Y_{kj}| \cdot \left|V_j\right| \sin\left(\delta_k - \delta_j - \theta_{kj}\right) - |V_k|^2 |Y_{kk}| \sin(\theta_{kk}) \qquad ⑪$$

Where:

- P_k is active power injections at bus k
- Q_k is reactive power injections at bus k
- V_k is voltage magnitude at bus k
- Y_{kj} is admittance of line between bus k and bus j
- V_j is voltage at bus j
- δ_k is voltage angle at bus k
- δ_j is voltage angle at bus j
- θ_{kj} is admittance angle from bus k to bus j
- θ_{kk} is admittance angle at bus k

For larger networks where there are n buses, 2n equations are required relating 4n variables.

Even though Newton-Raphson Method typically converges after a short number of iterations (Powell 2005), each iteration can take some time due to the need to form the $(2n-1) \times (2n-1)$ J matrix, which is then inverted on every iteration.

The Decoupled Newton-Raphson Method uses the following relationships to be able to perform the iterations faster:

- $P \propto \delta$
- $Q \propto |V|$

As these relationships suggest, there is a high degree of independence between P and |V|, and between Q and δ (Powell 2005). As such equation X can be reduced to:

$$\begin{bmatrix} \Delta P \\ \Delta Q \end{bmatrix} = \begin{bmatrix} J_1 & 0 \\ 0 & J_4 \end{bmatrix} \begin{bmatrix} \Delta\delta \\ \frac{\Delta|V|}{|V|} \end{bmatrix} \qquad ⑫$$

which on expansion and inversion produces the two matrix equations below:

$$\Delta\delta = J_1^{-1}\Delta P \qquad ⑬$$

$$\frac{\Delta|V|}{|V|} = J_4^{-1}\Delta Q \qquad ⑭$$

J_1^{-1} and J_4^{-1} can now be inverted separately, and since each one is a quarter of the size of the original J matrix, the iteration time is much faster.

The Fast Decoupled Method further simplifies the Decoupled Newton-Raphson Method by making the following assumptions:

- The difference in angle between adjacent busbars is small, meaning that $\cos(\delta_k - \delta_j) \cong 1$;
- $G_{kj}\sin(\delta_k - \delta_j) \ll B_{kj}$, which follows on from assumption 1;
- $Q_k \ll B_{kk}|V_k|^2$.

Where:

- δ_k is voltage angle at bus k
- G_{kj} is conductance of the line between bus k and adjacent bus j
- B_{kj} is susceptance of the line between bus k and adjacent bus j
- Q_k is reactive power of the load at bus k
- $|V_k|$ is voltage magnitude at bus k

Due to the assumptions listed previously, this method requires more iterations before the system converges, but the time to perform each iteration is only a fraction of that required by the Newton-Raphson Method for two reasons:

- Only a single $(n-1) \times (n-1)$ matrix is required, compared to the $(2n-1) \times (2n-1)$ J matrix required by the Newton-Raphson Method;
- The $(n-1) \times (n-1)$ matrix needs to be inverted only once during the entire solution, where the Newton-Raphson Method requires the $(2n-1) \times (2n-1)$ matrix to be inverted with every iteration.

5.2 Application to PV EG

As a static power source, generation from a PV array can be considered as a negative load. The P and Q values of the PV EG are set at each bus just as the P and Q values of the load at each bus is set. Since it is treated as a negative load, in relation to the P and Q values of the loads, the respective values are seen by the model as – P and – Q. The P and Q values at each bus are added together to get the total P and Q magnitude at each bus.

Figure 17 below is an example of a simplified power flow model showing load and generations at each PQ bus.

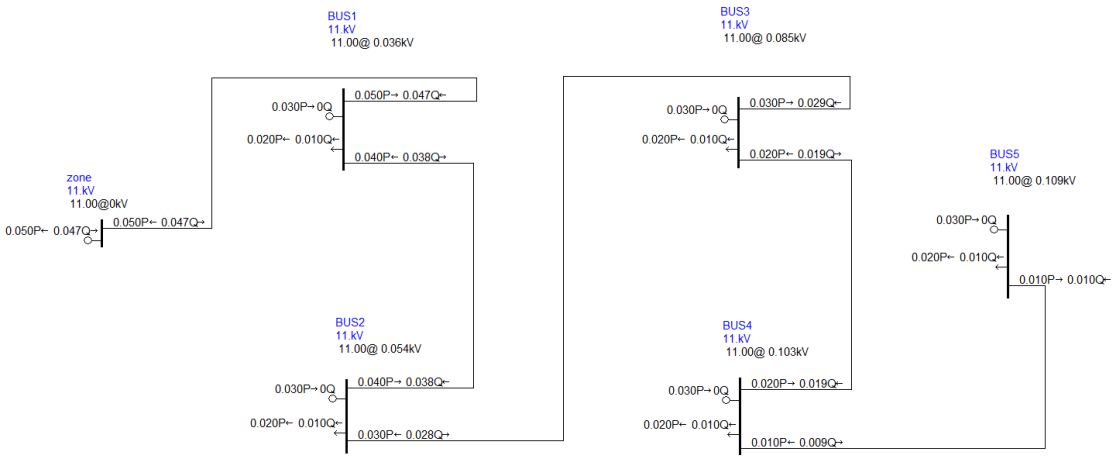

Figure 17: Simplified power flow model showing PV EGs at each bus (pf=1)

5.3 Network Feeder Models

5.3.1 'Test' Feeder Model

This was the feeder that was originally chosen for the power flow modelling to demonstrate the effects of future predicted levels of PV EG as it was one of the smallest feeders with the smallest number of connected customers, but with the highest penetration of PV EG. When attempting to validate the model however, the equipment on this feeder proved not to have sufficient measured data available to adequately prove the model.
It did however prove to be a valuable step in the project for several reasons:

- it indicated that further measured data was required to properly validate a model;
- it proved that the current method used by Distribution Planning to allocate load to Txs (proportional to kVA size of the Tx) on a feeder was inadequate for the purposes of this project;
- it allowed familiarisation with power flow modelling, and the ASPEN software itself to be carried out on a smaller feeder.

5.3.1.1 Construction

Initial construction of the model was carried out manually, using Ausgrid line tables, GIS based feeder data, system diagrams and a network mapping program called SCOUT.
This method ultimately proved accurate, but was very time consuming.

A secondary construction method was then trialled, utilising an Ausgrid line impedance database called LID. A conversion program called LIS2ASPEN was then used to convert the output of LID into a usable form for ASPEN.
Whilst providing the cable impedances of the feeder and default loadings for the Tx buses, LID also created a large number of tap-buses, at every point there was a shackle pole on the feeder, that were not necessary for the power flow simulation and make the diagram very congested. This method proved to not be completely without the need for manual input as each unnecessary tap bus had to be removed and the Tx buses relocated and extended for the solved diagram to be decipherable.

5.3.1.2 Validation

Due to distribution level data not being available, validation for what became the test feeder was only possible at the origin of the feeder. When compared to the average maximum demand over

that period for the feeder, the model provided accurate results using the default load values for the Tx on the feeder which were based on the kVA rating of the individual Tx.

The actual physical ABS that constitutes the open point between this feeder and the feeder adjacent to it was operated which resulted in 10 of 38 Txs being fed from the adjacent feeder. The loading on the new feeder configuration was measured and the average maximum demand determined. This was then simulated on the model and results were obtained for the new total feeder load under the altered conditions.

The manually constructed unsolved 1–Line diagram of the test feeder is shown below with the open point ABS shown in the open position.

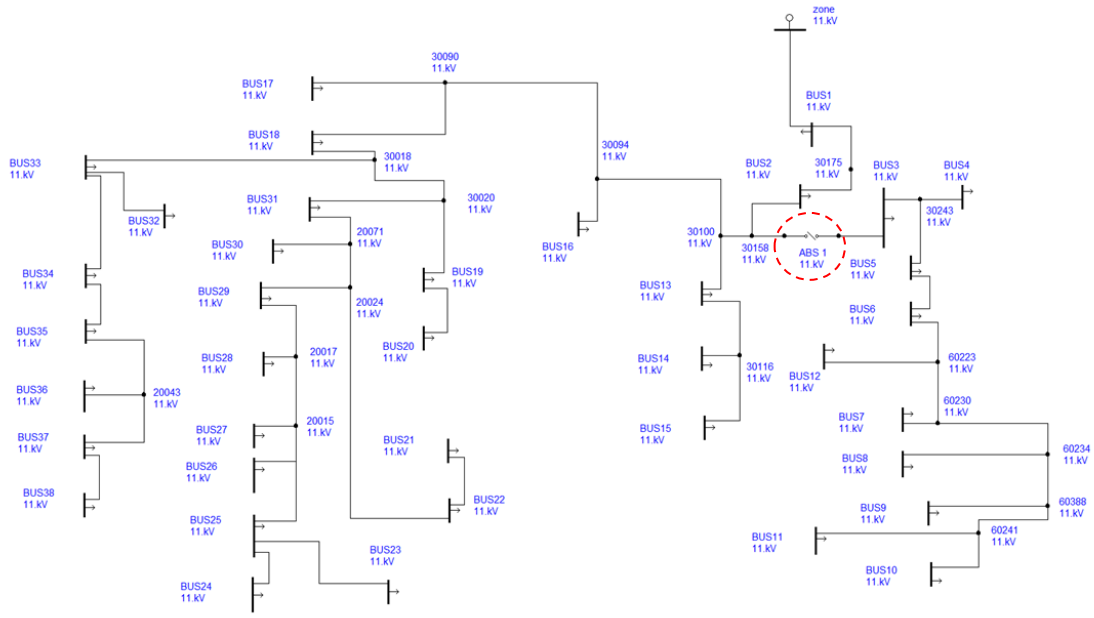

Figure 18: Unsolved 1-Line diagram of test feeder - ABS in open position

Table 1 below shows the results of the original feeder configuration model, the altered feeder configuration model and the real measured data obtained under both conditions.

	Model		Measured Feeder[9]	
	# Tx's	Feeder Loading (A)	# Tx's	Feeder Loading (A)
Original configuration	38	121	38	103.69
Altered configuration	28	71.1	28	46.75

Table 1: Comparison of feeder loading - model to actual – kVA based load allocation

[9] Refer Appendix D8 for Matlab code to produce results of feeder loading

It can be seen from the table above, that while the ‘Tx kVA’ method of allocating load to the Txs proved accurate for the total feeder loading when the feeder configuration was as expected, when any changes were made to the feeder it did not provide accurate results.
This led to the investigation into alternate methods of allocating load to Txs.

5.3.1.3 DM&C data

DM&C equipment is equipment that is installed on some Txs at distribution level. This in situ monitoring equipment takes interval measurements of the following components:

- Real power;
- Reactive power;
- Phase voltage for all 3 phases;
- Phase current for all 3 phases.

This type of distribution level monitoring would be an ideal source for the load data for each Tx to for the purposes of power flow modelling, however for the majority of feeders and networks DM&C data is not available as there are very few of these units installed at this level, making a comprehensive data set not readily available.
Figures 19 & 20 below show a DM&C unit installed on a distribution Tx.

Figure 19: Exterior of DM&C unit installed on a distribution Tx

Figure 20: Interior of a DM&C unit installed on a distribution Tx

5.3.1.4 LIS Data

The Load Information System (LIS) is an ongoing project within Ausgrid to establish an accurate load information database based on customers metering data. As stated previously, it is not yet available for distribution planning purposes, but was made available for the purposes of this project.

An initial search of the LIS data was conducted encompassing 4 different feeders. The initial data that was returned was based on Tx number with the Txs listed numerically, but not sorted by feeder number. This returned a spreadsheet containing data for 457 Txs, the data for each Tx broken up into the 29 days of February 2016 at 48 half hourly intervals.

After manually searching the initial spreadsheet for the Txs on the test feeder, it was found that only 23 out of the 38 Txs had LIS data allocated to them. In order to get data for the remaining 15 Txs, a subsequent search had to be made for the individual NMI data of all installations connected to the Txs that were missing data. This second search was for 422 individual installation NMIs, which returned a second spreadsheet, again with the NMI data being broken up into the 29 days of February 2016 at 48 half hourly intervals, arranged numerically by NMI number but not sorted to the Tx that it was supplied by.

The data from this spreadsheet was imported into Matlab and a script was written to allocate the individual NMI data to the Tx that supplied it, then summed all relevant NMI data to obtain the total load data for the Tx[10].

5.3.1.5 Comparison of LIS Data to DM&C Data to Validate LIS Data

To verify that the LIS data was an accurate representation of Tx load, LIS data obtained for 7 Txs on one of the other feeders that all had DM&C equipment installed. This data was then compared to the data that was measured by the DM&C equipment.

There was no manipulation of the LIS data or the DM&C measured real power data and they are shown on figure 21 below in blue and green respectively. The red graph is the calculated DM&C real power values which were obtained by multiplying each measured phase voltage by its corresponding phase current then multiplying by an assumed common power factor of 0.95. The common power factor was decided upon as the result of a sensitivity analysis that is outlined later in section 5.3.2.3.

The individual phase powers were then added together to obtain a total real power value for the Tx.

The following figure shows the data comparisons for one Tx, which is Tx18 from the feeder that was ultimately used for the power flow modelling as discussed later in section 5.3.2[11].

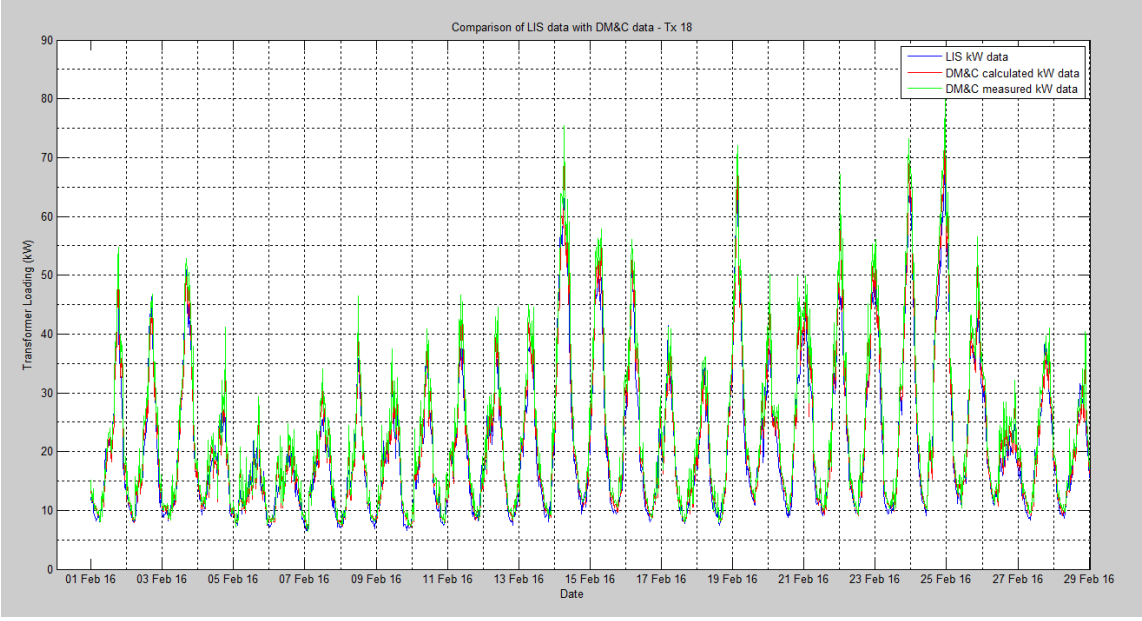

Figure 21: Comparison of LIS kW data with DM&C kW data – Tx18[12]

[10] Refer Appendix D9 for Matlab code for the data allocation
[11] Refer Appendix C for the remaining comparisons
[12] Refer Appendix D10 for Matlab code

As can be seen from figure 21 on the previous page, there is little variation between all three plots, thus verifying that the LIS data is a valid source for Tx load.

5.3.1.6 Revised Test Feeder Model

Once the LIS data was validated, it was applied to the test feeder model as the Tx loads[13]. As the LIS data is from customer metering data, it is measured on the LV side of the Tx. In the model, the loads were applied to the HV bus with a compensation factor of 2% to account for losses through the Tx.

This percent loss was decided upon due to the following considerations:

- From October 2004 distribution Txs used in Australia must comply with Minimum Energy Performance (MEPS) requirements. For a 500kVA rated Tx the minimum power efficiency at 50% load is 99.13%;
- There were a mix of pre and post 2004 Txs on this feeder;
- Pre 2004 Txs were likely to have a percent loss higher than 99.13%;
- 2% loss was decided upon as a common overall power loss through all Txs on the feeder.

5.3.1.7 Validation

The test feeder model was run and produced the following results shown in table 2 below.

	Feeder Loading (A)		
	kVA based model	LIS based model	Feeder actual data
Original configuration	121	110	103.69
Altered configuration	71.1	46.9	46.75

Table 2: Comparison of feeder loading - model to actual - LIS based load allocation

The discrepancy in the original configuration results was due to the fact that the LIS model was modelled from 2016 data only. The original configuration feeder loading was an average of the peak loads from the past 7 years 2009 – 2015, with the 2014 peak load being 109.38A which was very close to the maximum load as predicted by the LIS data model.

[13] Refer Appendix D11 for Matlab code used to ascertain LIS loading for test feeder Txs

5.3.2 Power Flow Model

It was proven from the results of the test feeder model that the model could not be properly validated through data measurements at the zone substation only, and that other measured data points around the feeder were required if the model was to be proven as a true representation of an actual feeder. To that end, the feeder with the largest number of distribution monitoring points was chosen.

5.3.2.1 Construction

Feeder model construction was done using the LID database and the LIS2ASPEN conversion program, which provided a model with 276 buses. Excess tap buses were manually removed and the remaining buses were modified and rearranged to enable the model to be easily read.

The resultant model had 85 buses consisting of:

- 1 slack bus;
- 64 PQ buses;
- 20 tap buses that represented t-off poles[14].

Default Tx loadings based on Tx kVA rating were replaced with loadings obtained from LIS data[15]. The LIS data was obtained using the same method that was outlined in section 5.3.1.4. After manually searching the data from the initial spreadsheet, it was found that 5 out of 64 Txs were missing LIS data. An individual NMI search was then carried out for data for each installation connected to these Txs, again as outlined in section 5.3.1.4. This search was for 127 individual installation NMIs.
The LIS data for one of the Txs on the feeder, Tx9, which also had DM&C data available, was found to have been incorrect. The reason for this was not evident, but the results are clear from the LIS/ DM&C data comparison shown in figure 22 on the next page.

[14] Refer Appendix E1 for power flow model 1-Line diagram – additional PV EG shown 'out of service'
[15] Refer Appendix D12for Matlab code used to ascertain LIS loading for power flow feeder Txs

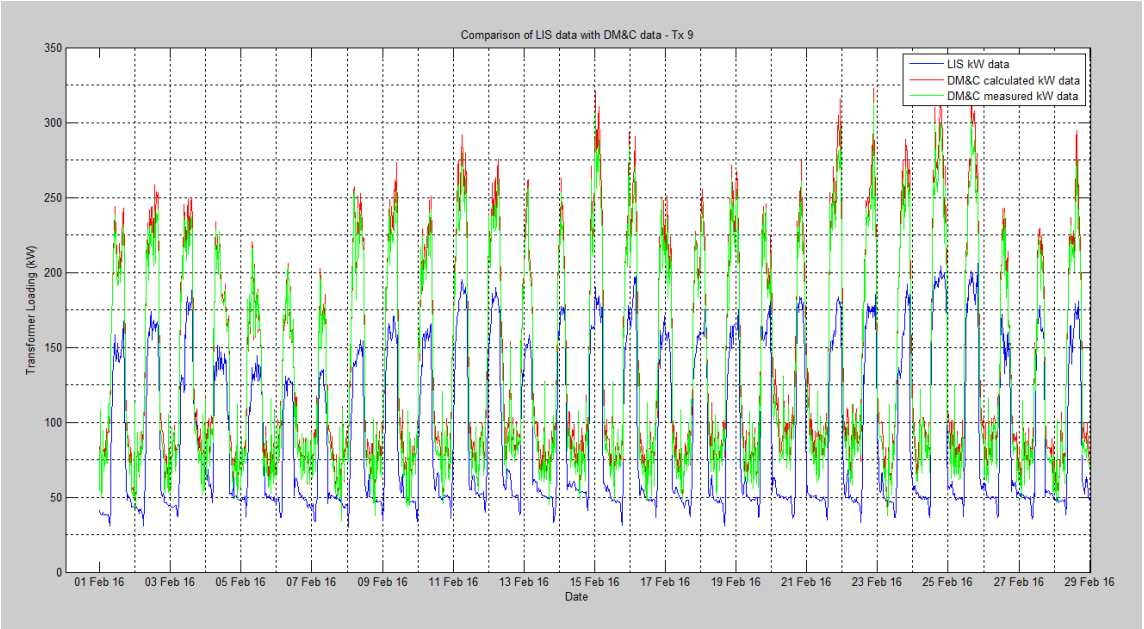

Figure 22: Comparison of LIS kW data with DM&C kW data – Tx9

The LIS data for this Tx could not be used as the loading for the Tx in the power flow model. In this case only the measured P data from the DM&C measurement unit was used. All other LIS/ DM&C comparisons, found in Appendix C, verify the LIS data to be accurate.
It was assumed that LIS data for all other Txs on the feeder was also accurate.

5.3.2.2 Model Validation

Power flow modelling is based on several variables. As discussed earlier, when the model has only one generation point, located at the slack or zone bus, and all other buses on the model are PQ fixed power buses, there are 4 variables that the conventional model uses, 2 known and 2 unknown which are the values that it solves for:

1. Load P – PQ bus known, slack bus unknown;
2. Load Q – PQ bus known, slack bus unknown;
3. Voltage magnitude – PQ bus unknown, slack bus known;
4. Voltage angle – PQ bus unknown, slack bus known.

In the case of the power flow model that was constructed, the ASPEN software also solved for:

5. Current magnitude – PQ bus unknown, slack bus unknown;
6. Current angle – PQ bus unknown, slack bus unknown.

When PV EG is added at the PQ load buses the following quantities are also known:

7. PV EG P – PQ bus known;
8. PV EG Q – PQ bus known.

For a standard PV EG connection, the inverter is at unity pf so the Q magnitude is zero.

There is no in-situ monitoring equipment that measures phase angle in real time so the viability of manually obtaining the voltage and current phase angles at the Txs and zone substation was investigated.

The Fluke 435 Power Quality Analyser was connected to the control panel of the zone substation bus that was used as the model slack bus and the voltage and current phase angles taken. The results of the current magnitudes and angles can be seen in figure 23 on the next page.

It took considerable time to take the necessary precautions, physically connect the instrument and take the measurements. Since this same process would have to be repeated at all 8 measurement points around the feeder, the time between measurements would likely see a significant change in loading not only on the Tx it was being connected to, but also at the zone bus which would be the reference point for all other readings.

For this reason manually obtaining the phase angles was found to be unviable with the measuring instrument that was available.

For the purposes of this project, the phase angle measurements not being available did not impact the results, or the ability to validate the model. For this reason, the values of the PQ buses voltage magnitude and PQ buses current magnitude, as well as slack bus current magnitude were the quantities used for comparison between the results provided by the model and the actual measurements taken around the feeder itself.

Figure 23: Fluke 435 Power Quality Analyser – zone bus phase currents

The model was run and the results were compared to the measured data obtained from the zone substation and the DM&C units on individual Txs.

Table 3 below contains the comparison between the model results and the measured data.

Reference	Voltage (V)			Current (A)		
	Measured	Model	% Difference	Measured	Model	% Difference
Tx 8	11088	11140	0.46897547	18.6	18.8	1.075268
Tx 9	11132	11140	0.07186489	9.7	9.75	0.515463
Tx 17	11088	11140	0.46897547	0.2	0.177	11.5
Tx 18	11044	11140	0.86925027	0.6	0.648	8
Tx 19	11176	11140	0.32211883	1.4	1.35	3.571428
Tx 20	11239	11150	0.7918854	1.2	1.2	0
Tx 23	11132	11140	0.07186489	0.2	0.151	24.5
Zone	11265	11265	0	97.6	100	2.459016

Table 3: Comparison of measured values and model values - initial

The results in the table above demonstrate that the voltages predicted by the power flow model when compared to those that were actually measured at the corresponding equipment present an error of less than 1% on all occasions. There was no variation between the feeder voltage of the model and that measured at the zone substation as the voltage is fixed at that point.
The errors between the predicted currents at these points compared to the measured currents were found to be much larger. On investigation, it was found that the PI DataLink used to obtain the measured figures rounded to one decimal place. Where the currents were larger, this did not pose a significant change, but on the lightly loaded Txs this caused large variation in the results.
The raw data for the measurements was sourced from a program called ION that allows historical and live raw network data to be accessed. The revised raw data figures are shown in table 4 below. Only current readings were altered, as decimal place changes to the voltage level caused no change.

Reference	Voltage (V)			Current (A)		
pf = 0.95	Measured	Model	% Difference	Measured	Model	% Difference
Tx 8	11088	11140	0.46897547	18.619	18.8	0.972125
Tx 9	11132	11140	0.07186489	9.731	9.75	0.195252
Tx 17	11088	11140	0.46897547	0.177	0.177	0
Tx 18	11044	11140	0.86925027	0.642	0.648	0.934579
Tx 19	11176	11140	0.32211883	1.362	1.35	0.881057
Tx 20	11239	11150	0.7918854	1.189	1.2	0.925147
Tx 23	11132	11140	0.07186489	0.150	0.151	0.666667
Feeder	11265	11265	0	97.625	100	2.432778

Table 4: Comparison of measured values and model values - revised

As can be seen from the revised current figures in table 4 above, when the actual measured current data was used, effectively removing the errors caused by rounding the raw data, all errors found on comparison of predicted model currents with the actual measured currents were less than 1% which was consistent with the voltage errors. The only point where this was not the case was the total feeder load, which had an error of 2.433%.
This can be accounted for by the slight inaccuracies that exist within the LIS data for the Txs that did not have 100% interval metering data available.
From the results presented in table 4 above, the power flow model was verified as an accurate representation of the actual physical feeder it was modelled on, and could be used to investigate the effects of increasing levels of PV EG on the feeder.

5.3.2.3 Sensitivity Analysis

This section demonstrates how change in power factor of the feeder effected the validation of the model.

The feeder was modelled with 3 power factors 0.9, 0.92, 0.95. The results for pf = 0.95 are shown in table 4 on the previous page.

Reference	Voltage (V)			Current (A)		
pf = 0.92	Measured	Model	% Difference	Measured	Model	% Difference
Tx 8	11088	11130	0.37878788	18.619	19.3	3.657554
Tx 9	11132	11130	0.01796622	9.731	10	2.764361
Tx 17	11088	11130	0.37878788	0.177	0.181	2.259887
Tx 18	11044	11130	0.77870337	0.642	0.664	3.426791
Tx 19	11176	11130	0.41159628	1.362	1.39	2.0558
Tx 20	11239	11140	0.88086129	1.189	1.22	2.607233
Tx 23	11132	11130	0.01796622	0.150	0.155	3.333333
Zone	11265	11265	0	97.625	102	4.481434

Table 5: Comparison of measured values and model values at pf = 0.92

Whilst all but one of the voltage errors reduced slightly in magnitude, all the current errors increased significantly with the power factor change from 0.95 to 0.92.

Reference	Voltage (V)			Current (A)		
pf = 0.90	Measured	Model	% Difference	Measured	Model	% Difference
Tx 8	11088	11120	0.2886	18.619	19.7	5.805897
Tx 9	11132	11120	0.107797	9.731	10.21	4.922413
Tx 17	11088	11120	0.2886	0.177	0.185	4.519774
Tx 18	11044	11120	0.688156	0.642	0.679	5.76324
Tx 19	11176	11120	0.501074	1.362	1.42	4.258443
Tx 20	11239	11130	0.969837	1.189	1.25	5.130362
Tx 23	11132	11120	0.107797	0.150	0.158	5.333333
Zone	11265	11265	0	97.625	104	6.53009

Table 6: Comparison of measured values and model values at pf = 0.90

In changing the power factor from 0.92 to 0.90, most of the voltage errors increased, some significantly. Again, all of the current errors increased significantly.

On examination of these results, it was decided to use a common power factor of 0.95 as it gave the lowest error factors when considering both voltage and current magnitudes of the model compared with those that were actually measured at the Txs themselves.

5.3.2.4 Introducing Additional PV EG to the Power Flow Model

Once the model was verified to be an accurate representation of the actual feeder, additional PV EG was introduced to investigate the effects on feeder load, power flow and voltage rise.
This involved the following steps:

a. Determine the total existing PV EG capacity connected to each Tx;
b. Introduce additional PV EG to each Tx consistent with the AEMO predicted increase outlined in section 2.2.2, figure 5;
c. Investigate effects on power flow around the feeder at this level of additional PV EG;
d. Investigate effects on voltage rise around the feeder at this level of additional PV EG;
e. Determine the required increase in PV EG where the grid begins to generate back into the zone substation;
f. Investigate effects on power flow around the feeder at this level of additional PV EG;
g. Investigate effects on voltage rise around the feeder at this level of additional PV EG;
h. Increase the PV EG to twice the level predicted by AEMO;
i. Investigate effects on power flow around the feeder at this level of additional PV EG;
j. Investigate effects in voltage rise around the feeder at this level of additional PV EG;
k. Investigate effects of a tap change at zone bus on voltage rise around the feeder at this level of additional PV EG;
l. Investigate voltage rise on LV side of DM&C Txs.

5.3.2.4.a Determining the Total Existing PV EG Capacity Connected to Each Tx

Before EG can be connected to the grid an application for connection must first be submitted to the relevant distributor. When notification has been received that the EG, in the case of this project PV EG, has been installed, metered and connected to the network, the size and type of connection (net or gross) is recorded against the NMI number for that installation.
A report of every individual NMI, on this feeder was run to determine the current level of connected PV EG on every Tx on the feeder.
As stated previously, since the Tx load P and Q values were based on LIS customer metering data, this current level of PV EG was accounted for in the loading of the existing feeder model.

5.3.2.4.b Introducing Additional PV EG to Each Tx Consistent With the AEMO Predicted Increase

After the current levels of PV EG for each Tx on the feeder had been determined, a PV EG was added to every Tx on the feeder[16], with the real power values of the generators those determined by multiplying each Txs current connected PV EG capacity by 2.25[17]. This multiplier was chosen to align the increase in the models PV EG with the AEMO predicted increase in rooftop PV EG over the next 10 years to 2025.

The Q value for each added PV EG was set to zero, as all existing inverters have a unity pf.

There were 3 stages of PV EG increase:

1. 1 x AEMO predicted increase;
2. 1.48 x AEMO predicted increase – the point where reverse power flow into the zone substation was found to occur;
3. 2 x AEMO predicted increase.

The effects of these increases on both power flow and voltage rise will now be considered at each stage.

5.3.2.4.c Investigating Effects on Power Flow at 1 x AEMO Predicted Additional PV EG on the Feeder

The additional PV EGs were added to the model, it was solved again and the effects of the generators on PF were observed[18].

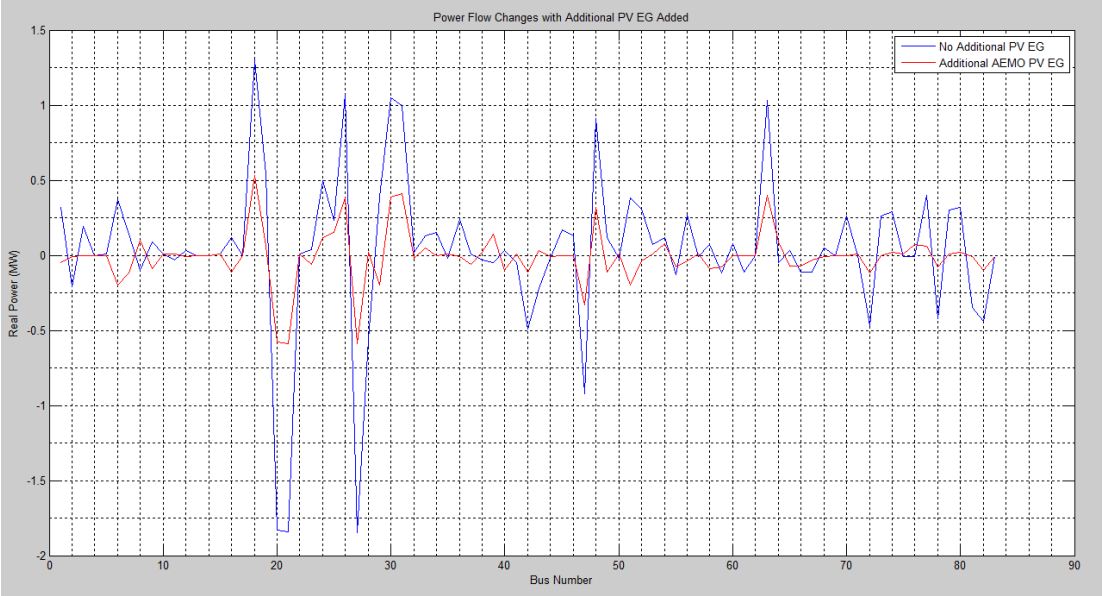

Figure 24: Changes in power flow at all buses with addition of PV EG – 1 x AEMO predicted increase

[16] Refer Appendix E2 for power flow model 1-Line diagram – additional PV EG shown 'in service'
[17] Refer Appendix F for existing and future levels of PV EG
[18] Refer Appendix D13 for Matlab code for all power flow comparisons

The figure on the previous page demonstrates the changes in power flow of the feeder when 1 x the AEMO predicted increase in PV EG was added to it. The blue plot was the power flow of real power only on the feeder in its existing state. The red plot was the power flow when the generators were added.

It can be seen that, for the most part, with the addition of this level of PV EG that the power flow at individual buses was in the same direction, though the magnitude greatly decreased.

5.3.2.4.d Investigating Effects on Voltage Rise at 1 x AEMO Predicted Additional PV EG on the Feeder

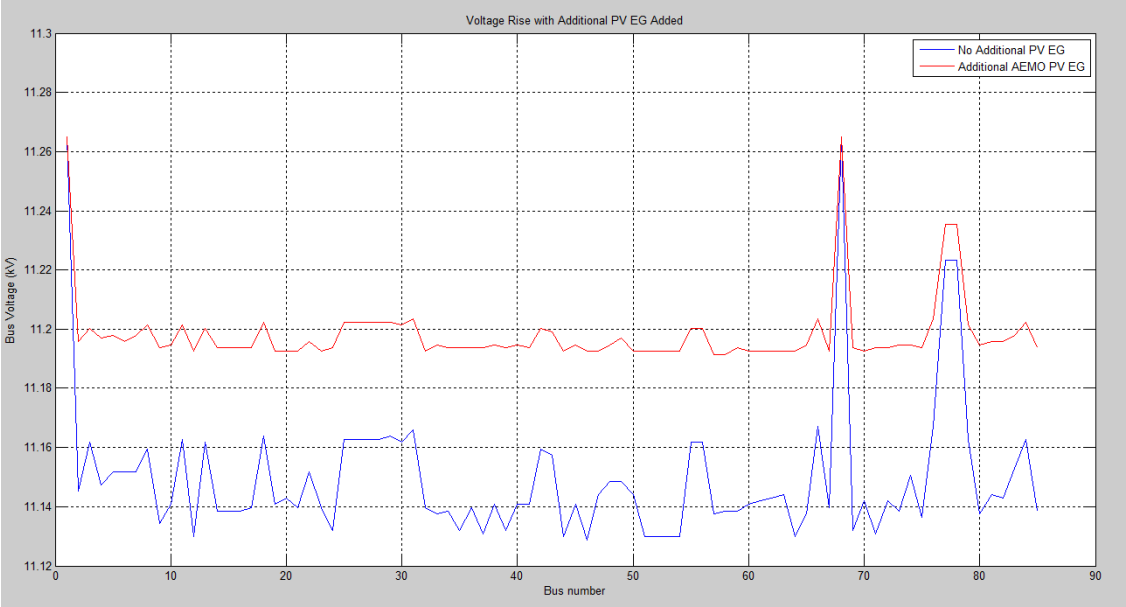

Figure 25: Changes in voltage rise at all buses with addition of PV EG – 1 x AEMO predicted increase[19]

It can be seen from figure 25 above that there are several points on the graph where the voltage 'spikes'. The one on the far left is the zone substation slack bus which is a fixed voltage bus, regulated by the on load tap changer (OLTC) at the zone substation. The second point on the figure located at bus 68, is the circuit breaker in the zone substation which protects the feeder. The third and fourth points located at buses 77 and 78, are the first two Tx buses on the feeder, which are close to the zone substation. The remainder of the buses are distributed around the feeder.

The results shown in figure 25 demonstrate that with the exception of these 4 points, there was significant voltage rise at every bus on the feeder. In the case of 1 x AEMO predicted increase in PV EG, this did not cause an adverse voltage rise effect, but actually served to provide a more even voltage distribution around the feeder.

[19] Refer Appendix D14 for Matlab code for all voltage rise comparisons

5.3.2.4.e Determining the Required Increase in PV EG for Reverse Real Power Flow Back into the Zone Substation

As could be seen from figure 24 on the previous page, the addition of 1 x AEMO predicted increase in PV EG was not sufficient in the case of this particular feeder to reverse the power flow to such an extent that the grid would begin to generate back into the zone substation. To determine the level of additional PV EG that would be needed for this to occur, the capacity of the generators were increased incrementally in steps of 0.1 x the AEMO predicted increase, from 1 x AEMO up to 2 x AEMO.

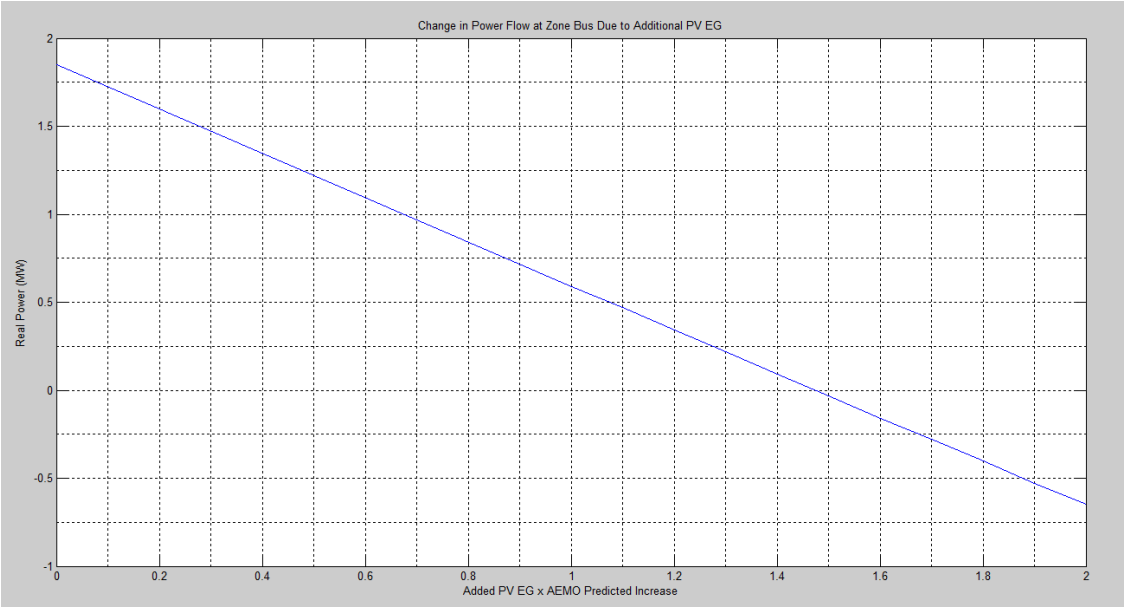

Figure 26: Change in power flow at zone bus[20]

As can be seen in figure 26 above, since all generators have been scaled equally, the change in power flow magnitude is linear. The point where the grid begins to generate back into the zone substation is at approximately 1.48 x the AEMO predicted increase. If 1 x AEMO increase is predicted to occur in 10 years, then it would be expected that this feeder would begin to generate back into the zone substation that supplies it in approximately 14 years. This is assuming that there are no other influences in the intervening period to increase the level of PV EG such as another government incentive to encourage consumers to install PV EG similar to the SBS that occurred in 2010/ 2011. The table on the next page contains the AEMO predicted increase multiplier and the resultant changes in power flow at the zone substation bus.

[20] Refer Appendix D15 for Matlab code

AEMO Predicted Increase	Power Flow at Zone Substation Bus	
Multiplier	Magnitude (MW)	Direction
0 (No additional PV EG)	+ 1.85	Out of Zone into Grid
1.0	+ 0.59	Out of Zone into Grid
1.1	+ 0.47	Out of Zone into Grid
1.2	+ 0.34	Out of Zone into Grid
1.3	+ 0.22	Out of Zone into Grid
1.4	+ 0.09	Out of Zone into Grid
1.5	- 0.03	From Grid Into Zone
1.6	- 0.16	From Grid Into Zone
1.7	- 0.28	From Grid Into Zone
1.8	- 0.4	From Grid Into Zone
1.9	- 0.53	From Grid Into Zone
2.0	- 0.65	From Grid Into Zone

Table 7: Power flow at zone substation slack bus

5.3.2.4.f Investigating Effects on Power Flow at 1.48 x AEMO Predicted Additional PV EG on the Feeder

It was determined in the previous section, that when the AEMO predicted increase in PV EG was multiplied by 1.48 the grid would begin to generate back into the zone substation. Figure 26 showed the changes in power flow at the zone bus. Figure 27 below shows the changes in power flow at all the buses around the feeder at this point.

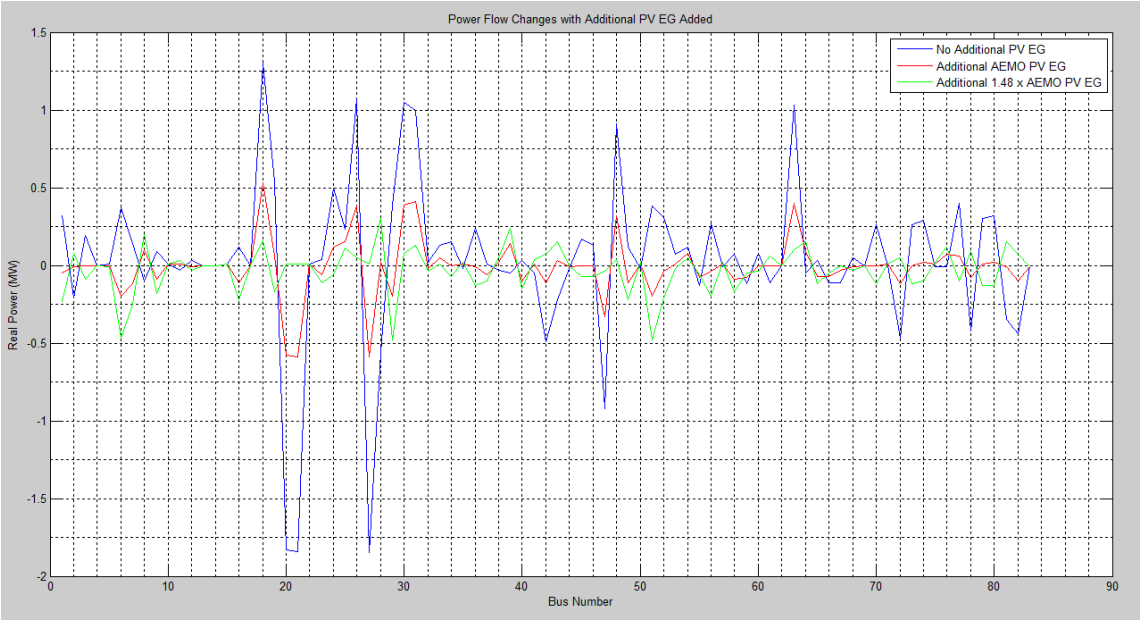

Figure 27 : Changes in power flow at all buses with addition of PV EG – 1.48 x AEMO predicted increase

It can be seen in figure 27 on the previous page, that at 1.48 x the predicted AEMO increase in PV EG, most buses around the feeder were experiencing power flow opposite to their original direction. Those that had already reversed direction with the 1 x AEMO increase had increased in magnitude. This demonstrated that the changes in power flow direction and magnitude that were experienced at the zone bus were also experienced at the majority of buses around the feeder with this level of additional PV EG.

5.3.2.4.g Investigating Effects on Voltage Rise at 1.48 x AEMO Predicted Additional PV EG on the Feeder

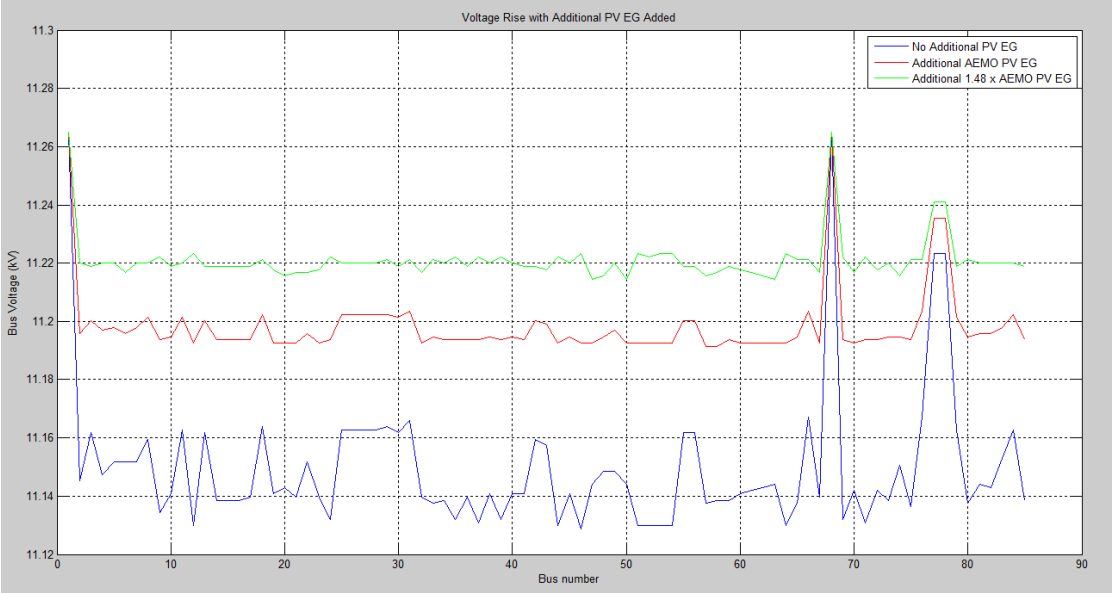

Figure 28: Effect on voltage rise of increase in additional PV EG – 1.48 x AEMO predicted increase

Figure 28 above shows the effects on voltage rise at all buses on the feeder at 1.48 x AEMO predicted increase in PV EG. Again it can be seen that the 4 points at or very close to the zone substation were not significantly impacted.

Again, though this level of PV EG was found to further increase voltage rise, it was not found to have caused a problematic rise in voltage on the feeder, but did in fact even out the voltage distribution around the feeder even further.

5.3.2.4.h Increasing the Additional PV EG to 2 x AEMO Predicted Level

The result of increasing the additional PV EG on the feeder to 2 x AEMO predicted levels was to cause reverse power flow from the grid into the zone substation to a magnitude of approximately 0.65MW. Figure 29 on the next page demonstrates the effects of this increase at all buses around the feeder.

5.3.2.4.i Investigating Effects on Power Flow at 2 x AEMO Predicted Additional PV EG on the Feeder

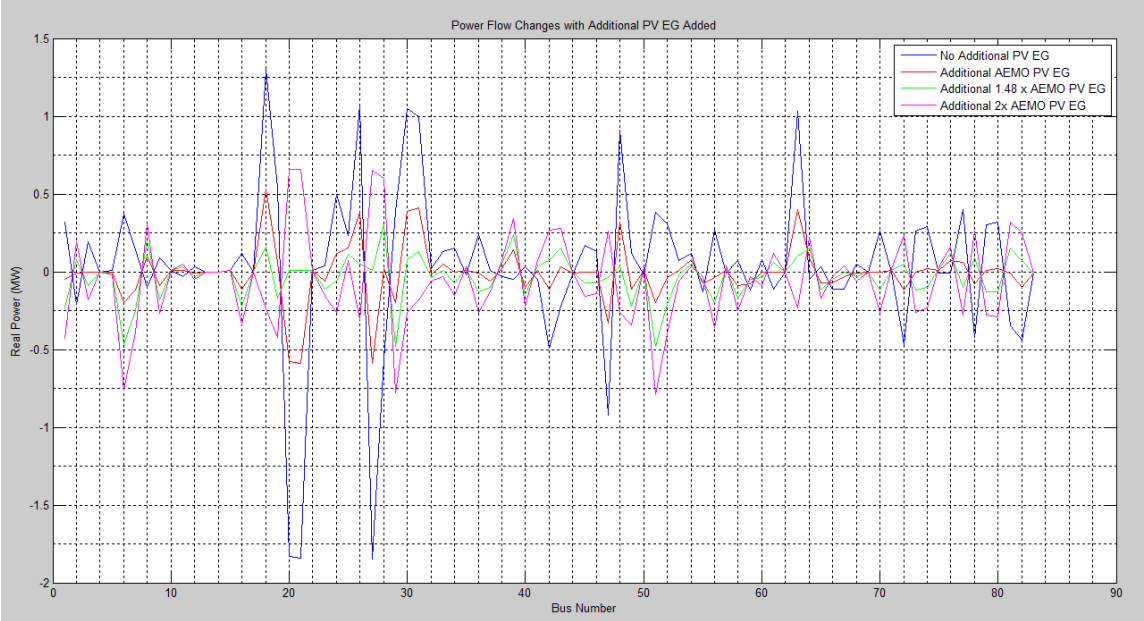

Figure 29: Changes in power flow at all buses with addition of PV EG – 2 x AEMO predicted increase

It can be seen from figure 29 above that any remaining buses that had not yet experienced power flow in the reverse direction to the existing feeder configuration had now experienced reverse power flow. All that had already experienced reverse power flow had increased in magnitude in that direction.

It was determined that at 2 x AEMO predicted increase in PV EG on this feeder, that all buses on the feeder were experiencing reverse power flow.

5.3.2.4.j Investigating Effects on Voltage Rise at 2 x AEMO Predicted Additional PV EG on the Feeder

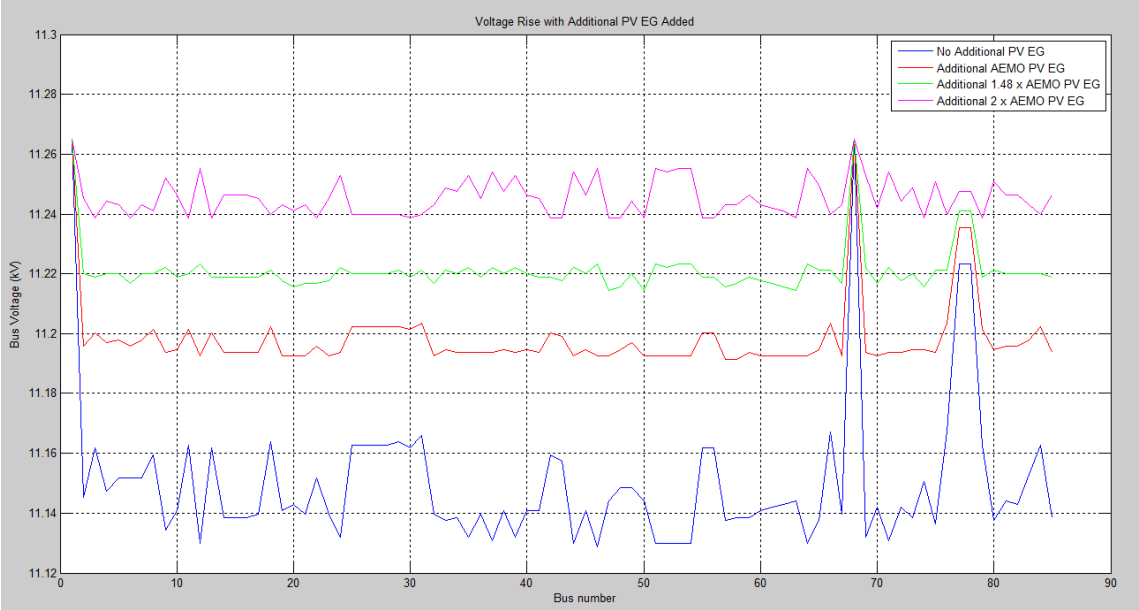

Figure 30: Effect on voltage rise of increase in additional PV EG – 2 x AEMO predicted increase

At 2 x AEMO predicted increase in PV EG all buses were experiencing reverse power flow of some magnitude. It can be seen from figure 30 above, that at this point voltage rise was also becoming exaggerated. Where at previous levels of PV EG the effects on voltage levels were not found to be detrimental and had the effect of evening out the voltage distribution around the feeder, at 2 x AEMO predicted level the voltage increase became more pronounced, with the individual bus voltages beginning to demonstrate increased deviation from each other, and in several cases they had reached the voltage level at the zone bus.

5.3.2.4.k Investigating the Effects of a Tap Change at the Zone Bus on Voltage Rise at 2 x AEMO Predicted Additional PV EG

As the voltage rise around the feeder continues to increase, a tap change at the zone bus may be initiated. This may serve to alleviate voltage rise problems on this feeder, but it must be kept in mind that the same zone bus supplies multiple feeders. If the adjacent feeders do not have elevated voltage levels at this time, a tap change to compensate for the voltage rise on this feeder may negatively impact voltage levels on adjacent feeders.

Figure 31 on the next page demonstrates the effect on the feeder bus voltage levels if a tap change occurred at the zone substation to alter the supply bus voltage from 11.27kV to 11kV.

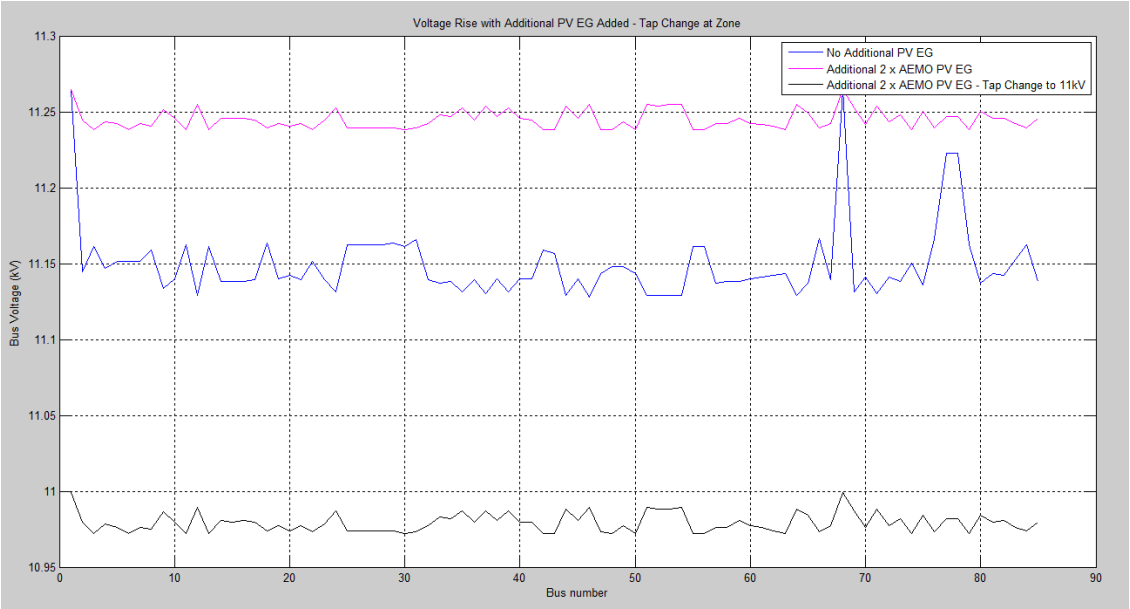

Figure 31: Effects of a tap change on voltage levels of the feeder

The blue plot in Figure 31 above shows the voltage level of the feeder with the existing level of PV EG. The magenta plot shows the voltage level at 2 x AEMO predicted increase in PV EG. The black plot shows the voltage level at this same level of PV EG after a tap change at the zone substation changes the zone bus voltage to 11kV.

While it can be demonstrated from the results shown in figure 31 above that a tap change at the zone substation would effectively decrease the voltage levels at all feeder buses for this level of additional PV EG, as discussed previously, depending on the voltage levels of other feeders also fed from the zone bus, this may not be a viable solution as voltage rise on one feeder cannot be managed in this way if it is to the detriment of adjacent feeders.

A tap change at the distribution Tx level would also not constitute a viable option as all distribution Txs have NLTCs only, which require the Tx to be de-energised before a manual tap change can be carried out.

5.3.2.4.l Investigating Effects on Voltage Rise on LV at 2 x AEMO Predicted Additional PV EG

Voltage rise on the LV side of the 7 Txs with DM&C equipment installed was investigated. The results are shown in the table below for a 2 x AEMO predicted increase of PV EG.

Tx	HV VR (V)	LV VR (V)
8	94.6	2.149936932
9	94.6	2.149936932
17	105.6	2.399929599
18	102.3	2.324931799
19	103.4	2.349931066
20	90.2	1.990232879
23	105.6	2.399929599

Table 8: Voltage Rise at DM&C Txs due to added PV EG

It can be seen from the results in table 8 above, that highest LV voltage rise that resulted was approximately 2.4V, which would not cause significant voltage rise issues.

With the transient nature of a PV array however, if this voltage rise was to occur rapidly and then subside rapidly, this could be sufficient to cause problems with OLTCs. Even though OLTCs operate automatically, the tap change itself is a physical process that can take up to several minutes to complete. If the voltage rise is sufficient to trigger a tap change, the tap changer would not have sufficient time to complete its transition before being required to change back again. This type of increase in the frequency of tap changes would cause considerable wear on the physical components of the OLTC.

.

Chapter 6

6 Solutions to Identified Issues

6.1 Imposing Export Limitations on Installed PV EG

The utilisation of export capacity limitation of PV EG is the most widespread solution to high penetrations of PV EG currently in use.
This constitutes the simplest and most economical solution available to electricity network distributors as it poses no cost to them.
By limiting export capacity it may alleviate forecasting problems as far as PV EG generating back into the grid, but it does not address the issues of decreased demand due to the installations containing the PV EG not importing from the grid.
With emphasis on accommodating increased levels of PV EG, rather than limiting it, this method of decreasing or limiting the effects of PV EG on the electricity distribution network may be the most common and thus far most economical, but it is not the most ideal.

6.2 Introducing a Reactive Power Component to PV EG

All inverters currently used for rooftop PV EG have no reactive power component, with their power factor pre-set to unity, although some manufacturers are now providing small scale inverters with a power factor setting that ranges from 0.9 leading to 0.9 lagging.
Since all loads that are not perfectly resistive have both a real and reactive power component, it follows that the electricity distribution network supplies power that has both a real and reactive component.
When PV EG supplies power with a real component only, it has a different effect on the network than if it supplied both real and reactive power.
Considering the relationships that were discussed in section 5.1:

- $P \; \alpha \; \delta$
- $Q \; \alpha \; |V|$

an increase in the value of P only would have more of an effect on phase angle rather than voltage magnitude, where an increase in Q should have more effect on voltage magnitude. Increase of both together, especially at a power factor closely matching that of the grid, would have the most effect on current magnitude. Since the power factor of the grid is constantly changing with the loads that are connected to it, exactly matching PV EG power factor with the

network would not be possible, though a close approximation to the most commonly experienced power factor may be possible with some inverters incorporating dynamic control of power factor.

There is also the possibility of using PV EG as a reactive power sink rather than a source. From the relationships above, this should have the effect of decreasing voltage magnitude, but could then also have the effect of increasing demand on the grid by further changing the relationship between grid real and reactive power.

The following sections investigate the application of a reactive power component to PV EG first as a source then as a sink.

6.2.1 PV EG as a Reactive Power Source

The following section investigates whether altering the generation characteristics of inverters such that the PV EGs produce a quantity of reactive power may be a solution to the possible issues identified in section 5.

While increasing the value of reactive power at each generator would have no effect on the real power flow around the feeder or at the zone substation, it would have an effect on magnitude and possibly direction of flow of current, as well as voltage magnitude and feeder power factor. The following figures demonstrate the effects on these components when the power factor at each PV EG was altered from pf=1, to pf=0.95, with PV EG set at 2 x AEMO predicted increase.

The results of figures 32 and 33 are indicative of the flow of reactive power, keeping in mind that although reactive power flow is theoretical only, it is indicative of effects on current flow, voltage magnitude and power factor. Knowing how this theoretical flow of reactive power is affected by changes in PV EG is therefore an important step in understanding how the physical components of current and voltage are affected.

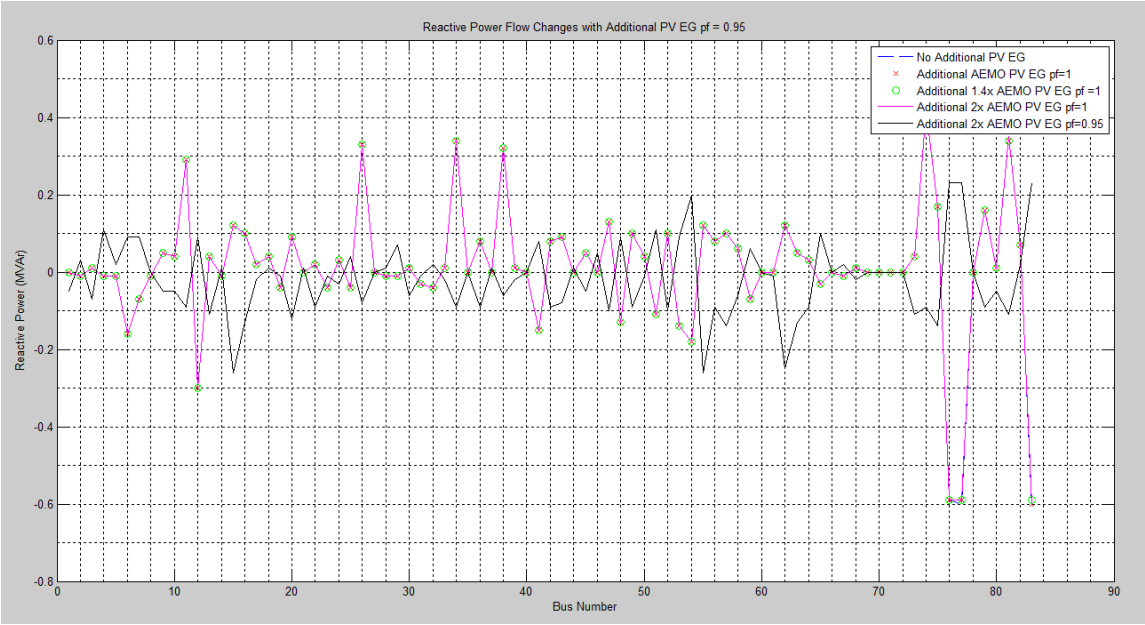

Figure 32: Changes in reactive power flow around the feeder with PV EG pf = 0.95

As expected, there was no change to reactive power flow when PV EG was added with a unity pf. This is demonstrated in the figure above as it shows all reactive power plots for all additional levels of PV EG at unity pf are the same as the plot for no additional PV EG[21].

The black plot in the figure above is the change in reactive power magnitude and flow when PV EG at a pf=0.95 at 2 x AEMO predicted increase is introduced.

As can be seen, this small adjustment in the output of the PV EG has had significant effects on the reactive power flow of the feeder.

The table below shows the effect on reactive power flow at the zone bus for PV EG pf range of 1 to 0.85, again at 2 x AEMO predicted PV EG increase.

Power factor of PV EG	Magnitude of reactive power flow at zone bus (MVAr)	Direction of reactive power flow at zone bus
1	+ 0.6	Out of zone
0.98	+ 0.09	Out of zone
0.95	-0.22	Into zone
0.92	-0.47	Into zone
0.90	-0.61	Into zone
0.88	-0.75	Into zone
0.85	-0.95	Into zone

Table 9: Effects of change in PV EG power factor on reactive power flow at zone bus

[21] Refer Appendix D16 for Matlab code

The figure below shows the difference in reactive power flow at the zone bus for PV EG pf range of 1.0 to 0.85.

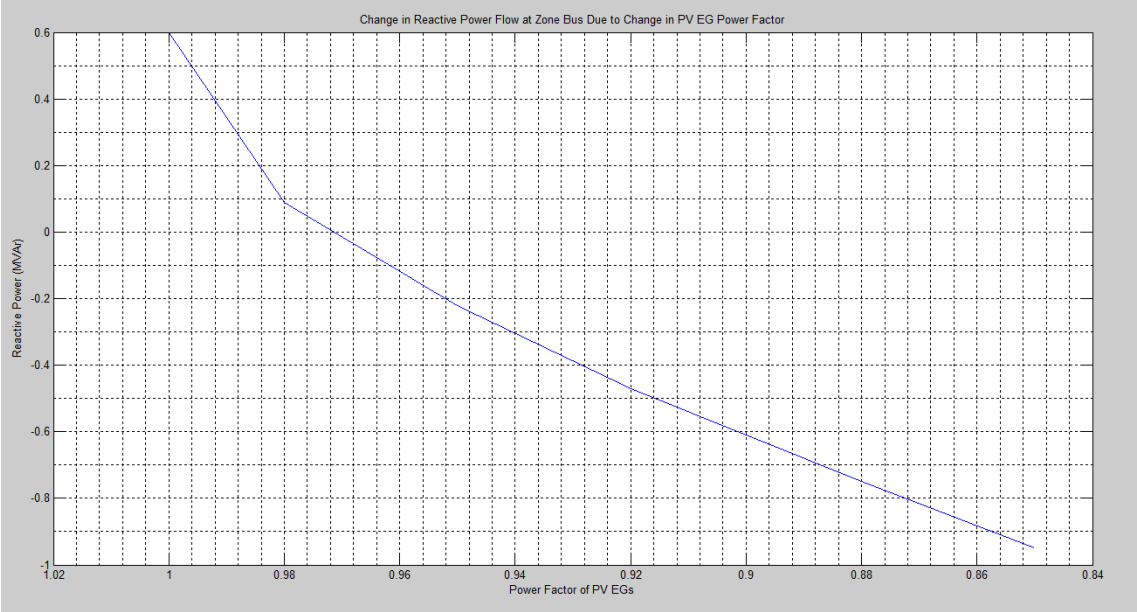

Figure 33: Change in reactive power flow magnitude and direction at zone bus with change in PV EG power factor - source[22]

The results in the figure above demonstrate the effect of PV EG power factor on the reactive power flow of the feeder at the zone bus. It can be seen that a PV EG power factor of only 0.972 the reactive power for this feeder had begun to reverse its flow from the grid back into the zone substation.

The effects of PV EG power factor on current flow at the zone bus are shown in the following tables.

Table 10 below contains the results of at 2 x AEMO increase in PV EG.

Power factor of PV EG (2 x AEMO PV EG)	Magnitude of current flow at zone bus (A)	Direction of current flow at zone bus
1	+ 46.7	Out of zone
0.98	+ 35.5	Out of zone
0.95	- 37.0	Into zone
0.92	- 42.5	Into zone
0.90	- 47.0	Into zone
0.88	- 52.0	Into zone
0.85	- 59.8	Into zone

Table 10: Effects on current flow at zone bus due to PV EG power factor at 2 x AEMO increase

[22] Refer Appendix D17 for Matlab code

From table 10 on the previous page, it can be seen that reverse current flow occurs at a point where PV EG is between 0.98 and 0.95.

In section 5.3.2.4.e, it was found that reverse real power flow into the zone substation occurred at 1.48 x AEMO predicted increase in PV EG. Using this and the power factor range discussed above as a starting point, it was found that the point where current began to flow in reverse from the grid into the zone substation was at 1.45 x AEMO predicted increase in PV EG, with a PV EG power factor of 0.972. At any point beyond this, i.e. pf<0.972 and AEMO increase > 1.45 x, current flow at the zone bus will be in reverse.

These results are shown in table 11 below.

Power factor of PV EG (1.45 x AEMO PV EG)	Magnitude of current flow at zone bus (A)	Direction of current flow at zone bus
1	+ 30.5	Out of zone
0.98	+ 4.38	Out of zone
0.972	- 0.598	Into zone
0.95	- 11.7	Into zone
0.92	- 24.1	Into zone
0.90	- 31.5	Into zone
0.88	- 38.5	Into zone
0.85	- 48.7	Into zone

Table 11: Effects on current flow at zone bus due to PV EG power factor at 1.45 x AEMO increase

The effects of PV EG power factor on feeder current are shown below.

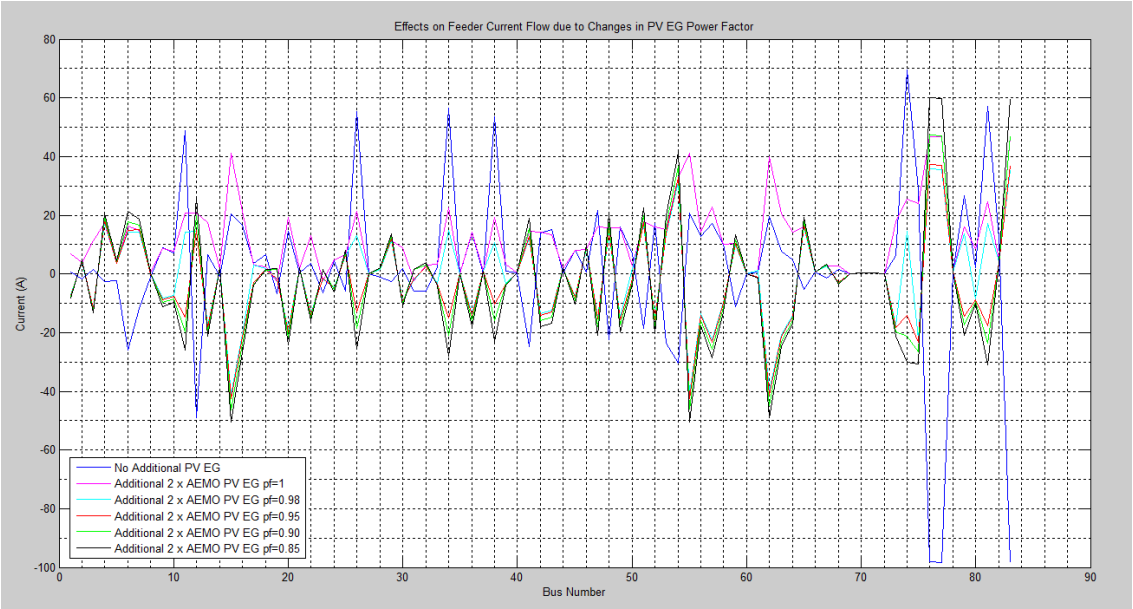

Figure 34: Effects on feeder current flow due to changes in PV EG power factor[23]

It can be seen from figure 34 above that the major effect on feeder current magnitude and flow occurs when the PV EG power factor is changed from unity. The amount the power factor is changed from 0.98 to 0.85, in most cases, did not have a significant effect.

The effects of PV EG power factor on feeder voltage rise are shown below.

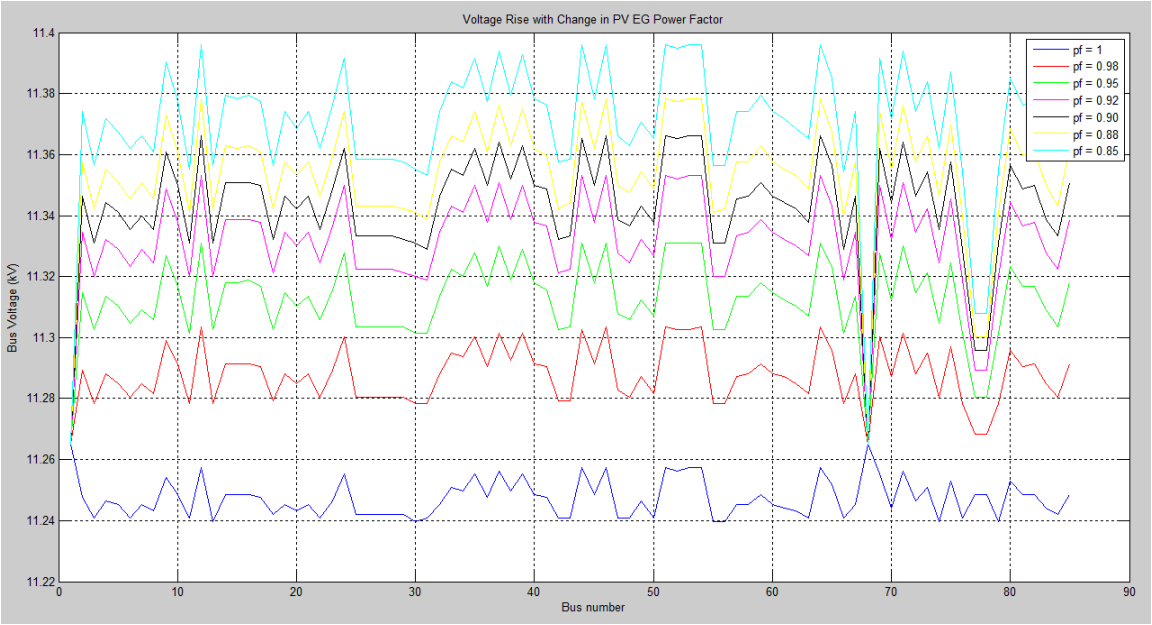

Figure 35: Effect of PV EG as a reactive power source on feeder voltage rise[24]

[23] Refer Appendix D18 for Matlab code
[24] Refer Appendix D19 for Matlab code

As demonstrated in figure 35 on the previous page, changes in PV EG power factor had significant effects on voltage rise of the feeder, with every decrease in power factor causing voltage at every bus to rise above the voltage at the zone bus.
Average bus voltage rise due to change in PV EG power factor is shown in the table below.

PV EG power factor	Average Voltage Rise across feeder (V)
0.98	40.35
0.95	65.06
0.92	84.27
0.9	95.71
0.88	106.4
0.85	122.1

Table 12: Average voltage rise across feeder with change in PV EG power factor

The results in table 12 above demonstrate that as power factor decrease the feeder voltage increases.

The effects of changes in PV EG power factor on the LV side of the network are shown in table 13 below. The first two columns are a reproduction of the LV voltage rise shown in table 8 in section 5.3.2.4.l.

Tx	HV VR (V) PV EG pf = 1	LV VR (V) PV EG pf = 1	HV VR (V) PV EG pf = 0.95	LV VR (V) PV EG pf = 0.95
8	94.6	2.149936932	162.8	3.699891465
9	94.6	2.149936932	162.8	3.699891465
17	105.6	2.399929599	177.1	4.024881932
18	102.3	2.324931799	172.7	3.924884865
19	103.4	2.349931066	173.8	3.949884132
20	90.2	1.990232879	156.2	3.44650084
23	105.6	2.399929599	177.1	4.024881932

Table 13: LV voltage rise at distribution Tx LV terminals with change in PV EG power factor

The results in table 13 above demonstrate that a decrease in PV EG power factor also causes voltage to rise on the LV side of the Txs by an amount approximately 67% greater than PV EG at unity power factor.

As discussed in section 5.3.2.4.k, a tap change at the zone substation may not be a viable solution to voltage rise problems caused by change in PV EG power factor if adjacent feeders are not experiencing similar levels of voltage rise.

6.2.2 PV EG as a Reactive Power Sink

The following section investigates whether altering the generation characteristics of inverters such that the PV EGs sink a quantity of reactive power may be a solution to the possible issues identified in section 5.

The modelling software would not allow a negative value to be entered for Q, so all PV EG Q values were set to zero, with a second load being added at each bus having a Q only component that was equal to that of the PV EG from the previous section.

While effectively modelling the PV EGs as reactive power sinks would have no effect on the real power flow around the feeder or at the zone substation, it would have an effect on magnitude and possibly direction of flow of current, as well as voltage magnitude.

The following figures demonstrate the effects on these components when the power factor at each PV EG was altered from pf=1, to pf=0.95 but acting as a reactive power sink rather than a source. Again PV EG was set at 2 x AEMO predicted increase.

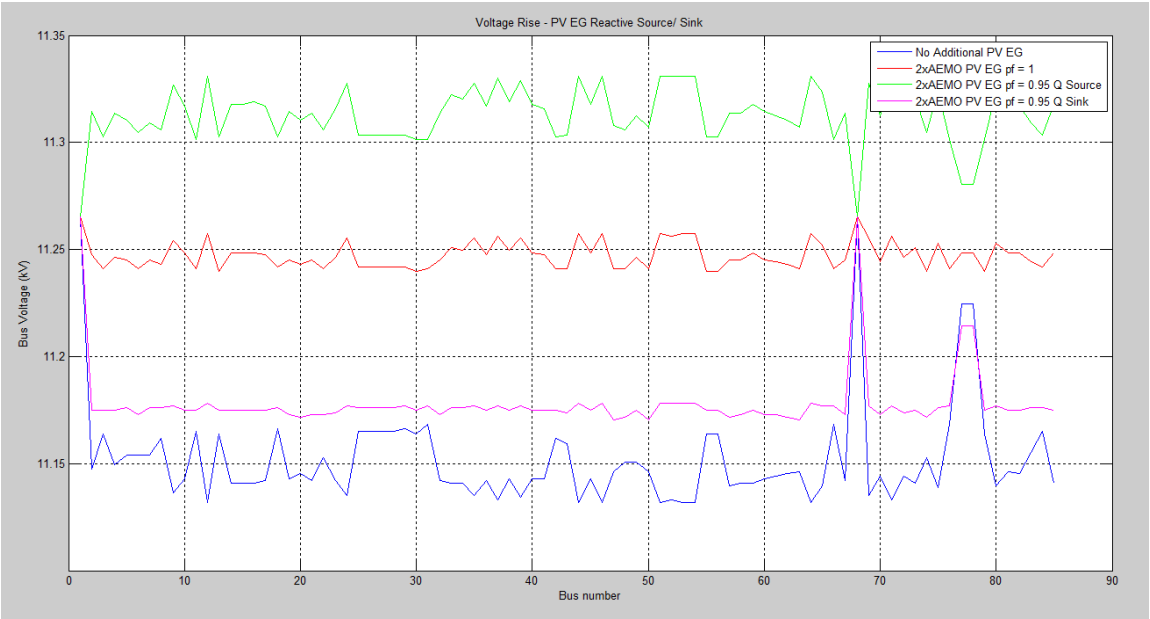

Figure 36: Effect of PV EG as a reactive power sink on feeder voltage rise

The red plot in figure 36 above is the 2xAEMO PV EG increase with the PV EG at unity power factor. The power factor was then changed to 0.95, the green plot when PV EG was used as reactive power source as shown in the previous section, the magenta plot when the PV EG was used as a reactive power sink.

The differences in voltage rise between using the PV EG as a reactive power source or sink are apparent from the graph, the sink decreasing the voltage around the feeder considerably, almost to the level it was prior to any PV EG being added. It also has the beneficial effect of making the voltage around the feeder more uniform.

The figure below demonstrates the effects of PV EG as a reactive power sink on feeder current flow.

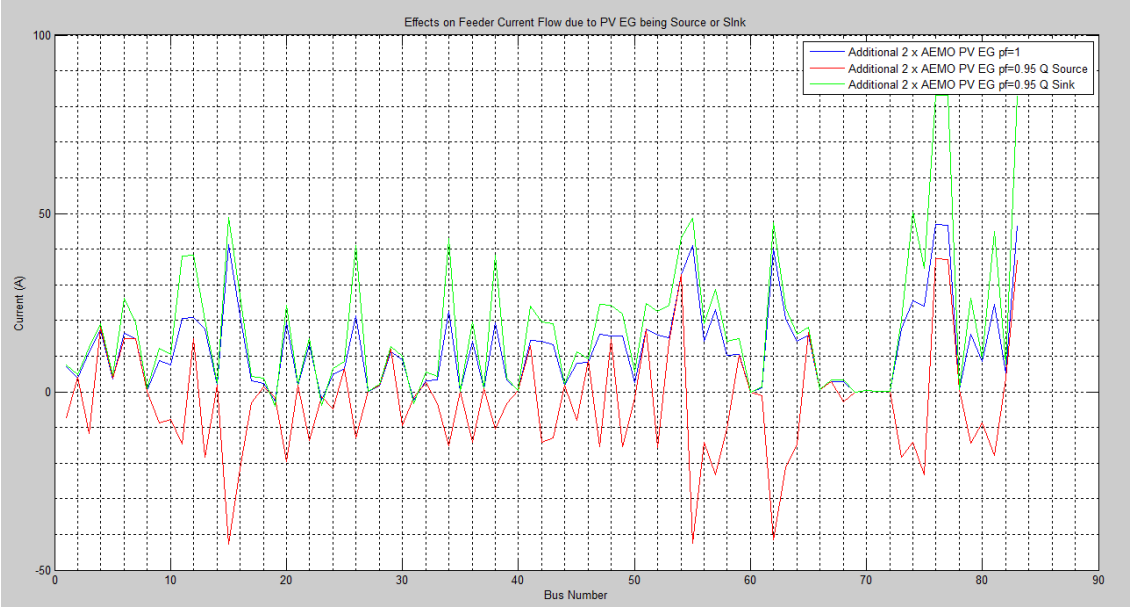

Figure 37: Effects on Feeder Current Flow PV EG as Source/ Sink

As was discussed in the previous section, utilising PV EG as a reactive power source has the potential to reverse current flow from the grid back into the zone substation. That relationship is shown again in figure 37 above, the blue plot representing current magnitude at each bus at an increase in PV EG of 2 x AEMO at unity power factor, the red plot representing current magnitude at the same increase in PV EG but at a pf = 0.95, with the PV EG acting as a reactive power source.

The green plot is the current magnitude around the feeder, again at the same increase in PV EG also at a pf = 0.95, but now acting as a reactive power sink.

It was found in the previous section that when PV EG is used as a reactive power source, it causes not only a decrease in demand, but also a reverse in the direction of current flow.

When PV EG is used as a reactive power sink it causes no reverse in current flow, but actually further increases the load on the feeder.

To further investigate the effects of PV EG as a reactive power sink, the power factor of the PV EG was decreased to 0.90. The effects on feeder voltage rise and feeder current are shown in the following figures.

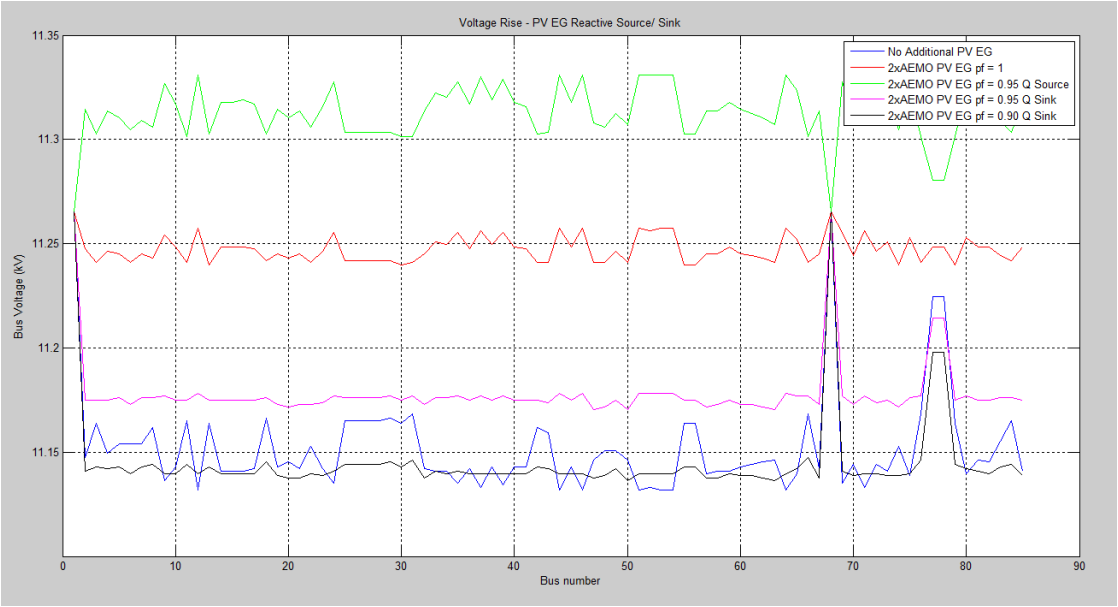

Figure 38: Effect of PV EG as a reactive power sink on feeder voltage rise pf = 0.90

By further reducing the power factor on the PV EG when it is used as a reactive power sink, it can be seen in figure 38 above that the voltage level drops considerably, at most points around the feeder dropping below the voltage level prior to PV EG being added. It also begins to become less uniform again. Where altering the PV EG to become a reactive power sink at pf = 0.95 improved the voltage level, decreasing that power factor to 0.90 has caused adverse effects to the voltage level, causing it to drop too low.

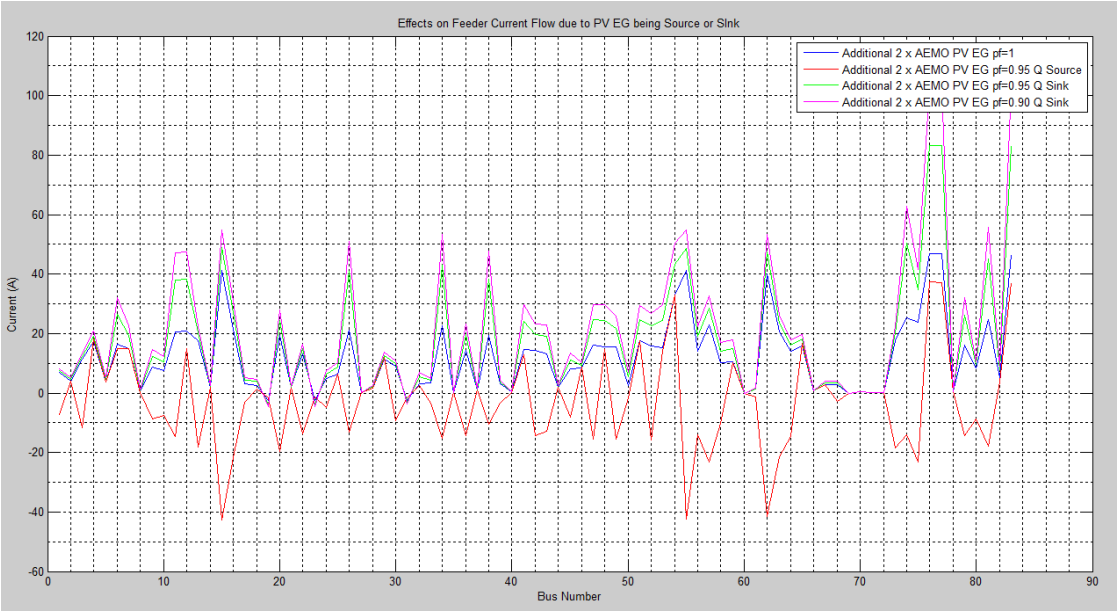

Figure 39: Effects on Feeder Current Flow PV EG as Source/ Sink pf = 0.90

Figure 39 above demonstrates the effects on feeder current of altering the PV EG power factor to 0.90. As can be seen, the magenta plot represents the feeder loading at PV EG pf = 0.90. This decrease in power factor has caused an even greater increase on feeder loading.

With revision of AS/NZS 4777.2 – Grid connection of energy systems via inverters – inverter requirements, allowance for Demand Response Modes (DRM) within PV EG inverters was made.

This allows for the modes shown in the following table to be operational, though currently all but DRM 0 are disabled by default.

Demand Response Modes	
Mode	Requirement
DRM 0	Operate the disconnection device
DRM 1	Do not consume power
DRM 2	Do not consume at more than 50% of rated power
DRM 3	Do not consume at more than 75% of rated power AND Source reactive power if capable
DRM 4	Increase power consumption (subject to the constraints from other active DRMs)
DRM 5	Do not generate power
DRM 6	Do not generate at more than 50% of rated power
DRM 7	Do not generate at more than 75% of rated power AND Sink reactive power if capable
DRM 8	Increase power generation (subject to the constraints from other active DRMs)

Table 14: Demand response modes as allowed by AS/NZS 4777.2 (StandardsAustralia 2015)

From the table above, the standard has allowed for some measure of reactive power to be produced by PV EG, though only under certain conditions.
DRM 7 which specifies PV EG shall not generate at more than 75% of rated power and sink reactive power if capable, supports the results presented in this section that, under certain conditions, PV EG used as a reactive power sink is a viable solution to the issues identified in section 5, particularly voltage rise.
As was demonstrated, the power factor of the PV EG would be required to be set within a very specific range.

6.3 Intentional Islanding

Intentional islanding, or establishing a micro grid, would be a configuration where a section of the network would be intentionally cut off from the bulk of the network when certain conditions occurred, such as reverse power flow.
Currently, it is a requirement of AS/NZS4777 series of standards that PV EG inverters have anti-islanding protection installed, so that on loss of mains (LoM) the inverter would shut down DC to AC power conversion and open off from the grid. This is a safety measure to ensure that the PV EG cannot continue to generate back into the grid under network fault conditions.
If the idea of intentional islanding were to be entertained, there would need to be significant testing and alterations to the current standards to allow islanding under certain conditions.

Besides regulatory requirements, there are certain physical conditions that would need to exist before islanding could occur:

- The load on the micro grid would have to closely match the generation capacity of the PV EG in both real and reactive power requirements;
- Some type of energy storage would be required so as to sustain the loads if the level of PV EG dropped. This would be required to ensure that the system was not trying to disconnect/ reconnect every time a cloud bank passed;
- When the micro grid is disconnected from the bulk of the network, it would lose the frequency and voltage reference provided by the rotating power generators, so a substitute reference would be need to be established to hold voltage and frequency within a certain range;
- There would need to be some agreement between consumers and generators on the micro grid and the network distributor;
- Operating protocols would need to be established to prevent the micro grid from operating if the network is required to be shut down for maintenance, or if the feeder protection operated due to a fault on that part of the network.

6.4 Conclusions

For the immediate future it seems as though imposing export limitations on PV EG will continue to be the main solution used by electricity distributors to deal with network problems caused by increased penetrations of PV EG.

Adding a reactive power component to PV EG has the potential to both cause and alleviate problems. Where PV EG as a reactive power source can cause excessive voltage rise, used as a reactive power sink, with the correct power factor, it can decrease effects of PV EG on voltage rise, though this is at the cost of increasing the loading on the feeder.
Introducing a reactive power component to PV EG could be a potential solution to electricity distribution network issues providing that it is managed correctly.

With current standards, as well as very real safety concerns, it is also unlikely that intentional islanding will present a solution to these problems in the near future.

Chapter 7

7 Suggested Changes to Regulatory Requirements

7.1 Local Electricity Network Distributor Requirements

Currently, any PV EG system exceeding 5kW/ phase is load assessed prior to approval for connection to the network. In order to make connection faster and cheaper for customers seeking to install PV EG, Ausgrid has increased that threshold to 10kW/ phase. This could lead to the case of every 3 phase installation being able to connect a 30kW PV EG without assessment to determine how they may adversely affect the network. This includes rural installations that are potentially supplied by long, high impedance feeders. This would have significant effects on the network with respect to voltage rise and reverse power flow. It could also lead to a situation where the connected PV EG capacity exceeds the reverse power rating of the Tx that supplies the installation.

For example, a common 3 phase rural Tx size is 15kVA. The base current rating of a 3 phase Tx is 1.3x its kVA rating, rating the Tx at only 19.5A/ phase. A 30kW 3 phase PV EG system is rated at approximately 44A/ phase which is twice the current rating of the Tx. For domestic loads, the Tx can be rated to a maximum 1.4x its base rating which would put the Tx at 27.3A/ phase as an absolute maximum. Without first being load assessed, it may be the responsibility of the electricity distributor to replace the Tx with one of a higher rating.

Urban properties may be limited by physical space in installing a 30kW system, but with 300W panels now available, it would only require 100 panels for a 30kW system. It was not uncommon during the SBS for 10kW systems to be installed on urban installations which at the time required approximately 60 x 175W panels to produce 10kW. 60 panels at 300W each would create an 18kW system.

With increases in PV EG causing increases in existing problems as well as causing new ones, it may not be prudent to increase the level of auto approved PV EG connections to 10kW/ phase.

7.2 Australian Standards

In order to allow the possible solution outlined in section 7.3, standards would have to be revised with respect to anti-islanding. Currently PV EG inverters must disconnect from the grid within 2 seconds of sensing LoM. This corresponds with the only mandatory DRM requirement as shown in table 14 above. For intentional islanding to occur, this requirement would need to be revised so that islanding would be allowable under strict conditions as agreed by the electricity distributor.

Chapter 8

8 Conclusions and Further Work

8.1 Conclusions

Current levels of rooftop PV EG have already had significant impacts on feeder loading, both through the decrease in power imported by individual installations they are connected to as well as significant amounts of power generation back onto the grid.
While it could not be proven that any one individual installation had a significant effect on feeder conditions, it was demonstrated that many distributed PV EG systems do.
Through modelling it was also proven to have the potential to cause problems with respect to demand profiling, voltage rise, reverse power flow, and reverse current flow.

Through the same modelling, it was also demonstrated that not all effects of PV EG on the network are negative. As was demonstrated in section 5, at certain levels of PV EG, the power factor of the network can be improved as well as improving the voltage levels at different points around the feeder. Without some amount of energy storage, this cannot be sustained however during evening and early morning peak load times, or at times of low solar exposure.

Reverse power flow was one of the network issues that were identified through the modelling, though this may not constitute the primary concern as it is not likely that reverse power flow would penetrate to the transmission level even if one or more 11kV feeders are generating back into a zone substation, as it is unlikely that all 11 kV feeders would be. So even though loadings on 11kV, 33kV and 66kV feeders may decrease, it is unlikely with the current predicted increases in PV EG levels that reverse power generation would occur past a sub transmission station and back to a network power generator.

Increased difficulty in accurately predicting network load was another problem that was identified. Where contemporary load prediction used historical figures and BoM temperature data, it may come to depend more on daily solar exposure levels, as it was demonstrated in section 4 how much daytime feeder loading can depend on the daily solar exposure levels.
The transient nature of PV EG is also a concern for accurate load predictions. Without some measure of energy storage PV EG is very dependent on weather conditions which causes generation stability issues on days with high cloud cover.

Voltage rise was the primary concern identified by the project.
As voltage rise cannot be controlled at a local distribution Tx level, if not all feeders supplied by a zone bus have a similar level of voltage rise, this is difficult to compensate for at a zone level with OLTCs, as a tap change may be required due to the voltages on one feeder, but not on another adjacent feeder. If a tap change is triggered, then it may lower the problem voltage rise to an acceptable level, but cause the voltage levels on an adjacent feeder to be too low.
This can also be a problem with transient voltage rise that could occur on a cloudy day. PV EG arrays are instantaneous in their response to solar exposure so that voltage and current rise are instantaneous when the panels are exposed to the sun. The same is true for the drop in voltage and current levels when cloud cover obscures the sun from the panels. It takes some time for an OLTC to operate as it is a mechanical operation. This could also cause increased wear on the tap changer components.

As yet there are no ideal methods for electricity network distributors to address the problems that will continue due to the increases in PV EG. The one that is utilised the most at present is simply limiting the amount of power that can be exported from PV EG. Other solutions that were investigated as part of this project included adding a reactive power component to the PV EG and also the possibility of intentional islanding.
While the possibility of a reactive power component within PV EG has been considered to a certain extent as part of the revision of some Australian Standards, and was proven through modelling that under certain conditions it can improve voltage rise effects, it is yet to reach a level that would make it a viable solution to the issues that have been identified as it is not available on existing rooftop PV EG systems, and most ‘domestic’ inverters still have no option to alter power factor.
The possibility of intentional islanding is more problematic as there are significant safety issues that would have to be overcome before this could be a viable solution.

8.2 Further Work

Suggestions for further work following on from this project and on the topic in general are:

- Fault analysis;
- Investigate the possibilities of islanding – both intentional and unintentional;
- Investigate the effects of cloud cover over PV EG arrays on the distribution network.

8.2.1 Fault Analysis

Fault analysis has the potential to be used not only to investigate the possible contributory effects of PV EG to network faults, but also to investigate the possibility of nuisance tripping of overcurrent protection relays in the following manner:

- Introduce PV EG close to origin of feeder to see if it will cause a nuisance trip of the OC protection if at times of low loading it generates a higher current magnitude than the protection relay is looking for – model at lowest daytime feeder loading;
- Introduce PV EG at the end of feeder to see if, under a high impedance fault condition where not enough fault current flows for the OC protection to operate (e.g. a HV cable falls to the ground), PV EG will contribute to fault current;
- Further to the previous point, if PV EG causes voltage rise and the fault is acting like a load, investigate whether it could cause the fault current to decrease even further so that the OC protection is even less likely to operate.

8.2.1.1 Background

There are 4 types of faults that can occur on a distribution feeder:

- 3 phase
- Phase to ground
- Phase to phase
- Phase to phase to ground

The type of fault that produces the lowest fault current and that is possible on all types of distribution feeder is phase to ground, with the probability of ground resistance leading to an even lower prospective fault current, so this would be an ideal type of fault to be investigated.

8.2.1.2 Application to Photovoltaic Embedded Generation

All PV inverters approved for use in Australia have anti-islanding protection built into them. This specifies that the inverter must shut down its AC generation within 2 seconds of mains supply failing. This should theoretically mean that PV EG should have no contributory effect to fault current when a fault occurs and the protection operates. Also, since PV generation is a current limited source, it should have little or no effect on the fault current prior to the protection operating. This may not be the case if there is a level of resistance involved with the fault, for

example a section of overhead line in a rural area that has fallen to the ground or onto a fence. If this does not present a high enough fault current for the protection relay to operate then any surrounding EG will not disconnect from the network and could potentially feed into the fault if the load it is connected to is not sufficient to use all the generation.
In the past it was a common practice to have spur protection/ isolation on long rural feeders in the form of pole top HV fuses that would operate if a high enough fault was detected on the spur line. This would avoid the entire feeder tripping out in the case of a fault at the end of the line. It would also provide a means of allowing the protection relay at the zone substation to be set slightly higher than it otherwise could be. In recent years, when lines are redesigned or replaced, these pole top fuses have not been reinstated.

8.2.1.3 Fault Analysis Model and Adding PV EG

Utilising the modelling techniques outlined in this project, a long rural radial feeder would be ideal to model for fault analysis as it would have the highest line impedance and therefore the lowest phase to earth current.

With addition of PV EG in particular areas the ability of PV EG to cause or contribute to the problems outlined in the following sections could be investigated.

8.2.1.4 Potential for PV EG to Cause Nuisance Tripping of Overcurrent Protection Relays

The fault analysis model could be utilised to investigate the possibility of PV EG causing nuisance tripping of overcurrent protection relays located at the zone substation by generating a higher magnitude of current back into the grid than the pick-up current setting of the relay. This would best be achieved by placing a PV EG system close to the zone substation so there is little line impedance. It would also be more likely to occur during the middle of the day when feeder load is lowest, but PV EG potential is highest.

8.2.1.5 Contribution of PV EG to a Feeder Fault

PV EG is a current limited source, limited by the maximum available output of the PV panels themselves. As such, the likelihood of a PV EG significantly increasing the prospective fault current available at a fault point is low. There is the possibility however, that PV EG can have a different effect on a feeder fault, one that may inhibit the feeder overcurrent protection operating as intended.
As has been demonstrated in the power flow modelling, the addition of PV EG can have

a significant effect on voltage rise on the feeder.

If a feeder fault occurs that constitutes the following conditions:

- High impedance phase to ground fault – this is a common occurrence in the case of a HV feeder cable making contact with the ground or a fence for example;
- Feeder OC protection does not operate as the magnitude of the fault current is not high enough;
- Since the feeder protection has not operated and no loss of mains (LoM) has occurred, PV inverter anti-islanding protection will not operate and PV EG will stay connected to the network;
- In this case, the impedance of the fault then acts like a load, with the generation of the PV EG heading towards the fault. In this manner, connected EG can contribute to a fault. Investigate whether due to the voltage rise effect of the PV EG, the fault now acts like any other load, as voltage rises, current decreases which would further inhibit the overcurrent protection operating;
- This would best be achieved by locating the fault at the end of the feeder furthest from the zone substation and introducing the PV EG so that it is in close proximity to the fault.

8.2.2 Islanding – Unintentional and Intentional

8.2.2.1 Unintentional Islanding

Unintentional islanding is where PV EG fails to disconnect even though a LoM condition has occurred. It could occur as a result of either feeder protection operating in response to a fault on the feeder, or as a result of that section of feeder being isolated for maintenance work by the electricity distributor.
While, with the requirements of current standards AS/NZS 4777 series, it is unlikely an unintentional island would happen, there is the possibility it could occur.
There are very specific conditions however that would need to be met for this condition to occur:

- Closely balanced generation and load conditions;
- Several PV EG units or energy storage systems feeding into each other, so that the inverters would have the perception that there has been no LoM condition.

On long rural feeders there is also the capacitance of the lines that would factor into how closely the load and generation could match, though there is a chance this could be compensated for by the types of loads that are common in these areas, namely large irrigation pumps run by large induction motors.

Unintentional islanding would have the potential to cause problems with frequency drift and voltage shift, though if the frequency or voltage did stray outside certain limits:

- 48 – 52 Hz
- 207 – 267 V

the inverters have internal limitations that would cause them to trip out.
In some instances where it is considered that unintentional islanding may occur, it may then be prudent to decrease these limits so that the inverters operate earlier.

Unintentional islanding poses serious safety risks to distribution workers who believe the network is isolated, and with increasing numbers of both PV EG and energy storage systems it is an important issue to be considered.

8.2.2.2 Intentional Islanding

Intentional islanding, as discussed in section 7.3, constitutes the same result as unintentional islanding, where PV EG does not disconnect when a LoM condition occurs, though as the name suggests, the formation of the micro-grid in this case is intentional.
The same specific conditions mentioned in the previous section would also need to occur for intentional islanding and the establishing of a micro-grid to be possible.
The possibly of frequency drift and voltage shift wold also be present. If attempting to establish a micro-grid it would be necessary to provide an alternative frequency and voltage reference point that would normally be provided by the grid so that the inverters have a reference point to sync to. If energy storage is utilised this may be able to perform this function.
The same frequency and voltage limits as mentioned in the previous section would also apply and possibly be a barrier to the micro-grid successfully forming. In this case it may be necessary for the allowable limits specified in the AS/NZS 4777 series to be increased so that the inverter internal protection does not operate as soon as it would when connected to the grid.

Intentional islanding has the potential to be utilised as a solution to network problems arising as a result of high penetrations of PV EG and would be a very important extension of this project.

Where the modelling carried out as part of this project was steady state, to model whether islanding – intentional or unintentional – was possible the model would have to be dynamic so that the model was a ‘running’ approximation of the network.

8.2.3 Effect of Cloud Cover over PV EG Arrays on the Distribution Network

As discussed previously, the effect of cloud cover on a PV array output is instantaneous with voltage and current levels decreasing instantly when the PV modules are covered by cloud. Whether this happens on a mass level that involves many PV EG sites with large cloud masses, or it occurs on a 'sliding scale' with the same cloud cover travelling quickly over a region, instantaneous voltage and current rise can cause loading problems as well as tap change problems.

To some degree, network augmentation could also become a concern as peak loads at times of little or no PV EG continue to increase, but daytime loads continue to decrease sometimes to the point of reverse power flow.

There is great potential for the investigation into how the effects of 'clouding' of arrays could be lessened.

References

AEMO 2015, *NATIONAL TRANSMISSION NETWORK DEVELOPMENT PLAN* viewed 22/03/2016 <http://www.aemo.com.au/Electricity/Planning/National-Transmission-Network-Development-Plan>.

APVI 2016, *Australian PV Institute (APVI) Solar Map*, viewed 24/5/2016, <pv-map.apvi.org.au>.

Ausgrid 2009, *Connection of Embedded Generators*, Ausgrid.

Ausgrid 2011, *ES11 Requirements for connection of embedded generators*, Ausgrid.

Ausgrid 2013, *NS194 Protection Requirements of Embedded Generators >30kW*.

Ausgrid 2015a, *NIS436 Distribution Planning*.

Ausgrid 2015b, *NIS 418 Embedded Generation*.

Ausgrid to cut fees and fast-track solar and battery applications, 2016, created by Ausgrid, viewed 20/08/16 <http://www.ausgrid.com.au/solarfasttrack>.

Balaguer, IJ, Lei, Q, Yang, S, Supatti, U & Peng, FZ 2011, 'Control for Grid-Connected and Intentional Islanding Operations of Distributed Power Generation', *IEEE Transactions on Industrial Electronics*, vol. 58, no. 1, pp. 147-57.

Bayliss, CR & Hardy, BJ 2012, *Transmission and distribution electrical engineering*, 4th edn, Newnes, Oxford.

Caamaño-Martín, E, Laukamp, H, Jantsch, M, Erge, T, Thornycroft, J, De Moor, H, Cobben, S, Suna, D & Gaiddon, B 2008, 'Interaction between photovoltaic distributed generation and electricity networks', *Progress in Photovoltaics: Research and Applications*, vol. 16, no. 7, pp. 629-43.

CEC 2016, *Renewable Energy Map*, viewed 5/22, <https://www.cleanenergycouncil.org.au/technologies/renewable-energy-map.html>.

Cipcigan, LM & Taylor, PC 2007, 'Investigation of the reverse power flow requirements of high penetrations of small-scale embedded generation', *IET Renewable Power Generation*, vol. 1, no. 3, p. 160.

Eftekharnejad, S, Vittal, V, Heydt, GT, Keel, B & Loehr, J 2013, 'Impact of increased penetration of photovoltaic generation on power systems', *IEEE Transactions on Power Systems*, vol. 28, no. 2, pp. 893-901.

ENA 2015, *The Electricity Network Transformation Roadmap*, viewed 13/05/2016 <http://www.ena.asn.au/sites/default/files/151215_ntr-wp1-iwp2_fgf_refresh_technical_report.pdf>.

ENA, Ca 2015, *Electricity Network Transformation Roadmap: Interim Program Report*, CSIRO and Energy Networks Association(ENA), viewed 13/05/2016 <http://www.ena.asn.au/sites/default/files/roadmap_execsummary_interim_program_report.pdf>.

Horowitz, SH & Phadke, AG 2014, *Power system relaying*, vol. Fourth, John Wiley & Sons Inc, Chichester, West Sussex.

Jenkins, N 2000, *Embedded generation*, vol. no. 31., Institution of Electrical Engineers, London.

Kolenc, M, Papič, I & Blažič, B 2015, 'Assessment of maximum distributed generation penetration levels in low voltage networks using a probabilistic approach', *International Journal of Electrical Power and Energy Systems*, vol. 64, pp. 505-15.

Liu, X, Aichhorn, A, Liu, L & Li, H 2012, 'Coordinated Control of Distributed Energy Storage System With Tap Changer Transformers for Voltage Rise Mitigation Under High Photovoltaic Penetration', *IEEE Transactions on Smart Grid*, vol. 3, no. 2, pp. 897-906.

Namin, MH & Agelidis, VG 2013, 'Voltage sensitivity study of LV/MV networks under high penetration of photovoltaic generation considering residential and industrial load profiles', IEEE, pp. 2309-14.

Nourbakhsh, G, Thomas, B, Mokhtari, G, Ghosh, A & Ledwich, G 2013, 'Distribution tap changer adjustment to improve small-scale embedded generator penetration and mitigate voltage rise', Australasian Committee for Power Engineering (ACPE, pp. 1-5.
Powell, L 2005, *Power system load flow analysis*, McGraw-Hill, New York.
Quezada, VHM, Abbad, JR & Roman, TGS 2006, 'Assessment of energy distribution losses for increasing penetration of distributed generation', *IEEE Transactions on Power Systems*, vol. 21, no. 2, pp. 533-40.
RedbankEnergy 2006, *Redbank*, <http://redbankenergy.com/assets/redbank.aspx>.
REN21 2010, *Renewables 2010 Global Status Report*, Paris: REN21 Secretariat. viewed 23/05/2016 <http://www.ren21.net/Portals/0/documents/activities/gsr/REN21_GSR_2010_full_revised%20Sept2010.pdf>.
REN21 2015, *Renewables 2015 Global Status Report*, Paris: REN21 Secretariat. viewed 24/05/2016 <http://www.ren21.net/status-of-renewables/global-status-report/>.
S&IRNSW 2012, *Service and Installation Rules of New South Wales*.
Simpson, R 2011, Solar Photovoltaics - what effect is this having on the grid?, Internal Ausgrid document, viewed 5/22/16 <http://www.ausgrid.com.au/~/media/Files/About%20Us/Newsroom/Discussions/Solar%20Effect%20on%20the%20Grid.pdf>.
Soroudi, A, Ehsan, M, Caire, R & Hadjsaid, N 2011, 'Possibilistic Evaluation of Distributed Generations Impacts on Distribution Networks', *IEEE Transactions on Power Systems*, vol. 26, no. 4, pp. 2293-301.
StandardsAustralia 2005, *Grid connection of energy systems via inverters*, Part 1: Installation requirements, Standards Australia, Sydney, Australia.
StandardsAustralia 2007, *Wiring Rules*.
StandardsAustralia 2014, *Installation and safety requirements for photovoltaic (PV) arrays*.
StandardsAustralia 2015, *Grid connection of energy systems via inverters*, Part 2: Inverter requirements, Standards Australia, Sydney, Australia.
UNFCCC 2016, *United Nations Framework Convention for Climate Control*, viewed 5/22, <http://unfccc.int/2860.php>.
Vovos, PN, Kiprakis, AE, Wallace, AR & Harrison, GP 2007, 'Centralized and Distributed Voltage Control: Impact on Distributed Generation Penetration', *IEEE Transactions on Power Systems*, vol. 22, no. 1, pp. 476-83.
Zeineldin, HH & Kirtley, JL 2008, 'Islanding operation of inverter based Distributed Generation with static load models', IEEE, pp. 1-6.

Appendix A – Project Specification

ENG4111/4112 Research Project

Project Specification

For: Karen Hourigan

Title: Effect of Private Embedded Generation on Electricity Distribution Networks

Major: Electrical and Electronic Engineering

Supervisors: Associate Professor Tony Ahfock
Dr. Les Bowtell

Enrolment: ENG4111 – EXT S1, 2016
ENG4112 – EXT S2, 2016

Project Aim: To analyse the effect the current level of penetration of private embedded generation has had on electricity distribution networks, and investigate the ongoing effects to networks if this trend in installing private embedded generation continues and their implications for network design reform.

Programme: Issue B, 8th October 2016

1. Research the level of penetration of embedded generation (EG) over a finite period;
2. Investigate specific areas of Ausgrid's network that have higher rates of EG penetration;
3. Examine existing relevant Australian, State and local standards that apply to the connection of EG;
4. Investigate what effect the current level of EG has on electricity distribution networks;
5. Develop a feeder model to see how current levels of EG are affecting the network;
6. Further develop model to see how network will be affected if trend in increase in EG installation continues;
7. Evaluate the configuration of different network designs and how they are affected by EG – changing open points on ring fed feeders compared to radial feeders.

If time and resources permit:

8. Investigate and suggest possibilities for improving local standards for EG connections;
9. Investigate feasibility of isolating the bulk of the grid from areas of high reverse power flow from EG;
10. Investigate possible solutions to any problems identified.

Appendix B - Resource Analysis

The main resources that have been required to achieve the project objectives are:

1. Matlab – owned;

2. ASPEN Powerflow simulation software – software, databases and licence obtained through Ausgrid;

3. ASPEN DistriView simulation software – software, databases and licence obtained through Ausgrid;

4. Advice/ mentoring from Ausgrid staff in the use of ASPEN Powerflow/ DistriView – Senior Engineer Distribution Planning and Senior Engineer Protection;

5. Manual data loggers – Polylogger II instruments and software obtained through Ausgrid;

6. Access to kiosk substations for purposes of manual logging and nameplate data/ tap position and required training – part of current position;

7. Access to Ausgrid distribution network data – line and area managers have approved the use of network data, both present and historical, required to complete the project;

8. Access to embedded generation statistics – generalised data available online. Line manager has approved the use of Ausgrid specific data;

9. Access to Australian, State and distributor specific standards –
    i. Australian Standards (AS) available through either USQ or Ausgrid licences;
    ii. State standards are available online free of charge;
    iii. Most Ausgrid specific standards are freely available to the public online. Any standards that are not will be redacted prior to inclusion in the report if required;

10. Textbooks/ online resources – available through USQ library service;

11. Word and data processing software – data specific software accessed through Ausgrid. All software exported results as .csv files for use in generic software programs such as those available in Microsoft Office 365 which was accessed through USQ licence.

Appendix C – LIS vs DM&C Comparisons

The following figures are the comparisons of LIS data for the Txs on the power flow model feeder that have DM&C capability. They show the deviation of the LIS data from the measured P values as well as the P values that were calculated using the measured phase voltages, currents and an assumed pf.

Refer Appendix D10 for Matlab code used to produce all graphs.

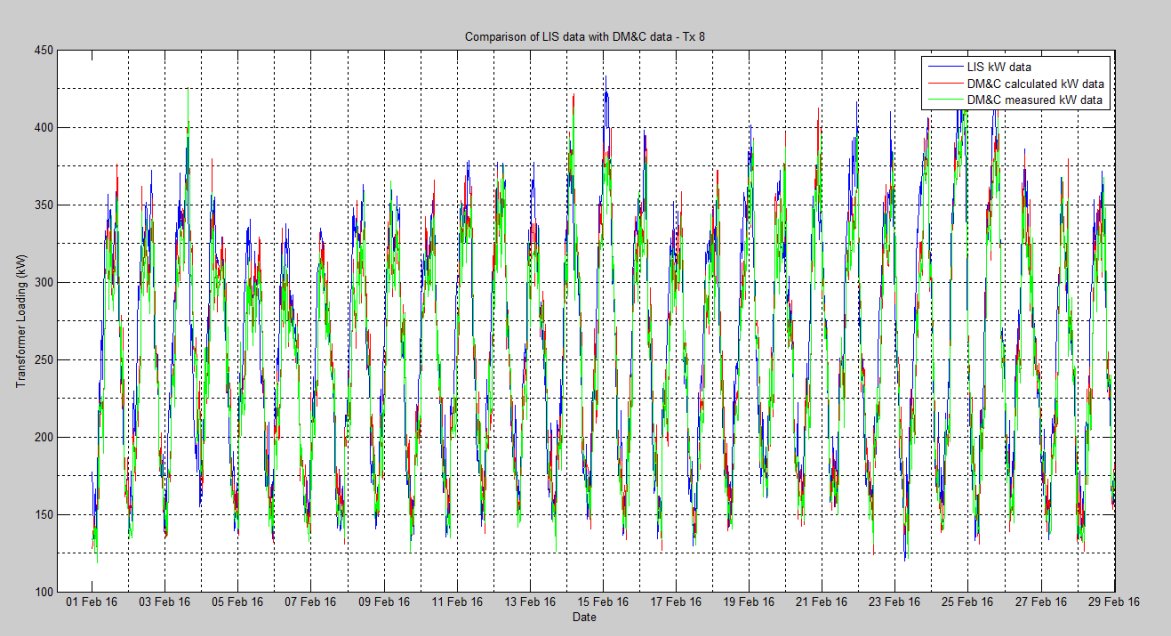

Figure 40: Comparison of LIS kW data with DM&C kW data – Tx8

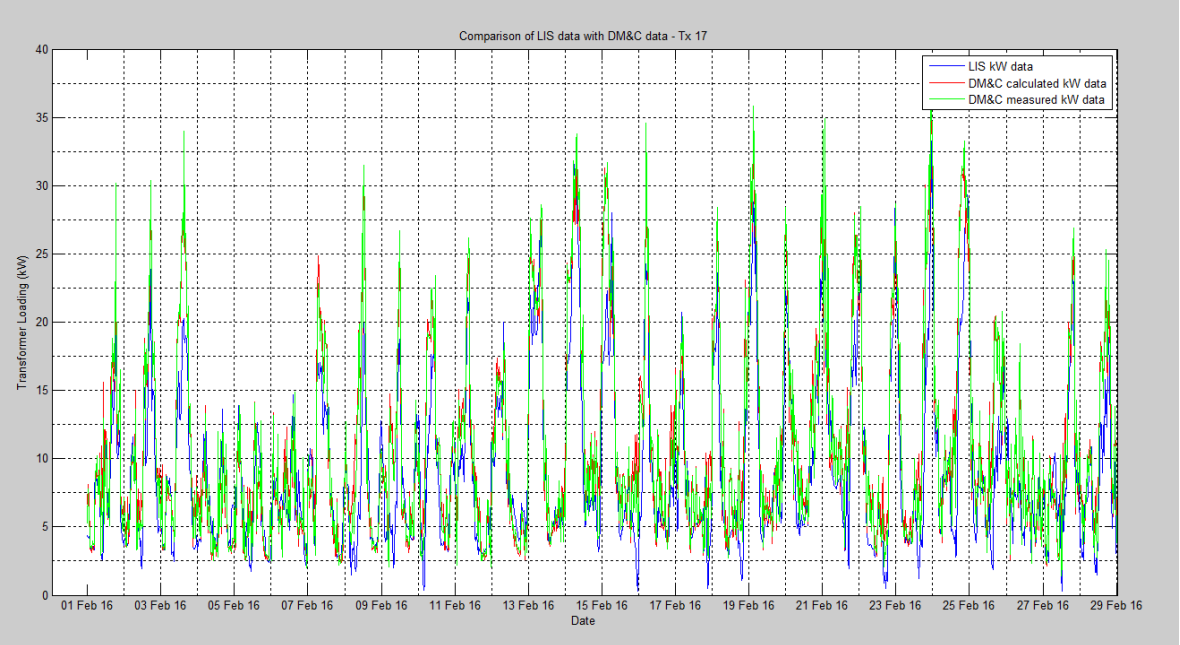

Figure 41: Comparison of LIS kW data with DM&C kW data – Tx17

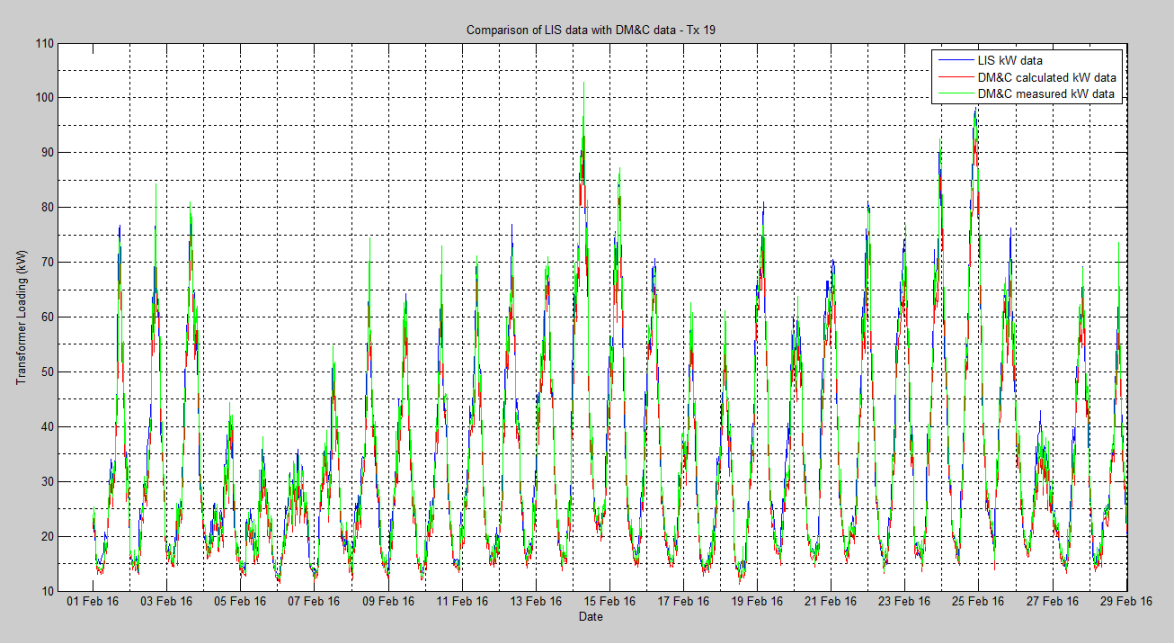

Figure 42: Comparison of LIS kW data with DM&C kW data – Tx19

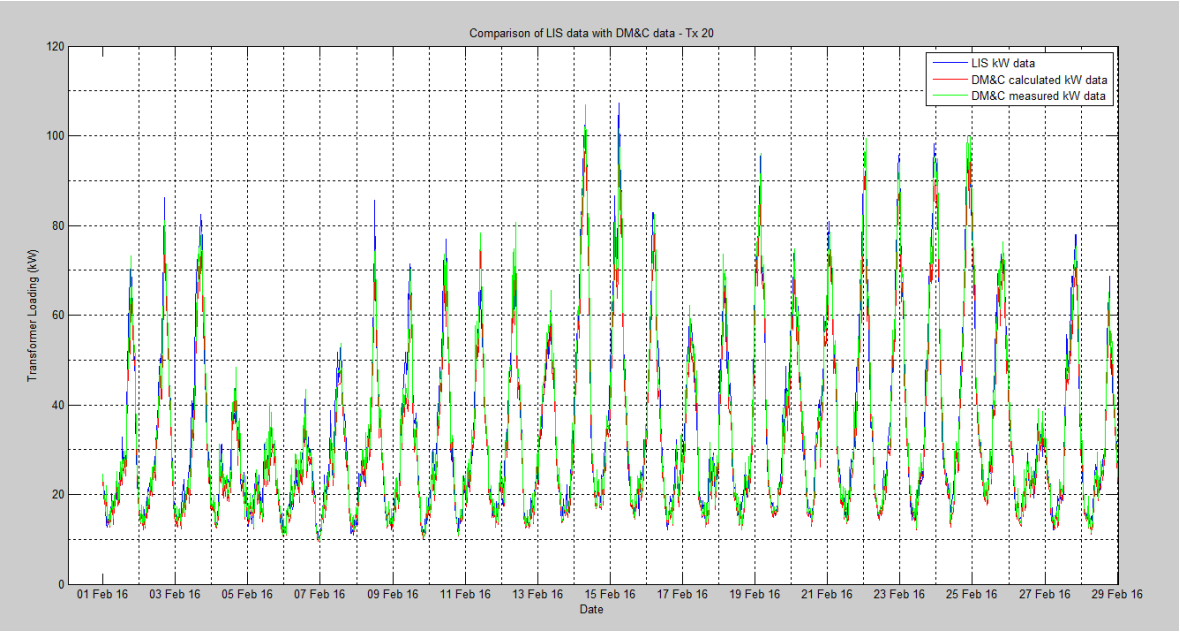

Figure 43: Comparison of LIS kW data with DM&C kW data – Tx20

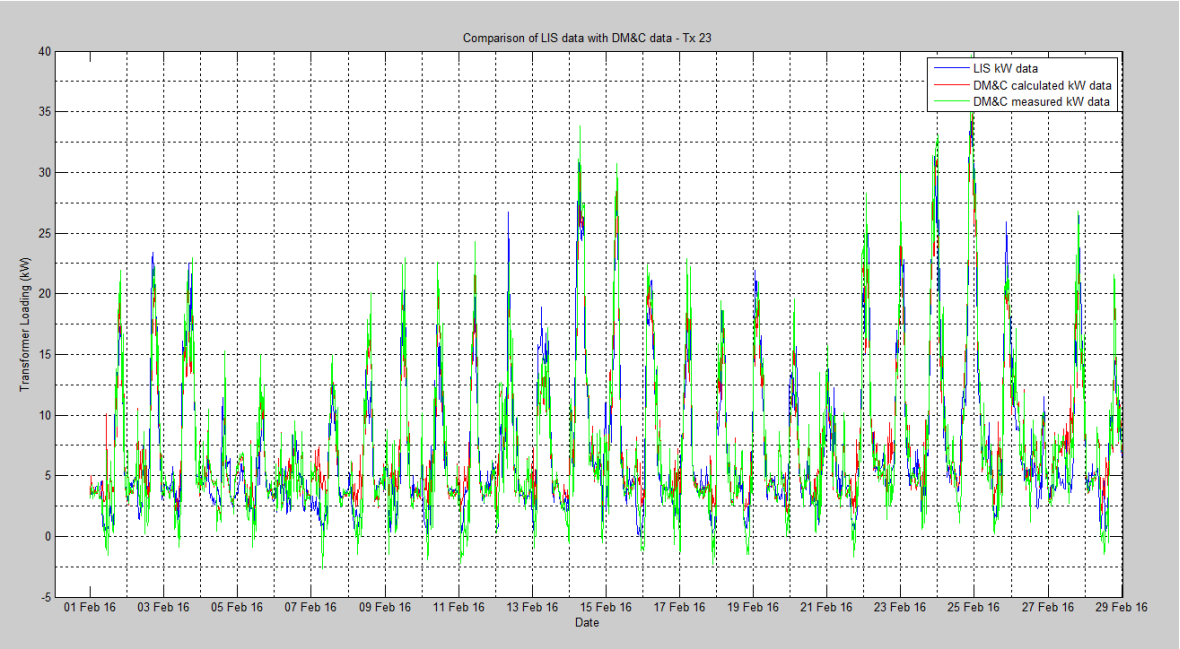

Figure 44: Comparison of LIS kW data with DM&C kW data – Tx23

With the exception of Tx9, shown in figure 22, it can be seen from the preceding figures that the LIS data was consistently accurate when compared to the measured DM&C P data as well as the P values that were calculated using the DM&C measured phase voltage and phase current data, applying an assumed common power factor of 0.95.

Appendix D – Matlab Codes

Appendix D1 – Section 4.2.1 Load Comparison for School
Appendix D2 – Section 4.2.2 Load Comparison for Social Club
Appendix D3 – Section 4.2.3 Load Comparison for Office Building
Appendix D4 – Section 4.3.1 Feeder Comparison for School
Appendix D5 – Section 4.3.2 Feeder Comparison for Social Club
Appendix D6 – Section 4.3.3 Feeder Comparison for Office Building
Appendix D7 – Section 4.4 Change in Load on HV Feeder
Appendix D8 – Section 5.3.1.2 Test Feeder Model Validation
Appendix D9 – Section 5.3.1.4 LIS Dara Allocations
Appendix D10 – Section 5.3.1.5 LIS vs DM&C Data Comparisons
Appendix D11 – Section 5.3.1.6 Tx LIS Loadings
Appendix D12 – Section 5.3.2.1 Tx LIS Loadings for Power Flow Feeder
Appendix D13 – Section 5.3.2.4 Power Flow Comparisons
Appendix D14 – Section 5.3.2.4 Voltage Rise Comparisons
Appendix D15 – Section 5.3.2.4 Change in Power Flow at Zone Bus
Appendix D16 – Section 6.2.1 PV EG Q Source Effect on Feeder Power Flow
Appendix D17 – Section 6.2.1 PV EG Q Source Effect on Zone Bus Power Flow
Appendix D18 – Section 6.2.1 PV EG Q Source Effect on Feeder Current
Appendix D19 – Section 6.2.1 Effect of PV EG Q Source on Feeder Voltage Rise

Appendix D1 – Section 4.2.1 Load Comparison for School

```
% matlab code to import manual logging data for the school
% to use in load profile comparison for before and after the PV EG was
% installed
filename1 = 'school_SOLAR.xlsx'; % excel spreadhseet containing the logging data after PV EG
installation
filename2 = 'school_NO_SOLAR.xlsx'; % excel spreadsheet containing the logging data prior to
PV EG installation
sheet = 1;  %Pick which sheet of the excel spreadsheet that is to be imported
xlsxRange1 = 'D2:L51906';   %Pick all phase current and kW data - solar
xlsxRange2 = 'D2952:I54736';  %Pick all phase current and kW data - non solar
xlsxRange3 = 'C2:C51906';       % read in solar times
xlsxRange4 = 'C2952:C54736';       % read in non solar times
xlsxRange5 = 'B2:B51906';       % read in solar dates
xlsxRange6 = 'B2952:B54736';       % read in non solar dates
xlsxRange7 = 'N2:N51906';       % read in solar timestamp
solar_data=xlsread(filename1, sheet, xlsxRange1);  %Read the excel file for phase current and
power data - solar
nonsolar_data = xlsread(filename2, sheet, xlsxRange2); %Read the excel file for phase current
and power data - non solar
[time_PV,~] = xlsread(filename1, sheet, xlsxRange3); % read in time for solar data
[time_noPV,~] = xlsread(filename2, sheet, xlsxRange4); % read in time for non solar data
[~,date_PV] = xlsread(filename1, sheet, xlsxRange5);  % read in date for solar data
[~,date_noPV] = xlsread(filename2, sheet, xlsxRange6);  % read in date for non solar data
[~,timestamp_PV] = xlsread(filename1, sheet, xlsxRange7); % read in timestamp for solar data
VAS=solar_data(:,1); % voltage Aph solar
VBS=solar_data(:,2); % voltage Bph solar
VCS=solar_data(:,3); % voltage Cph solar
IAS=solar_data(:,4);            % A phase current solar
IBS=solar_data(:,5);            % B phase current solar
ICS=solar_data(:,6);            % C phase current solar
kWAS=solar_data(:,7);           % A phase power solar
kWBS=solar_data(:,8);           % B phase power solar
kWCS=solar_data(:,9);           % C phase power solar
p=length(VAS);

VANS=nonsolar_data(:,1); % voltage Aph non solar
VBNS=nonsolar_data(:,2); % voltage Bph non solar
VCNS=nonsolar_data(:,3); % voltage Cph non solar
IANS=nonsolar_data(:,4); % current Aph non solar
IBNS=nonsolar_data(:,5); % current Bph non solar
ICNS=nonsolar_data(:,6); % current Cph non solar

%%
% when kW reading is zero and voltage and current readings are positive,
% the current flow is actually reverse current flow from the EG back into
% the network. This for loop and if statement section is to convert the
% 'false' positive current readings into negative readings.
for x=1:p
   if kWAS(x)==0
   IAA(x,1)=-IAS(x);
   else
      IAA(x,1)=IAS(x);
   end
      if kWBS(x)==0
   IBB(x,1)=-IBS(x);
   else
      IBB(x,1)=IBS(x);
      end
      if kWCS(x)==0
```

```
    ICC(x,1)=-ICS(x);
    else
        ICC(x,1)=ICS(x);
    end
end
IS_data=[IAA IBB ICC]; % phase currents - solar
IS_data = -1*IS_data; % logging CTs were installed for reverse power flow hence muliplying
factor of -1
INS_data=[IANS IBNS ICNS]; % phase currents - non solar

% sets date for use as date ticks on figure x axis
 t1 = datenum('2016-04-15 11:22:00');
 dt = 30/(24*60*60); % 30 second
 t2 = datestr(t1 + (1:size(IS_data,1))*dt);
 t_PV = datenum(t2);
 t11 = datenum('2008-07-25 11:22:00');
 dt = 30/(24*60*60); % 30 second
 t22 = datestr(t11 + (1:size(INS_data,1))*dt);
 t_noPV = datenum(t22);

% set up subplot to plot both graphs on the same figure
subplot(2,1,1);
plot(t_noPV,INS_data); % plots the non solar load data
grid minor
title('Load Profile/ Usage Comparision - Installation 1 - School');
set(gca, 'XTick', linspace(t_noPV(1),t_noPV(end), 7))
datetick('x', 'dd mmm yy','keepticks');
ylabel('Load (A)');
legend('No PV EG connected');
subplot(2,1,2);
plot(t_PV,IS_data);
grid minor
set(gca, 'XTick', linspace(t_PV(1),t_PV(end), 7))
datetick('x', 'dd mmm yy','keepticks');
xlabel('Date');
ylabel('Load (A)');
legend('PV EG connected');
```

Appendix D2 – Section 4.2.2 Load Comparison for Social Club

```
% matlab code to import manual logging data for the social club
% to use in load profile comparison for before and after the PV EG was
% installed
filename1 = 'club_SOLAR.xlsx'; % excel spreadhseet containing the
% logging data after PV EG installation
filename2 = 'club_NO_SOLAR.xlsx'; % excel spreadsheet containing
% the logging data prior to PV EG installation
sheet = 1;  %Pick which sheet of the excel spreadsheet that is to be imported
xlsxRange1 = 'D6246:L43405'; %Pick all phase current and kW data - solar
xlsxRange2 = 'D2:I37161'; %Pick all phase current and kW data - non solar
solar_data=xlsread(filename1, sheet, xlsxRange1);  %Read the excel file
% for phase current and power data - solar
nonsolar_data = xlsread(filename2, sheet, xlsxRange2); %Read the excel
% file for phase current and power data - non solar

% solar data
VAS=solar_data(:,1); % voltage Aph solar
VBS=solar_data(:,2); % voltage Bph solar
VCS=solar_data(:,3); % voltage Cph solar
IAS=solar_data(:,4);            %A phase current
```

```
IBS=solar_data(:,5);            % B phase current
ICS=solar_data(:,6);            % C phase current
kWA=solar_data(:,7);            % A phase power
kWB=solar_data(:,8);            % B phase power
kWC=solar_data(:,9);            % C phase power
p=length(VAS);

% non solar data
VANS=nonsolar_data(:,1); % voltage
VBNS=nonsolar_data(:,2);
VCNS=nonsolar_data(:,3);
IANS=nonsolar_data(:,4); % current
IBNS=nonsolar_data(:,5);
ICNS=nonsolar_data(:,6);


%%
% when kW reading is zero and voltage and current readings are positive,
% the current flow is actually reverse current flow from the EG back into
% the network. This for loop and if statement section is to convert the
% 'false' positive current readings into negative readings.
for x=1:p
    if kWA(x)==0
    IAA(x,1)=-IAS(x);
    else
        IAA(x,1)=IAS(x);
    end
        if kWB(x)==0
    IBB(x,1)=-IBS(x);
    else
        IBB(x,1)=IBS(x);
        end
        if kWC(x)==0
    ICC(x,1)=-ICS(x);
    else
        ICC(x,1)=ICS(x);
    end
end
IS_data=[IAA IBB ICC]; % phase currents - solar
INS_data=[IANS IBNS ICNS]; % phase currents - non solar

% sets date for use as date ticks on figure x axis
 t1 = datenum('2016-04-14 13:03:00');  % solar dates
 dt = 30/(24*60*60); % 30 second intervals
 t2 = datestr(t1 + (1:size(IS_data,1))*dt);
 t_PV = datenum(t2);

 t11 = datenum('2011-09-22 13:03:00');
 dt = 30/(24*60*60); % 30 second
 t22 = datestr(t11 + (1:size(INS_data))*dt);
 t_noPV = datenum(t22);

 % set up subplot to plot both graphs on the same figure
subplot(2,1,1);
plot(t_noPV,INS_data); % plots the non solar load data
grid minor
title('Load Profile/ Usage Comparision - Installation 2 - Social Club');
set(gca, 'XTick', linspace(t_noPV(1),t_noPV(end), 7))
datetick('x', 'dd mmm yy','keepticks');
ylabel('Load (A)');
legend('No PV EG connected');
subplot(2,1,2);
```

```
plot(t_PV,IS_data); % plots solar data
grid minor
set(gca, 'XTick', linspace(t_PV(1),t_PV(end), 7))
datetick('x', 'dd mmm yy','keepticks');
xlabel('Date');
ylabel('Load (A)');
legend('PV EG connected');
```

Appendix D3 – Section 4.2.3 Load Comparison for Office Building

```
% matlab code to import manual logging data for the office building
% to use in load profile comparison for before and after the PV EG was
% installed
filename1 = 'office_SOLAR.xlsx'; % excel spreadhseet containing the
% logging data after PV EG installation
filename2 = 'office_NO_SOLAR.xlsx'; % excel spreadsheet containing
% the logging data prior to PV EG installation
sheet = 1; %Pick which sheet of the excel spreadsheet that is to be imported
xlsxRange1 = 'D2:L55289';  %Pick all phase current and kW data - solar
xlsxRange2 = 'D2872:L58159'; %Pick all phase current and kW data - non solar
solar_data=xlsread(filename1, sheet, xlsxRange1);    %Read the excel file
% for phase current and power data - solar
nonsolar_data1 = xlsread(filename2, sheet, xlsxRange2); %Read the excel
% file for phase current and power data - non solar

%solar data
VAS=solar_data(:,1); % voltage Aph solar
VBS=solar_data(:,2); % voltage Bph solar
VCS=solar_data(:,3); % voltage Cph solar
IAS=solar_data(:,4);            % A phase current
IBS=solar_data(:,5);            % B phase current
ICS=solar_data(:,6);            % C phase current
kWAS=solar_data(:,7);           % A phase power
kWBS=solar_data(:,8);           % B phase power
kWCS=solar_data(:,9);           % C phase power
p=length(VAS);

% non solar data
VANS1=nonsolar_data1(:,1);
VBNS1=nonsolar_data1(:,2);
VCNS1=nonsolar_data1(:,3);
IANS1=nonsolar_data1(:,4);
IBNS1=nonsolar_data1(:,5);
ICNS1=nonsolar_data1(:,6);
kWANS1=nonsolar_data1(:,7);
kWBNS1=nonsolar_data1(:,8);
kWCNS1=nonsolar_data1(:,9);

%%
% when kW reading is zero and voltage and current readings are positive,
% the current flow is actually reverse current flow from the EG back into
% the network. This for loop and if statement section is to convert the
% 'false' positive current readings into negative readings.
for x=1:p
   if kWAS(x)==0
   IAA(x,1)=-IAS(x);
   else
      IAA(x,1)=IAS(x);
   end
      if kWBS(x)==0
   IBB(x,1)=-IBS(x);
```

```
    else
        IBB(x,1)=IBS(x);
        end
        if kWCS(x)==0
    ICC(x,1)=-ICS(x);
    else
        ICC(x,1)=ICS(x);
    end
end
IS_data=[IAA IBB ICC]; % phase currents - solar
INS_data1=[IANS1 IBNS1 ICNS1]; % phase currents - non solar

% sets date for use as date ticks on figure x axis
 t1 = datenum('2016-04-12 09:25:00');  % solar dates for 2008 comparison
 dt = 30/(24*60*60); % 30 second
 t2 = datestr(t1 + (1:size(IS_data,1))*dt);
 t_PV = datenum(t2);
 t111 = datenum('2008-12-16 9:25:00');
 dt = 30/(24*60*60); % 30 second
 t222 = datestr(t111 + (1:size(INS_data1,1))*dt);
 t_noPV1 = datenum(t222);

 % set up subplot to plot both graphs on the same figure
subplot(2,1,1); % plot for 2008 data
plot(t_noPV1,INS_data1);
grid minor
title('Load Profile Comparision - Installation 3 - Office Building');
set(gca, 'XTick', linspace(t_noPV1(1),t_noPV1(end), 7))
datetick('x', 'dd mmm yy','keepticks');
ylabel('Load (A)');
legend('No PV EG connected');
subplot(2,1,2);
plot(t_PV,IS_data);
grid minor
set(gca, 'XTick', linspace(t_PV(1),t_PV(end), 7))
datetick('x', 'dd mmm yy','keepticks');
xlabel('Date');
ylabel('Load (A)');
legend('PV EG connected');
```

Appendix D4 – Section 4.3.1 Feeder Comparison for School

```
% matlab code to compare school load profile with the load profile of the
% HV feeder that supplies the Tx it is connected to
filename1 = 'school_feeder_2016_30.xlsx'; % HV feeder data
filename2 = 'school_SOLAR.xlsx'; % school data
xlsxRange1 = 'B1366:B57601';
xlsxRange2 = 'G2:L56237';
sheet1 = 1;
sheet2 = 2;

fdr_data = xlsread(filename1, sheet2, xlsxRange1); % read in feeder data
solar_data = xlsread(filename2, sheet1, xlsxRange2); % read in school data

%% this section sorts negative load flow from the installation
IAS=solar_data(:,1);          % 1st column of solar_data is A phase current
IBS=solar_data(:,2);          % 2nd column of solar_data is B phase current
ICS=solar_data(:,3);          % 3rd column of solar_data is C phase current
kWAS=solar_data(:,4);         % 4th column of solar_data is A phase power
kWBS=solar_data(:,5);         % 5th column of solar_data is B phase power
kWCS=solar_data(:,6);         % 6th column of solar_data is C phase power
p=length(IAS);
```

```
% when kW reading is zero and voltage and current readings are positive,
% the current flow is actually reverse current flow from the EG back into
% the network. This for loop and if statement section is to convert the
% 'false' positive current readings into negative readings.
for x=1:p
   if kWAS(x)==0
   IAA(x,1)=-IAS(x);
   else
      IAA(x,1)=IAS(x);
   end
      if kWBS(x)==0
   IBB(x,1)=-IBS(x);
   else
      IBB(x,1)=IBS(x);
      end
      if kWCS(x)==0
   ICC(x,1)=-ICS(x);
   else
      ICC(x,1)=ICS(x);
   end
end
IS_data=[IAA IBB ICC]; % solar phase currents
IS_data = (-1)*IS_data; % compensate for logger CT's in reverse

%% this section sets up the date codes
t1fdr = datenum('2016-04-15 11:22:00');  % solar dates
dtfdr = 30/(24*60*60); % 30 second
t2fdr = datestr(t1fdr + (1:size(fdr_data,1))*dtfdr);
t_fdr = datenum(t2fdr);
t1inst3 = datenum('2016-04-15 11:22:00');  % solar dates
dtinst3 = 30/(24*60*60); % 30 second
t2inst3 = datestr(t1inst3 + (1:size(IS_data,1))*dtinst3);
t_inst3 = datenum(t2inst3);

% subplot HV feeder data and school data
subplot(2,1,1)
plot(t_fdr,fdr_data);
grid minor
title('Load Profile Comparision - Feeder to Individual Installation');
set(gca, 'XTick', linspace(t_fdr(1),t_fdr(end), 7))
datetick('x', 'dd mmm yy','keepticks');
ylabel('Load HV (A)');
legend('Feeder Load');
subplot(2,1,2)
plot(t_inst3,IS_data);
grid minor
set(gca, 'XTick', linspace(t_inst3(1),t_inst3(end), 7))
datetick('x', 'dd mmm yy','keepticks');
xlabel('Date');
ylabel('Load LV (A)');
legend('Installation Load');
```

Appendix D5 – Section 4.3.2 Feeder Comparison for Social Club

```
% matlab code to compare feeder load profile with club load profile
filename1 = 'club_feeder_2016_30.xlsx'; % feeder data
filename2 = 'club_SOLAR.xlsx'; % club data
xlsxRange1 = 'B1084:B57601';
```

```
xlsxRange2 = 'G2:L56519';
sheet1 = 1;
sheet2 = 2;

fdr_data = xlsread(filename1, sheet2, xlsxRange1); % read in feeder data
solar_data = xlsread(filename2, sheet1, xlsxRange2); % read in club data

%% this section sorts negative load flow from the installation
IAS=solar_data(:,1);          % 1st column of solar_data is A phase current
IBS=solar_data(:,2);          % 2nd column of solar_data is B phase current
ICS=solar_data(:,3);          % 3rd column of solar_data is C phase current
kWAS=solar_data(:,4);          % 4th column of solar_data is A phase power
kWBS=solar_data(:,5);          % 5th column of solar_data is B phase power
kWCS=solar_data(:,6);          % 6th column of solar_data is C phase power
p=length(IAS);

% when kW reading is zero and voltage and current readings are positive,
% the current flow is actually reverse current flow from the EG back into
% the network. This for loop and if statement section is to convert the
% 'false' positive current readings into negative readings.
for x=1:p
   if kWAS(x)==0
   IAA(x,1)=-IAS(x);
   else
      IAA(x,1)=IAS(x);
   end
      if kWBS(x)==0
   IBB(x,1)=-IBS(x);
   else
      IBB(x,1)=IBS(x);
      end
      if kWCS(x)==0
   ICC(x,1)=-ICS(x);
   else
      ICC(x,1)=ICS(x);
   end
end
IS_data=[IAA IBB ICC]; % solar phase currents

%% this section sets up the date codes
t1fdr = datenum('2016-04-12 09:01:00');  % solar dates
dtfdr = 30/(24*60*60); % 30 second
t2fdr = datestr(t1fdr + (1:size(fdr_data,1))*dtfdr);
t_fdr = datenum(t2fdr);
t1inst3 = datenum('2016-04-12 09:01:00');  % solar dates
dtinst3 = 30/(24*60*60); % 30 second
t2inst3 = datestr(t1inst3 + (1:size(IS_data,1))*dtinst3);
t_inst3 = datenum(t2inst3);

% sets subplot for feeder and club
subplot(2,1,1)
plot(t_fdr,fdr_data);
grid minor
title('Load Profile Comparision - Feeder to Individual Installation');
set(gca, 'XTick', linspace(t_fdr(1),t_fdr(end), 7))
datetick('x', 'dd mmm yy','keepticks');
ylabel('Load HV (A)');
legend('Feeder Load');
subplot(2,1,2)
plot(t_inst3,IS_data);
grid minor
set(gca, 'XTick', linspace(t_inst3(1),t_inst3(end), 7))
```

```
datetick('x', 'dd mmm yy','keepticks');
xlabel('Date');
ylabel('Load LV (A)');
legend('Installation Load');
```

Appendix D6 – Section 4.3.3 Feeder Comparison for Office Building

```
% matlab code to compare office load profile with feeder load profile
filename1 = 'office_feeder_2016_30.xlsx'; % feeder data
filename2 = 'office_SOLAR.xlsx'; % office data
xlsxRange1 = 'B1132:B59289';
xlsxRange2 = 'G2:L58159';
sheet1 = 1;
sheet2 = 2;

fdr_data = xlsread(filename1, sheet2, xlsxRange1); % read in feeder data
solar_data = xlsread(filename2, sheet1, xlsxRange2); % read in office data

%% this section sorts negative load flow from the installation
IAS=solar_data(:,1);          % 1st column of solar_data is A phase current
IBS=solar_data(:,2);          % 2nd column of solar_data is B phase current
ICS=solar_data(:,3);          % 3rd column of solar_data is C phase current
kWAS=solar_data(:,4);           % 4th column of solar_data is A phase power
kWBS=solar_data(:,5);           % 5th column of solar_data is B phase power
kWCS=solar_data(:,6);           % 6th column of solar_data is C phase power
p=length(IAS);

% when kW reading is zero and voltage and current readings are positive,
% the current flow is actually reverse current flow from the EG back into
% the network. This for loop and if statement section is to convert the
% 'false' positive current readings into negative readings.
for x=1:p
   if kWAS(x)==0
   IAA(x,1)=-IAS(x);
   else
      IAA(x,1)=IAS(x);
   end
      if kWBS(x)==0
   IBB(x,1)=-IBS(x);
   else
      IBB(x,1)=IBS(x);
      end
      if kWCS(x)==0
   ICC(x,1)=-ICS(x);
   else
      ICC(x,1)=ICS(x);
   end
end
IS_data=[IAA IBB ICC]; % office phase currents


%% this section sets up the date codes
t1fdr = datenum('2016-04-12 09:25:00');  % solar dates
dtfdr = 30/(24*60*60); % 30 second
t2fdr = datestr(t1fdr + (1:size(fdr_data,1))*dtfdr);
t_fdr = datenum(t2fdr);
t1inst3 = datenum('2016-04-12 09:25:00');  % solar dates
dtinst3 = 30/(24*60*60); % 30 second
t2inst3 = datestr(t1inst3 + (1:size(IS_data,1))*dtinst3);
t_inst3 = datenum(t2inst3);
```

```
% sets up subplots for feeder and office load profiles
subplot(2,1,1)
plot(t_fdr,fdr_data);
grid minor
title('Load Profile Comparision - Feeder to Individual Installation');
set(gca, 'XTick', linspace(t_fdr(1),t_fdr(end), 7))
datetick('x', 'dd mmm yy','keepticks');
ylabel('Load HV (A)');
legend('Feeder Load');
subplot(2,1,2)
plot(t_inst3,IS_data);
grid minor
set(gca, 'XTick', linspace(t_inst3(1),t_inst3(end), 7))
datetick('x', 'dd mmm yy','keepticks');
xlabel('Date');
ylabel('Load LV (A)');
legend('Installation Load');
```

Appendix D7 – Section 4.4 Change in Load on HV Feeder

```
% matlab code to compare feeder loadings 2009 - 2015
formatin='mm/dd/yy HH:MM:SS';
sheet = 2;
xlsxRangedate = 'A17282:A30242'; % date range 19/04 00:00:00 to 28/04 00:00:00
xlsxRangeload = 'B17282:B30242';
xlsxRangevolts = 'C17282:C30242';
xlsxRangeBOM = 'F2:F10';

xlsxRangedatea = 'A2:A40321'; % date range to get average maximums
xlsxRangeloada = 'B2:B40321';
xlsxRangevoltsa = 'C2:C40321';

filename1 = 'feeder_2009.xlsx';  % 2009 feeder data
feeder_data_load1 = xlsread(filename1, sheet, xlsxRangeload);          %Read the excel file for
phase current data for plots
feeder_data_load1a = xlsread(filename1, sheet, xlsxRangeloada);    % used for max demand
feeder_data_volts1 = xlsread(filename1, sheet, xlsxRangevolts);
[~, timestamp] = xlsread(filename1, sheet, xlsxRangedatea);    %Read the excel file for date/time
data
x = datenum(timestamp);

filename7 = 'feeder_2015.xlsx';  % 2015 feeder data
feeder_data_volts7 = xlsread(filename7, sheet, xlsxRangevolts);          %Read the excel file for
phase current data
feeder_data_load7 = xlsread(filename7, sheet, xlsxRangeload);
feeder_data_load7a = xlsread(filename7, sheet, xlsxRangeloada);    % used for max demand

filename8 = 'feeder_2016.xlsx'; % 2016 feeder data - used for power flow model comparison in
section 5
feeder_data_volts8 = xlsread(filename8, sheet, xlsxRangevolts);          %Read the excel file for
phase current data
feeder_data_load8 = xlsread(filename8, sheet, xlsxRangeload);
feeder_data_load8a = xlsread(filename8, sheet, xlsxRangeloada);    % used for max demand

BOM_data = xlsread(filename7, sheet, xlsxRangeBOM); % read in BoM data for daily solar
exposure

% sets time/date axis
y1 = feeder_data_load1;
t1 = datenum('2009-04-19 00:00:00');
dt = 60/(24*60*60); % 60 second
t12 = datestr(t1 + (1:size(y1,1))*dt);
t_1 = datenum(t12);
```

```
y7 = feeder_data_load7;
t7 = datenum('2015-04-19 00:00:00');
dt = 60/(24*60*60); % 60 second
t72 = datestr(t7 + (1:size(y7,1))*dt);
t_7 = datenum(t72);

% plot for 2009/2015 feeder loadings
figure(1)
plot(t_1,y1,'b')
hold
plot(t_1,y7,'r')
set(gca, 'XTick', linspace(t_1(1),t_1(end), 7))
datetick('x', 'dd mmm  HH MM','keepticks');
title('Load Profile HV Feeder 2009 - 2015');
xlabel('Timestamp');
ylabel('Load (A)');
grid minor
legend('2009','2015');

% sets BoM plot date axis
yBOM = BOM_data;
tBOM = datenum('2015-04-18 13:30:00');
dtBOM = 1; % 1 day
tBOM2 = datestr(tBOM + (1:size(yBOM,1))*dtBOM);
t_BOM = datenum(tBOM2);

% plots BoM data
figure(2)
bar(t_BOM,yBOM,0.5,'r')
set(gca, 'XTick', linspace(t_BOM(1),t_BOM(end), 9))
datetick('x', 'dd mmm yy','keeplimits','keepticks');
title('Daily Solar Exposure April 2015 - BOM');
xlabel('Timestamp');
ylabel('Solar Exposure (kWh/m^2)');
grid
```

Appendix D8 – Section 5.3.1.2 Test Feeder Model Validation

```
% feeder data 2009 - 2016 to get maximum demands using PI Data - February
% for use in power flow modelling for test feeder in section 5
formatin='mm/dd/yy HH:MM:SS';
sheet = 2;
xlsxRangedatea = 'G1:G1344'; % date range to get maximums 1st Feb to 28th Feb
xlsxRangeloada = 'H1:H1344'; % load range

% read in feeder data for all years 2009 - 2016
filename1 = 'feeder_2009.xlsx';
feeder_data_load1a = xlsread(filename1, sheet, xlsxRangeloada);    % used for max demand
[~, timestamp] = xlsread(filename1, sheet, xlsxRangedatea);    %Read the excel file for date/time
data
x = datenum(timestamp); % convert timestamp to datenum to sort maximum and minimum
demands for feeder data years 2009 - 2016

filename2 = 'feeder_2010.xlsx';
feeder_data_load2a = xlsread(filename2, sheet, xlsxRangeloada);

filename3 = 'feeder_2011.xlsx';
feeder_data_load3a = xlsread(filename3, sheet, xlsxRangeloada);

filename4 = 'feeder_2012.xlsx';
feeder_data_load4a = xlsread(filename4, sheet, xlsxRangeloada);
```

```
filename5 = 'feeder_2013.xlsx';
feeder_data_load5a = xlsread(filename5, sheet, xlsxRangeloada);

filename6 = 'feeder_2014.xlsx';
feeder_data_load6a = xlsread(filename6, sheet, xlsxRangeloada);

filename7 = 'feeder_2015.xlsx';
feeder_data_load7a = xlsread(filename7, sheet, xlsxRangeloada);    % used for max demand

filename8 = 'feeder_2016.xlsx';
feeder_data_load8a = xlsread(filename8, sheet, xlsxRangeloada);    % used for max demand


%%
% this section sorts all of the February load data for each year 2009 -
% 2016 by day excluding February 29th. It then finds the minimum and
% maximum loading for each day in February for each year 2009 - 2016

n = x(end) - x(1);
d1st = x(1);
dlast = x(end);

% for loop to sort data into days
for l=1:n
   for m=1:length(x)
         if x(m)==d1st % if 1st day find and allocate maximum demand
         d1(m,1)=feeder_data_load1a(m); % 2009 amps
         d2(m,1)=feeder_data_load2a(m);  % 2010
         d3(m,1)=feeder_data_load3a(m);  % 2011
         d4(m,1)=feeder_data_load4a(m);  % 2012
         d5(m,1)=feeder_data_load5a(m);  % 2013
         d6(m,1)=feeder_data_load6a(m);  % 2014
         d7(m,1)=feeder_data_load7a(m);  % 2015
         d8(m,1)=feeder_data_load8a(m);  % 2016
         elseif x(m)==d1st+l % if 1st day plus l find and allocate maximum demand
         d1(m,1+l)=feeder_data_load1a(m); %2009 amps
         d2(m,1+l)=feeder_data_load2a(m); %2010
         d3(m,1+l)=feeder_data_load3a(m); %2011
         d4(m,1+l)=feeder_data_load4a(m); %2012
         d5(m,1+l)=feeder_data_load5a(m); %2013
         d6(m,1+l)=feeder_data_load6a(m); %2014
         d7(m,1+l)=feeder_data_load7a(m); %2015
         d8(m,1+l)=feeder_data_load8a(m); %2016
         end
   end

   d11(:,l)=nonzeros(d1(:,l)); % remove zeros from load matrix
   [peakd1(l), locnd1(l)]=max(d11(:,l));  % finds the peak demand for each day in Feb 2009
   d22(:,l)=nonzeros(d2(:,l));
   peakd2(l)=max(d22(:,l));  % 2010
   d33(:,l)=nonzeros(d3(:,l));
   peakd3(l)=max(d33(:,l));  % 2011
   d44(:,l)=nonzeros(d4(:,l));
   peakd4(l)=max(d44(:,l));  % 2012
   d55(:,l)=nonzeros(d5(:,l));
   peakd5(l)=max(d55(:,l));  % 2013
   d66(:,l)=nonzeros(d6(:,l));
   peakd6(l)=max(d66(:,l));  % 2014
   d77(:,l)=nonzeros(d7(:,l));
   peakd7(l)=max(d77(:,l));  % 2015
   d88(:,l)=nonzeros(d8(:,l));
   peakd8(l)=max(d88(:,l));  % 2016
```

```
end

% finds maximums for Feb each year
maxpeakd1=max(peakd1);
maxpeakd2=max(peakd2);
maxpeakd3=max(peakd3);
maxpeakd4=max(peakd4);
maxpeakd5=max(peakd5);
maxpeakd6=max(peakd6);
maxpeakd7=max(peakd7);
maxpeakd8=max(peakd8);

% puts all Feb peaks 2009 - 2016 into one array
maxpeaks = [maxpeakd1 maxpeakd2 maxpeakd3 maxpeakd4 maxpeakd5 maxpeakd6
maxpeakd7 maxpeakd8];

% peak for altered feeder configuration - 2016
altpeak = maxpeakd8;

% average of peaks for original feeder configuration 2009 - 2015
origpeak = mean(maxpeaks(1:7));
```

Appendix D9 – Section 5.3.1.4 LIS Dara Allocations

```
% This matlab code is used to sort individual NMI LIS data for Txs on the test
% feeder and allocate that data to the correct Tx, then write it back to
% the correct sheet in the excel spreadsheet that was created for the Txs
% that did originally contain LIS data
xlsxRangeSubs1 = 'A2:A15';
xlsxRangeSubs2 = 'B2:B423';
xlsxRangeNMIs = 'C2:C423';
filename1 = 'test_feeder_nmis.xlsx'; % contains the 422 NMIs on the test feeder that didn't
populate
% to their respective Txs
sheet1 = 1;
Subs1 = xlsread(filename1, sheet1, xlsxRangeSubs1); % reads list of sub numbers
Subs2 = xlsread(filename1, sheet1, xlsxRangeSubs2); % reads list of subs as they relate to
NMIs
NMIs = xlsread(filename1, sheet1, xlsxRangeNMIs); % reads NMIs
filename2 = 'test_feeder_nmis_LIS.xlsx'; % contains the LIS data for the NMIs in
'test_feeder_nmis.xlsx'
xlsxRangeNMIsLIS = 'A2:A11949';
xlsxRangeNMIdata = 'E2:AZ11949';
sheet2 = 1;
NMIsLIS = xlsread(filename2, sheet2, xlsxRangeNMIsLIS); % reads NMIs from LIS s/sheet
NMIdata = xlsread(filename2, sheet2, xlsxRangeNMIdata); % reads NMI data from LIS s/sheet
% if subs number = 'x' then allocate NMI to that sub
days = 29;  % number of days in the test month of February 2016
d = 0;
e = 1;
for a = 1:size(Subs1,1)  % for loop 1:14 - this is for 14 Txs only, not 15 as 1 Tx had no
connections to it
   for b = 1:size(Subs2,1)  % for loop 1:422
   if Subs2(b) == Subs1(a)
      NMIalloc(b,a) = NMIs(b);
   end
   end
end

% separate NMI data into individual Tx number arrays
NMIs27 = NMIalloc(:,1);
NMIs27(NMIs27 == 0) = []; % remove zeros
```

```
NMIs10 = NMIalloc(:,2);
NMIs10(NMIs10 == 0) = [];

NMIs5 = NMIalloc(:,3);
NMIs5(NMIs5 == 0) = [];

NMIs13 = NMIalloc(:,4);
NMIs13(NMIs13 == 0) = [];

NMIs23 = NMIalloc(:,5);
NMIs23(NMIs23 == 0) = [];

NMIs12 = NMIalloc(:,6);
NMIs12(NMIs12 == 0) = [];

NMIs3 = NMIalloc(:,7);
NMIs3(NMIs3 == 0) = [];

NMIs31 = NMIalloc(:,8);
NMIs31(NMIs31 == 0) = [];

NMIs6 = NMIalloc(:,9);
NMIs6(NMIs6 == 0) = [];

NMIs4 = NMIalloc(:,10);
NMIs4(NMIs4 == 0) = [];

NMIs16 = NMIalloc(:,11);
NMIs16(NMIs16 == 0) = [];

NMIs9 = NMIalloc(:,12);
NMIs9(NMIs9 == 0) = [];

NMIs19 = NMIalloc(:,13);
NMIs19(NMIs19 == 0) = [];

NMIs22 = NMIalloc(:,14);
NMIs22(NMIs22 == 0) = [];

% data for each NMI for each sub for 29 days
% repeated for each of the 14 Txs requiring data
j = 1;
for i = 1 : length(NMIs27)
   for c = 1:size(NMIsLIS,1)  % for loop 1:11949
       if NMIsLIS(c) == NMIs27(i);
          NMIs27data(j,:) = NMIdata(c,:);
          j = j + 1;
       end
   end
end
% sum each NMI data for each day at each interval to get total Tx load
for m = 1:29
   data27(m,:) = sum(NMIs27data(m:29:end,:),1);
end

j = 1;
for i = 1 : length(NMIs12)
   for c = 1:size(NMIsLIS,1)  % for loop 1:11949
       if NMIsLIS(c) == NMIs12(i);
          NMIs12data(j,:) = NMIdata(c,:);
          j = j + 1;
```

```
        end
    end
end
for m = 1:29
    data12(m,:) = sum(NMIs12data(m:29:end,:),1);
end

j = 1;
for i = 1 : length(NMIs10)
    for c = 1:size(NMIsLIS,1)  % for loop 1:11949
        if NMIsLIS(c) == NMIs10(i);
            NMIs10data(j,:) = NMIdata(c,:);
            j = j + 1;
        end
    end
end
for m = 1:29
    data10(m,:) = sum(NMIs10data(m:29:end,:),1);
end

j = 1;
for i = 1 : length(NMIs23)
    for c = 1:size(NMIsLIS,1)  % for loop 1:11949
        if NMIsLIS(c) == NMIs23(i);
            NMIs23data(j,:) = NMIdata(c,:);
            j = j + 1;
        end
    end
end
for m = 1:29
    data23(m,:) = sum(NMIs23data(m:29:end,:),1);
end

j = 1;
for i = 1 : length(NMIs22)
    for c = 1:size(NMIsLIS,1)  % for loop 1:11949
        if NMIsLIS(c) == NMIs22(i);
            NMIs22data(j,:) = NMIdata(c,:);
            j = j + 1;
        end
    end
end
for m = 1:29
    data22(m,:) = sum(NMIs22data(m:29:end,:),1);
end

j = 1;
for i = 1 : length(NMIs5)
    for c = 1:size(NMIsLIS,1)  % for loop 1:11949
        if NMIsLIS(c) == NMIs5(i);
            NMIs5data(j,:) = NMIdata(c,:);
            j = j + 1;
        end
    end
end
for m = 1:29
    data5(m,:) = sum(NMIs5data(m:29:end,:),1);
end

j = 1;
for i = 1 : length(NMIs9)
    for c = 1:size(NMIsLIS,1)  % for loop 1:11949
```

```
        if NMIsLIS(c) == NMIs9(i);
          NMIs9data(j,:) = NMIdata(c,:);
          j = j + 1;
        end
    end
end
for m = 1:29
    data9(m,:) = sum(NMIs9data(m:29:end,:),1);
end

j = 1;
for i = 1 : length(NMIs16)
    for c = 1:size(NMIsLIS,1)  % for loop 1:11949
        if NMIsLIS(c) == NMIs16(i);
          NMIs16data(j,:) = NMIdata(c,:);
          j = j + 1;
        end
    end
end
for m = 1:29
    data16(m,:) = sum(NMIs16data(m:29:end,:),1);
end

j = 1;
for i = 1 : length(NMIs4)
    for c = 1:size(NMIsLIS,1)  % for loop 1:11949
        if NMIsLIS(c) == NMIs4(i);
          NMIs4data(j,:) = NMIdata(c,:);
          j = j + 1;
        end
    end
end
for m = 1:29
    data4(m,:) = sum(NMIs4data(m:29:end,:),1);
end

j = 1;
for i = 1 : length(NMIs6)
    for c = 1:size(NMIsLIS,1)  % for loop 1:11949
        if NMIsLIS(c) == NMIs6(i);
          NMIs6data(j,:) = NMIdata(c,:);
          j = j + 1;
        end
    end
end
for m = 1:29
    data6(m,:) = sum(NMIs6data(m:29:end,:),1);
end

j = 1;
for i = 1 : length(NMIs31)
    for c = 1:size(NMIsLIS,1)  % for loop 1:11949
        if NMIsLIS(c) == NMIs31(i);
          NMIs31data(j,:) = NMIdata(c,:);
          j = j + 1;
        end
    end
end
for m = 1:29
    data31(m,:) = sum(NMIs31data(m:29:end,:),1);
end
```

```
j = 1;
for i = 1 : length(NMIs3)
   for c = 1:size(NMIsLIS,1)  % for loop 1:11949
      if NMIsLIS(c) == NMIs3(i);
         NMIs3data(j,:) = NMIdata(c,:);
         j = j + 1;
      end
   end
end
for m = 1:29
   data3(m,:) = sum(NMIs3data(m:29:end,:),1);
end

j = 1;
for i = 1 : length(NMIs13)
   for c = 1:size(NMIsLIS,1)  % for loop 1:11949
      if NMIsLIS(c) == NMIs13(i);
         NMIs13data(j,:) = NMIdata(c,:);
         j = j + 1;
      end
   end
end
for m = 1:29
   data13(m,:) = sum(NMIs13data(m:29:end,:),1);
end

j = 1;
for i = 1 : length(NMIs19)
   for c = 1:size(NMIsLIS,1)  % for loop 1:11949
      if NMIsLIS(c) == NMIs19(i);
         NMIs19data(j,:) = NMIdata(c,:);
         j = j + 1;
      end
   end
end
for m = 1:29
   data19(m,:) = sum(NMIs19data(m:29:end,:),1);
end

% write Tx load data back to excel spreadsheet that contains the other Txs
% data for this feeder
filename3 = 'test feeder sub data_LIS.xlsx';
xlsxRangeWrite = 'D2:AY30';
xlswrite(filename3, data3, 4, xlsxRangeWrite);
xlswrite(filename3, data4, 5, xlsxRangeWrite);
xlswrite(filename3, data5, 6, xlsxRangeWrite);
xlswrite(filename3, data6, 7, xlsxRangeWrite);
xlswrite(filename3, data9, 10, xlsxRangeWrite);
xlswrite(filename3, data10, 11, xlsxRangeWrite);
xlswrite(filename3, data12, 13, xlsxRangeWrite);
xlswrite(filename3, data13, 14, xlsxRangeWrite);
xlswrite(filename3, data16, 17, xlsxRangeWrite);
xlswrite(filename3, data19, 20, xlsxRangeWrite);
xlswrite(filename3, data27, 26, xlsxRangeWrite);
xlswrite(filename3, data31, 29, xlsxRangeWrite);
```

Appendix D10 – Section 5.3.1.5 LIS vs DM&C Data Comparisons

```
% LIS data validation using DM&C data from Txs 8,9,17,18,19,20,23
formatin='mm/dd/yy';
xlsxRangeP1 = 'E11602:AZ11630'; % LIS data range for Tx8
xlsxRangeP2 = 'E11573:AZ11601'; % LIS data range for Tx9
```

```
xlsxRangeP3 = 'E11892:AZ11920'; % LIS data range for Tx17
xlsxRangeP4 = 'E11921:AZ11949'; % LIS data range for Tx18
xlsxRangeP5 = 'E11950:AZ11978'; % LIS data range for Tx19
xlsxRangeP6 = 'E11979:AZ12007'; % LIS data range for Tx20
xlsxRangeP7 = 'E12066:AZ12094'; % LIS data range for Tx23
xlsxRangeDate = 'C11602:C11630';
xlsxRangeTime = 'E1:AZ1';
filename = 'LIS_DATA_DCs.xlsx';
sheet1 = 1;
P1 = xlsread(filename, sheet1, xlsxRangeP1); % read in LIS data for Tx8
P2 = xlsread(filename, sheet1, xlsxRangeP2); % read in LIS data for Tx9
P3 = xlsread(filename, sheet1, xlsxRangeP3); % read in LIS data for Tx17
P4 = xlsread(filename, sheet1, xlsxRangeP4); % read in LIS data for Tx18
P5 = xlsread(filename, sheet1, xlsxRangeP5); % read in LIS data for Tx19
P6 = xlsread(filename, sheet1, xlsxRangeP6); % read in LIS data for Tx20
P7 = xlsread(filename, sheet1, xlsxRangeP7); % read in LIS data for Tx23
[~, Date] = xlsread(filename, sheet1, xlsxRangeDate);
Time = xlsread(filename, sheet1, xlsxRangeTime);
x = datenum(Date,formatin);
P1a = P1'; % transform P from 29 x 48 to P1 48 x 29
P1b = reshape(P1a,[],1); % reshape 48 x 29 P1 matrix into P2 1392 x 1 array
P2a = P2'; % transform P from 29 x 48 to P1 48 x 29
P2b = reshape(P2a,[],1); % reshape 48 x 29 P1 matrix into P2 1392 x 1 array
P3a = P3'; % transform P from 29 x 48 to P1 48 x 29
P3b = reshape(P3a,[],1); % reshape 48 x 29 P1 matrix into P2 1392 x 1 array
P4a = P4'; % transform P from 29 x 48 to P1 48 x 29
P4b = reshape(P4a,[],1); % reshape 48 x 29 P1 matrix into P2 1392 x 1 array
P5a = P5'; % transform P from 29 x 48 to P1 48 x 29
P5b = reshape(P5a,[],1); % reshape 48 x 29 P1 matrix into P2 1392 x 1 array
P6a = P6'; % transform P from 29 x 48 to P1 48 x 29
P6b = reshape(P6a,[],1); % reshape 48 x 29 P1 matrix into P2 1392 x 1 array
P7a = P7'; % transform P from 29 x 48 to P1 48 x 29
P7b = reshape(P7a,[],1); % reshape 48 x 29 P1 matrix into P2 1392 x 1 array
for k = 1:length(x)
    L1(:,k) = x(k) + Time;
end
L2 = datestr(L1);
L3 = datenum(L2); % convert date string data to num data to plot

% DM&C PI data Txs_Feb_30min intervals
xlsxRangeP = 'O3:O1394';  % DM&C measured kW
xlsxRangeQ = 'P3:P1394';  % DM&C measured kVAr
xlsxRangeIa = 'Q3:Q1394'; % DM&C measured A phase current
xlsxRangeIb = 'R3:R1394'; % DM&C measured B phase current
xlsxRangeIc = 'S3:S1394'; % DM&C measured C phase current
xlsxRangeVa = 'T3:T1394'; % DM&C measured A phase voltage
xlsxRangeVb = 'U3:U1394'; % DM&C measured B phase voltage
xlsxRangeVc = 'V3:V1394'; % DM&C measured C phase voltage
filename1 = 'Tx8 2016 Feb.xlsx'; % Tx8 DM&C data
filename2 = 'Tx9 2016 Feb.xlsx'; % Tx9 DM&C data
filename3 = 'Tx17 2016 Feb.xlsx'; % Tx17 DM&C data
filename4 = 'Tx18 2016 Feb.xlsx'; % Tx18 DM&C data
filename5 = 'Tx19 2016 Feb.xlsx'; % Tx19 DM&C data
filename6 = 'Tx20 2016 Feb.xlsx'; % Tx20 DM&C data
filename7 = 'Tx23 2016 Feb.xlsx'; % Tx23 DM&C data
% pf = 0.9;
pf = 0.95;
sheet2 = 2;

%%
% Tx8
RP1 = xlsread(filename1, sheet2, xlsxRangeP); % real power
```

```
QP1 = xlsread(filename1, sheet2, xlsxRangeQ); % reactive power
Ia1 = xlsread(filename1, sheet2, xlsxRangeIa); % Aph current
Ib1 = xlsread(filename1, sheet2, xlsxRangeIb); % Bph current
Ic1 = xlsread(filename1, sheet2, xlsxRangeIc); % Cph current
Va1 = xlsread(filename1, sheet2, xlsxRangeVa); % Aph voltage
Vb1 = xlsread(filename1, sheet2, xlsxRangeVb); % Bph voltage
Vc1 = xlsread(filename1, sheet2, xlsxRangeVc); % Cph voltage
% out of balance load powers - pf averaged pf = 0.95
Pa1 = Va1.*Ia1*pf;  % Aph
Pb1 = Vb1.*Ib1*pf; % Bph
Pc1 = Vc1.*Ic1*pf; % Cph

Pt1 = Pa1 + Pb1 + Pc1; % total power in W

Ptotal1 = Pt1/1000; % calculated DM&C total power in kW
RPkW1 = RP1/1000; % measured DM&C power in kW

figure(1)
plot(L3,P1b,'b'); % plot Date vs LIS power
hold
plot(L3,Ptotal1,'r');  % plot Date vs DM&C power - from individual phase load and voltages
plot(L3,RPkW1,'g'); % plot Date vs DM&C power - measured real power
grid minor
set(gca, 'XTick', linspace(L3(1),L3(end), 15));
datetick('x', 'dd mmm yy','keeplimits','keepticks');
title('Comparison of LIS data with DM&C data - Tx 8');
xlabel('Date');
ylabel('Tx Loading (kW)');
legend('LIS kW data', 'DM&C calculated kW data' , 'DM&C measured kW data')

%%
% Tx9
RP2 = xlsread(filename2, sheet2, xlsxRangeP); % real power
QP2 = xlsread(filename2, sheet2, xlsxRangeQ); % reactive power
Ia2 = xlsread(filename2, sheet2, xlsxRangeIa); % Aph current
Ib2 = xlsread(filename2, sheet2, xlsxRangeIb); % Bph current
Ic2 = xlsread(filename2, sheet2, xlsxRangeIc); % Cph current
Va2 = xlsread(filename2, sheet2, xlsxRangeVa); % Aph voltage
Vb2 = xlsread(filename2, sheet2, xlsxRangeVb); % Bph voltage
Vc2 = xlsread(filename2, sheet2, xlsxRangeVc); % Cph voltage
% out of balance load powers - pf averaged pf = 0.95
Pa2 = Va2.*Ia2*pf;  % Aph
Pb2 = Vb2.*Ib2*pf; % Bph
Pc2 = Vc2.*Ic2*pf; % Cph

Pt2 = Pa2 + Pb2 + Pc2; % total power in W

Ptotal2 = Pt2/1000; % calculated DM&C total power in kW
RPkW2 = RP2/1000; % measured DM&C power in kW

figure(2)
plot(L3,P2b,'b'); % plot Date vs LIS power
hold
plot(L3,Ptotal2,'r');  % plot Date vs DM&C power - from individual phase load and voltages
plot(L3,RPkW2,'g'); % plot Date vs DM&C power - measured real power
grid minor
set(gca, 'XTick', linspace(L3(1),L3(end), 15));
datetick('x', 'dd mmm yy','keeplimits','keepticks');
title('Comparison of LIS data with DM&C data - Tx 9');
xlabel('Date');
ylabel('Tx Loading (kW)');
legend('LIS kW data', 'DM&C calculated kW data' , 'DM&C measured kW data')
```

```
%%
% Tx 17
RP3 = xlsread(filename3, sheet2, xlsxRangeP); % real power
QP3 = xlsread(filename3, sheet2, xlsxRangeQ); % reactive power
Ia3 = xlsread(filename3, sheet2, xlsxRangeIa); % Aph current
Ib3 = xlsread(filename3, sheet2, xlsxRangeIb); % Bph current
Ic3 = xlsread(filename3, sheet2, xlsxRangeIc); % Cph current
Va3 = xlsread(filename3, sheet2, xlsxRangeVa); % Aph voltage
Vb3 = xlsread(filename3, sheet2, xlsxRangeVb); % Bph voltage
Vc3 = xlsread(filename3, sheet2, xlsxRangeVc); % Cph voltage
% out of balance load powers - pf averaged pf = 0.95
Pa3 = Va3.*Ia3*pf;  % Aph
Pb3 = Vb3.*Ib3*pf; % Bph
Pc3 = Vc3.*Ic3*pf; % Cph

Pt3 = Pa3 + Pb3 + Pc3; % total power in W

Ptotal3 = Pt3/1000; % calculated DM&C total power in kW
RPkW3 = RP3/1000; % measured DM&C power in kW

figure(3)
plot(L3,P3b,'b'); % plot Date vs LIS power
hold
plot(L3,Ptotal3,'r');  % plot Date vs DM&C power - from individual phase load and voltages
plot(L3,RPkW3,'g'); % plot Date vs DM&C power - measured real power
grid minor
set(gca, 'XTick', linspace(L3(1),L3(end), 15));
datetick('x', 'dd mmm yy','keeplimits','keepticks');
title('Comparison of LIS data with DM&C data - Tx 17');
xlabel('Date');
ylabel('Tx Loading (kW)');
legend('LIS kW data', 'DM&C calculated kW data' , 'DM&C measured kW data')

%%
% Tx18
RP4 = xlsread(filename4, sheet2, xlsxRangeP); % real power
QP4 = xlsread(filename4, sheet2, xlsxRangeQ); % reactive power
Ia4 = xlsread(filename4, sheet2, xlsxRangeIa); % Aph current
Ib4 = xlsread(filename4, sheet2, xlsxRangeIb); % Bph current
Ic4 = xlsread(filename4, sheet2, xlsxRangeIc); % Cph current
Va4 = xlsread(filename4, sheet2, xlsxRangeVa); % Aph voltage
Vb4 = xlsread(filename4, sheet2, xlsxRangeVb); % Bph voltage
Vc4 = xlsread(filename4, sheet2, xlsxRangeVc); % Cph voltage
% out of balance load powers - pf averaged pf = 0.95
Pa4 = Va4.*Ia4*pf;  % Aph
Pb4 = Vb4.*Ib4*pf; % Bph
Pc4 = Vc4.*Ic4*pf; % Cph

Pt4 = Pa4 + Pb4 + Pc4; % total power in W

Ptotal4 = Pt4/1000; % calculated DM&C total power in kW
RPkW4 = RP4/1000; % measured DM&C power in kW

figure(4)
plot(L3,P4b,'b'); % plot Date vs LIS power
hold
plot(L3,Ptotal4,'r');  % plot Date vs DM&C power - from individual phase load and voltages
plot(L3,RPkW4,'g'); % plot Date vs DM&C power - measured real power
grid minor
set(gca, 'XTick', linspace(L3(1),L3(end), 15));
datetick('x', 'dd mmm yy','keeplimits','keepticks');
```

```
title('Comparison of LIS data with DM&C data - Tx 18');
xlabel('Date');
ylabel('Tx Loading (kW)');
legend('LIS kW data', 'DM&C calculated kW data' , 'DM&C measured kW data')

%%
% Tx19
RP5 = xlsread(filename5, sheet2, xlsxRangeP); % real power
QP5 = xlsread(filename5, sheet2, xlsxRangeQ); % reactive power
Ia5 = xlsread(filename5, sheet2, xlsxRangeIa); % Aph current
Ib5 = xlsread(filename5, sheet2, xlsxRangeIb); % Bph current
Ic5 = xlsread(filename5, sheet2, xlsxRangeIc); % Cph current
Va5 = xlsread(filename5, sheet2, xlsxRangeVa); % Aph voltage
Vb5 = xlsread(filename5, sheet2, xlsxRangeVb); % Bph voltage
Vc5 = xlsread(filename5, sheet2, xlsxRangeVc); % Cph voltage
% out of balance load powers - pf averaged pf = 0.95
Pa5 = Va5.*Ia5*pf;  % Aph
Pb5 = Vb5.*Ib5*pf; % Bph
Pc5 = Vc5.*Ic5*pf; % Cph

Pt5 = Pa5 + Pb5 + Pc5; % total power in W

Ptotal5 = Pt5/1000; % calculated DM&C total power in kW
RPkW5 = RP5/1000; % measured DM&C power in kW

figure(5)
plot(L3,P5b,'b'); % plot Date vs LIS power
hold
plot(L3,Ptotal5,'r');  % plot Date vs DM&C power - from individual phase load and voltages
plot(L3,RPkW5,'g'); % plot Date vs DM&C power - measured real power
grid minor
set(gca, 'XTick', linspace(L3(1),L3(end), 15));
datetick('x', 'dd mmm yy','keeplimits','keepticks');
title('Comparison of LIS data with DM&C data - Tx 19');
xlabel('Date');
ylabel('Tx Loading (kW)');
legend('LIS kW data', 'DM&C calculated kW data' , 'DM&C measured kW data')

%%
% Tx20
RP6 = xlsread(filename6, sheet2, xlsxRangeP); % real power
QP6 = xlsread(filename6, sheet2, xlsxRangeQ); % reactive power
Ia6 = xlsread(filename6, sheet2, xlsxRangeIa); % Aph current
Ib6 = xlsread(filename6, sheet2, xlsxRangeIb); % Bph current
Ic6 = xlsread(filename6, sheet2, xlsxRangeIc); % Cph current
Va6 = xlsread(filename6, sheet2, xlsxRangeVa); % Aph voltage
Vb6 = xlsread(filename6, sheet2, xlsxRangeVb); % Bph voltage
Vc6 = xlsread(filename6, sheet2, xlsxRangeVc); % Cph voltage
% out of balance load powers - pf averaged pf = 0.95
Pa6 = Va6.*Ia6*pf;  % Aph
Pb6 = Vb6.*Ib6*pf; % Bph
Pc6 = Vc6.*Ic6*pf; % Cph

Pt6 = Pa6 + Pb6 + Pc6; % total power in W

Ptotal6 = Pt6/1000; % calculated DM&C total power in kW
RPkW6 = RP6/1000; % measured DM&C power in kW

figure(6)
plot(L3,P6b,'b'); % plot Date vs LIS power
hold
plot(L3,Ptotal6,'r');  % plot Date vs DM&C power - from individual phase load and voltages
```

```
plot(L3,RPkW6,'g'); % plot Date vs DM&C power - measured real power
grid minor
set(gca, 'XTick', linspace(L3(1),L3(end), 15));
datetick('x', 'dd mmm yy','keeplimits','keepticks');
title('Comparison of LIS data with DM&C data - Tx 20');
xlabel('Date');
ylabel('Tx Loading (kW)');
legend('LIS kW data', 'DM&C calculated kW data' , 'DM&C measured kW data')

%%
% Tx23
RP7 = xlsread(filename7, sheet2, xlsxRangeP); % real power
QP7 = xlsread(filename7, sheet2, xlsxRangeQ); % reactive power
Ia7 = xlsread(filename7, sheet2, xlsxRangeIa); % Aph current
Ib7 = xlsread(filename7, sheet2, xlsxRangeIb); % Bph current
Ic7 = xlsread(filename7, sheet2, xlsxRangeIc); % Cph current
Va7 = xlsread(filename7, sheet2, xlsxRangeVa); % Aph voltage
Vb7 = xlsread(filename7, sheet2, xlsxRangeVb); % Bph voltage
Vc7 = xlsread(filename7, sheet2, xlsxRangeVc); % Cph voltage
% out of balance load powers - pf averaged pf = 0.95
Pa7 = Va7.*Ia7*pf;  % Aph
Pb7 = Vb7.*Ib7*pf; % Bph
Pc7 = Vc7.*Ic7*pf; % Cph

Pt7 = Pa7 + Pb7 + Pc7; % total power in W

Ptotal7 = Pt7/1000; % calculated DM&C total power in kW
RPkW7 = RP7/1000; % measured DM&C power in kW

figure(7)
plot(L3,P7b,'b'); % plot Date vs LIS power
hold
plot(L3,Ptotal7,'r');  % plot Date vs DM&C power - from individual phase load and voltages
plot(L3,RPkW7,'g'); % plot Date vs DM&C power - measured real power
grid minor
set(gca, 'XTick', linspace(L3(1),L3(end), 15));
datetick('x', 'dd mmm yy','keeplimits','keepticks');
title('Comparison of LIS data with DM&C data - Tx 23');
xlabel('Date');
ylabel('Tx Loading (kW)');
legend('LIS kW data', 'DM&C calculated kW data' , 'DM&C measured kW data')
```

Appendix D11 – Section 5.3.1.6 Tx LIS Loadings

```
% LIS data test feeder - gets load for every Tx
% when fdr max occurs - 14/02/16 19:00:00
xlsxRangeP = 'AP15';  % set data range to read from excel spreadsheet
filename1 = 'feeder sub data_LIS.xlsx';  % name of excel spreadsheet
pf = 0.9;  % set power factor
theta = acos(pf);  % angle between S & P corresponding to pf = 0.9
tan = tan(theta);  % tan of theta to work out Q from P
for b = 1:35  % for loop to read all Tx data from 35 sub spreadsheets
sheet = 1+b;  % set sheet number
P(b,1) = xlsread(filename1, sheet, xlsxRangeP);  % read power data from excel spreadsheet
end

% for loop to get Q for 14/02/16 19:00:00 for each tx
for g = 1:size(P,1)
RPMW(g) = P(g)/1000;
QPMW(g) = RPMW(g) * tan;
end
```

```
RPMW = RPMW' * 1.02; % compensation factor of 2% for load being applied to the HV bus
QPMW = QPMW' * 1.02;

%% write results back to excel spreadsheet
filename2 = 'Tx load test feeder.xlsx';
xlsxRangeRP = 'C2:C36';
xlsxRangeQP = 'D2:D36';
xlswrite(filename2, RPMW, xlsxRangeRP);
xlswrite(filename2, QPMW, xlsxRangeQP);
```

Appendix D12 – Section 5.3.2.1 Tx LIS Loadings for Power Flow Feeder

```
% LIS data for power flow feeder - gets load for every Tx
% when fdr daytime min occurs - 05/02/16 10:30:00
xlsxRangeP = 'Y6';  % set data range to read from excel spreadsheet
filename1 = 'PF feeder sub data_LIS.xlsx';  % name of excel spreadsheet
pf = 0.9;  % set power factor (this has been changed to pf=0.95 in the power flow modelling by
% applying a scaling factor to the Q value of the loads)
theta = acos(pf);  % angle between S & P corresponding to pf = 0.9
tan = tan(theta);  % tan of theta to work out Q from P
for b = 1:64  % for loop to read all Tx data from 64 sub spreadsheets
sheet = 1+b;  % set sheet number
P(b,1) = xlsread(filename1, sheet, xlsxRangeP);  % read power data from excel spreadsheet
end

% for loop to get Q for 05/02/16 11:00:00 for each tx
for g = 1:size(P,1)
RPMW(g) = P(g)/1000;
QPMW(g) = RPMW(g) * tan;
end

RPMW = RPMW';
QPMW = QPMW';

%% write results back to excel spreadsheet
filename2 = 'Tx min daytime load PF feeder_1.xlsx';
xlsxRangeRP = 'C2:C65';
xlsxRangeQP = 'D2:D65';
xlswrite(filename2, RPMW, xlsxRangeRP);
xlswrite(filename2, QPMW, xlsxRangeQP);
```

Appendix D13 – Section 5.3.2.4 Power Flow Comparisons

```
% Matlab script to show change in power flow when additional PV
% EG is introduced
sheet = 1;
filename1 = 'no gen lines.xlsx'; % PF data no additonal PV EG
filename2 = '1xaemolines.xlsx'; % PF data added AEMO 1xPV EG
filename3 = '148aemolines.xlsx'; % PF data added AEMO 1.4xPV EG
filename4 = '2aemolines.xlsx'; % PF data added AEMO 2xPV EG
xlsxRange1 = 'E8:E90'; % PF range
PF_NO_PV = xlsread(filename1, sheet, xlsxRange1);
PF_AEMO_PV = xlsread(filename2, sheet, xlsxRange1);
PF_1_48_AEMO_PV = xlsread(filename3, sheet, xlsxRange1);
PF_2_AEMO_PV = xlsread(filename4, sheet, xlsxRange1);
figure(1)
plot(PF_NO_PV);
title('Power Flow Changes with Additional PV EG Added');
xlabel('Bus Number');
ylabel('Real Power (MW)');
```

```
grid minor
hold on
plot(PF_AEMO_PV,'r');
% plot(PF_1_48_AEMO_PV,'g');
% plot(PF_2_AEMO_PV,'m');
legend('No Additional PV EG','Additional AEMO PV EG');
% legend('No Additional PV EG','Additional AEMO PV EG','Additional 1.48 x AEMO PV EG');
% legend('No Additional PV EG','Additional AEMO PV EG','Additional 1.48 x AEMO PV
EG','Additional 2x AEMO PV EG');
```

Appendix D14 – Section 5.3.2.4 Voltage Rise Comparisons

```
% read in results from ASPEN power flow for voltage rise
% existing network vs network with added generation at each tx
filename1 = 'no gen.xlsx';  % existing fdr model - no additional PV EG
filename2 = '1xaemo.xlsx'; % + 1 x AEMO predicted increase
filename3 = '148aemo.xlsx'; % + 1.4 x AEMO predicted increase - point where grid generates
back into zone
filename4 = '2aemo.xlsx'; % + 2 x AEMO predicted increase - point where all buses are
experiencing reverse power flow
filename5 = 'tap change_1.xlsx'; % + 2 x AEMO predicted increase - tap change at zone to 11kV
(1pu)
xlsxRange1 = 'F8:F92'; % V(pu)
sheet = 1;
Voltsexisting = xlsread(filename1, sheet, xlsxRange1);
VoltsAEMO1 = xlsread(filename2, sheet, xlsxRange1);
VoltsAEMO1_48 = xlsread(filename3, sheet, xlsxRange1);
VoltsAEMO2 = xlsread(filename4, sheet, xlsxRange1);
VoltsAEMO2TC = xlsread(filename5, sheet, xlsxRange1);
figure(1)
plot(Voltsexisting*11)
hold on
plot(VoltsAEMO1*11,'r')
plot(VoltsAEMO1_48*11,'g')
plot(VoltsAEMO2*11,'m')
grid
title('Voltage Rise with Additional PV EG Added')
xlabel('Bus number')
ylabel('Bus Voltage (kV)')
% legend('No Additional PV EG','Additional AEMO PV EG');
% legend('No Additional PV EG','Additional AEMO PV EG','Additional 1.48 x AEMO PV EG');
legend('No Additional PV EG','Additional AEMO PV EG','Additional 1.48 x AEMO PV
EG','Additional 2 x AEMO PV EG');

figure(2)
plot(Voltsexisting*11)
hold on
plot(VoltsAEMO2*11,'m')
plot(VoltsAEMO2TC*11,'k')
grid
title('Voltage Rise with Additional PV EG Added - Tap Change at Zone')
xlabel('Bus number')
ylabel('Bus Voltage (kV)')
% legend('No Additional PV EG','Additional AEMO PV EG');
% legend('No Additional PV EG','Additional AEMO PV EG','Additional 1.48 x AEMO PV EG');
legend('No Additional PV EG','Additional 2 x AEMO PV EG', 'Additional 2 x AEMO PV EG - Tap
Change to 11kV');
```

Appendix D15 – Section 5.3.2.4 Change in Power Flow at Zone Bus

```
% Matlab script to show change in power flow at zone bus when additional PV
% EG is introduced
sheet = 1;
filename1 = 'power flow_1.xlsx';
xlsxRange1 = 'A2:A13';
xlsxRange2 = 'B2:B13';
added_PV = xlsread(filename1, sheet, xlsxRange1);
power_flow_zone = xlsread(filename1, sheet, xlsxRange2);
figure(1)
plot(added_PV,power_flow_zone);
title('Change in Power Flow at Zone Bus Due to Additional PV EG');
xlabel('Added PV EG x AEMO Predicted Increase');
ylabel('Real Power (MW)');
grid minor
```

Appendix D16 – Section 6.2.1 PV EG Q Source Effect on Feeder Power Flow

```
% Matlab script to show change in reactive power flow around feeder when additional PV
% EG is introduced with pf=0.95
sheet = 1;
filename1 = 'no gen liines1.xlsx'; % PF data no additional PV EG
filename2 = '1xaemolines1.xlsx'; % PF data added AEMO 1xPV EG
filename3 = '145axaemolines1.xlsx'; % PF data added AEMO 1.48xPV EG
filename4 = '2xaemolines1.xlsx'; % PF data added AEMO 2xPV EG
filename5 = '2xaemolines095.xlsx'; % PF data added AEMO 2xPV EG pf = 0.95
xlsxRange1 = 'F8:F90'; % PF range Q
Q_PF_NO_PV = xlsread(filename1, sheet, xlsxRange1);
Q_PF_AEMO_PV = xlsread(filename2, sheet, xlsxRange1);
Q_PF_1_45_AEMO_PV = xlsread(filename3, sheet, xlsxRange1);
Q_PF_2_AEMO_PV = xlsread(filename4, sheet, xlsxRange1);
Q_PF_2_AEMO_PV_pf = xlsread(filename5, sheet, xlsxRange1);
figure(1)
plot(Q_PF_NO_PV,'--','color','b');
hold on
plot(Q_PF_AEMO_PV,'x','color','r');
plot(Q_PF_1_45_AEMO_PV,'o','color','g');
plot(Q_PF_2_AEMO_PV,'m');
title('Reactive Power Flow Changes with Additional PV EG pf = 0.95');
xlabel('Bus Number');
ylabel('Reactive Power (MVAr)');
grid minor
plot(Q_PF_2_AEMO_PV_pf,'k');
legend('No Additional PV EG','Additional AEMO PV EG pf=1','Additional 1.4x AEMO PV EG pf
=1','Additional 2x AEMO PV EG pf=1','Additional 2x AEMO PV EG pf=0.95');
```

Appendix D17 – Section 6.2.1 PV EG Q Source Effect on Zone Bus Power Flow

```
% Matlab script to show change in reactive power flow at zone bus when additional PV
% EG is introduced at changing power factors -
% 1,0.98,0.95,0.92.0.90,0.88,0.85
sheet = 1;
filename1 = 'power flow_1.xlsx';
xlsxRange1 = 'G2:G8';
xlsxRange2 = 'H2:H8';
power_factor = xlsread(filename1, sheet, xlsxRange1);
Q_power_flow_zone = xlsread(filename1, sheet, xlsxRange2);
figure(1)
plot(power_factor,Q_power_flow_zone);
set(gca,'xdir','reverse');
title('Change in Reactive Power Flow at Zone Bus Due to Change in PV EG Power Factor');
```

```
xlabel('Power Factor of PV EGs');
ylabel('Reactive Power (MVAr)');
grid minor
```

Appendix D18 – Section 6.2.1 PV EG Q Source Effect on Feeder Current

```
% Matlab script to show change in current when additional PV
% EG is introduced – PV EG Q soure
sheet = 1;
filename1 = 'no gen liines1.xlsx'; % current data no additional PV EG
filename2 = '1xaemolines1.xlsx'; % current data added AEMO 1xPV EG
filename3 = '145axaemolines1.xlsx'; % current data added AEMO 1.45xPV EG
filename4 = '2xaemolines1.xlsx'; % current data added AEMO 2xPV EG
filename5 = '2xaemolines095.xlsx'; % current data for 2xAEMO pf=0.95
filename6 = '2xaemolines090.xlsx'; % current data for 2xAEMO pf=0.90
filename7 = '2xaemolines085.xlsx'; % current data for 2xAEMO pf=0.85
filename8 = '2xaemolines098.xlsx'; % current data for 2xAEMO pf=0.98
xlsxRange1 = 'I8:I90'; % current range
xlsxRange2 = 'E8:E90'; % P range
xlsxRange3 = 'F8:F90'; % Q range
AMPS_NO_PV = xlsread(filename1, sheet, xlsxRange1);
AMPS_AEMO_PV = xlsread(filename2, sheet, xlsxRange1);
AMPS_1_4_AEMO_PV = xlsread(filename3, sheet, xlsxRange1);
AMPS_2_AEMO_PV = xlsread(filename4, sheet, xlsxRange1);
AMPS_2_AEMO_PV_095 = xlsread(filename5, sheet, xlsxRange1);
AMPS_2_AEMO_PV_090 = xlsread(filename6, sheet, xlsxRange1);
AMPS_2_AEMO_PV_085 = xlsread(filename7, sheet, xlsxRange1);
AMPS_2_AEMO_PV_098 = xlsread(filename8, sheet, xlsxRange1);
P_NO_PV = xlsread(filename1, sheet, xlsxRange2);
Q_NO_PV = xlsread(filename1, sheet, xlsxRange3);
P_AEMO_PV = xlsread(filename2, sheet, xlsxRange2);
Q_AEMO_PV = xlsread(filename2, sheet, xlsxRange3);
P_1_4_AEMO_PV = xlsread(filename3, sheet, xlsxRange2);
Q_1_4_AEMO_PV = xlsread(filename3, sheet, xlsxRange3);
P_2_AEMO_PV = xlsread(filename4, sheet, xlsxRange2);
Q_2_AEMO_PV = xlsread(filename4, sheet, xlsxRange3);
P_2_AEMO_PV_095 = xlsread(filename5, sheet, xlsxRange2);
Q_2_AEMO_PV_095 = xlsread(filename5, sheet, xlsxRange3);
P_2_AEMO_PV_090 = xlsread(filename6, sheet, xlsxRange2);
Q_2_AEMO_PV_090 = xlsread(filename6, sheet, xlsxRange3);
P_2_AEMO_PV_085 = xlsread(filename7, sheet, xlsxRange2);
Q_2_AEMO_PV_085 = xlsread(filename7, sheet, xlsxRange3);
P_2_AEMO_PV_098 = xlsread(filename8, sheet, xlsxRange2);
Q_2_AEMO_PV_098 = xlsread(filename8, sheet, xlsxRange3);

for k = 1:size(P_NO_PV,1)
   if P_NO_PV(k) < 0
      if Q_NO_PV(k) < 0
      AMPS_NO_PV(k) = -AMPS_NO_PV(k);
      end
   end
end

for k = 1:size(P_AEMO_PV,1)
   if P_AEMO_PV(k) < 0
      if Q_AEMO_PV(k) < 0
      AMPS_AEMO_PV(k) = -AMPS_AEMO_PV(k);
      end
   end
end

for k = 1:size(P_1_4_AEMO_PV,1)
```

```
    if P_1_4_AEMO_PV(k) < 0
        if Q_1_4_AEMO_PV(k) < 0
        AMPS_1_4_AEMO_PV(k) = -AMPS_1_4_AEMO_PV(k);
        end
    end
end

for k = 1:size(P_2_AEMO_PV,1)
    if P_2_AEMO_PV(k) < 0
        if Q_2_AEMO_PV(k) < 0
        AMPS_2_AEMO_PV(k) = -AMPS_2_AEMO_PV(k);
        end
    end
end

for k = 1:size(P_2_AEMO_PV_095,1)
    if P_2_AEMO_PV_095(k) < 0
        if Q_2_AEMO_PV_095(k) < 0
        AMPS_2_AEMO_PV_095(k) = -AMPS_2_AEMO_PV_095(k);
        end
    end
end

for k = 1:size(P_2_AEMO_PV_090,1)
    if P_2_AEMO_PV_090(k) < 0
        if Q_2_AEMO_PV_090(k) < 0
        AMPS_2_AEMO_PV_090(k) = -AMPS_2_AEMO_PV_090(k);
        end
    end
end

for k = 1:size(P_2_AEMO_PV_085,1)
    if P_2_AEMO_PV_085(k) < 0
        if Q_2_AEMO_PV_085(k) < 0
        AMPS_2_AEMO_PV_085(k) = -AMPS_2_AEMO_PV_085(k);
        end
    end
end

for k = 1:size(P_2_AEMO_PV_098,1)
    if P_2_AEMO_PV_098(k) < 0
        if Q_2_AEMO_PV_098(k) < 0
        AMPS_2_AEMO_PV_098(k) = -AMPS_2_AEMO_PV_098(k);
        end
    end
end

figure(1)
plot(AMPS_NO_PV);
title('Effects on Feeder Current Flow due to Changes in PV EG Power Factor');
xlabel('Bus Number');
ylabel('Current (A)');
grid minor
hold on
plot(AMPS_2_AEMO_PV,'m');
plot(AMPS_2_AEMO_PV_098,'c');
plot(AMPS_2_AEMO_PV_095,'r');
plot(AMPS_2_AEMO_PV_090,'g');
plot(AMPS_2_AEMO_PV_085,'k');
legend('No Additional PV EG','Additional 2 x AEMO PV EG pf=1','Additional 2 x AEMO PV EG
pf=0.98','Additional 2 x AEMO PV EG pf=0.95','Additional 2 x AEMO PV EG pf=0.90','Additional
2 x AEMO PV EG pf=0.85');
```

Appendix D19 – Section 6.2.1 Effect of PV EG Q Source on Feeder Voltage Rise

```
% read in results from ASPEN power flow for voltage rise
% existing network vs network with added generation at each tx with varying
% power factor. All added PV EG 2xAEMO predicted increase
filename1 = '2xaemo1.xlsx';  % pf=1
filename2 = '2xaemo098.xlsx'; % pf=0.98
filename2a = '2xaemo0972.xlsx'; % pf = 0.972
filename3 = '2xaemo0.95.xlsx'; % pf=0.95
filename4 = '2xaemo092.xlsx'; % pf=0.92
filename5 = '2xaemo090.xlsx'; % pf=0.90
filename6 = '2xaemo088.xlsx'; % pf=0.88
filename7 = '2xaemo085.xlsx'; % pf=0.85
xlsxRange1 = 'F8:F92'; % V(pu)
sheet = 1;
Volts1 = xlsread(filename1, sheet, xlsxRange1);
Volts098 = xlsread(filename2, sheet, xlsxRange1);
Volts095 = xlsread(filename3, sheet, xlsxRange1);
Volts092 = xlsread(filename4, sheet, xlsxRange1);
Volts090 = xlsread(filename5, sheet, xlsxRange1);
Volts088 = xlsread(filename6, sheet, xlsxRange1);
Volts085 = xlsread(filename7, sheet, xlsxRange1);
figure(1)
plot(Volts1*11)
hold on
plot(Volts098*11,'r')
plot(Volts095*11,'g')
plot(Volts092*11,'m')
plot(Volts090*11,'k')
plot(Volts088*11,'y')
plot(Volts085*11,'c')
grid
title('Voltage Rise with Change in PV EG Power Factor')
xlabel('Bus number')
ylabel('Bus Voltage (kV)')
legend('pf = 1','pf = 0.98','pf = 0.95','pf = 0.92','pf = 0.90','pf = 0.88','pf = 0.85');
```

Appendix E – Power Flow Model Unsolved 1-Line Diagrams

Appendix E1 – Model with additional PV EG 'out of service' to validate model under existing circumstances

Appendix E2 - Model with additional PV EG 'in service' to investigate effects of introduction of additional PV EG

Appendix E1 – Model with additional PV EG 'out of service' to validate model under existing circumstances

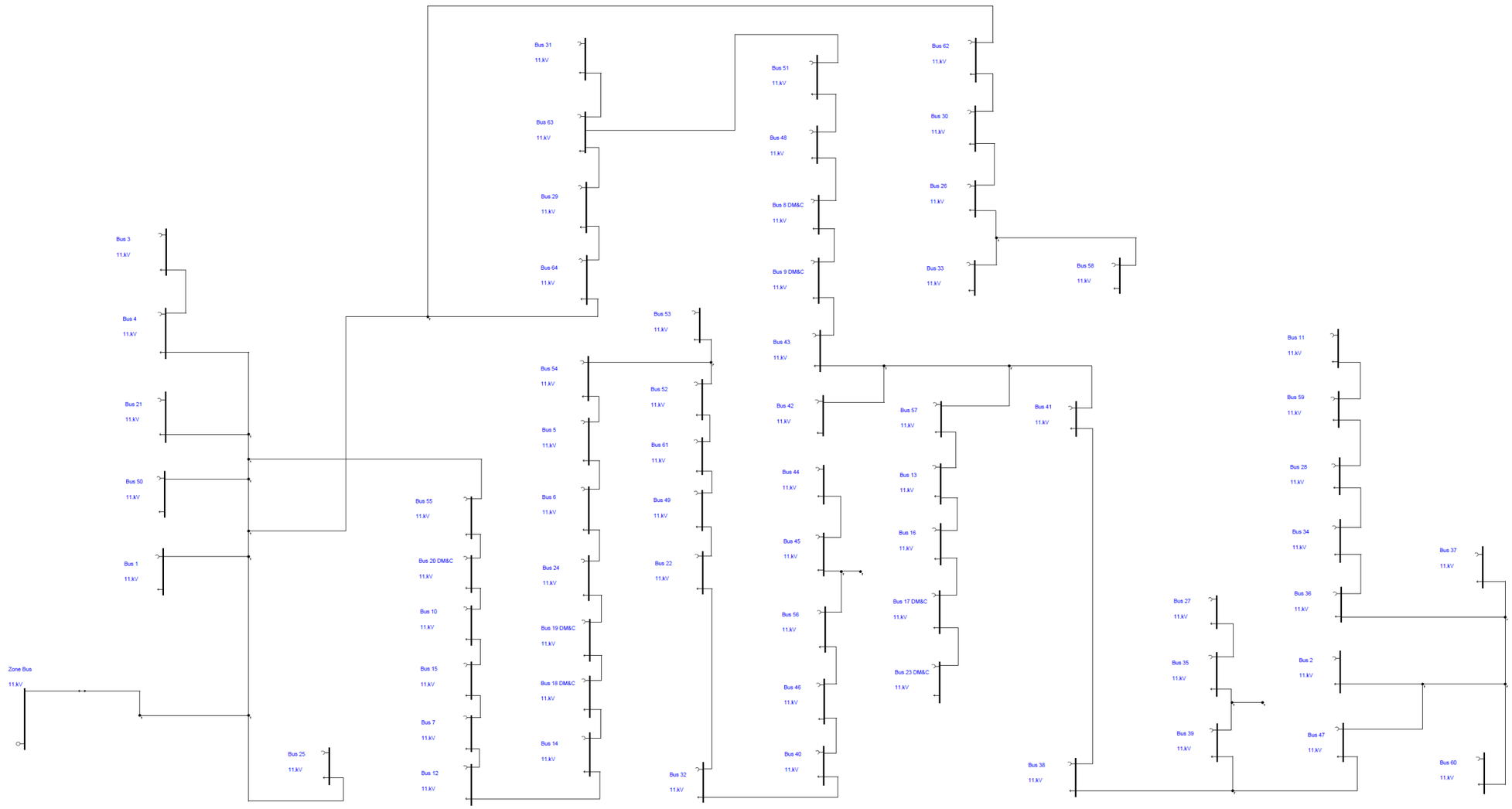

Figure 45: Unsolved 1-Line diagram of power flow model - PV EG 'out of service'

Appendix E2 - Model with additional PV EG ‘in service’ to investigate effects of introduction of additional PV EG

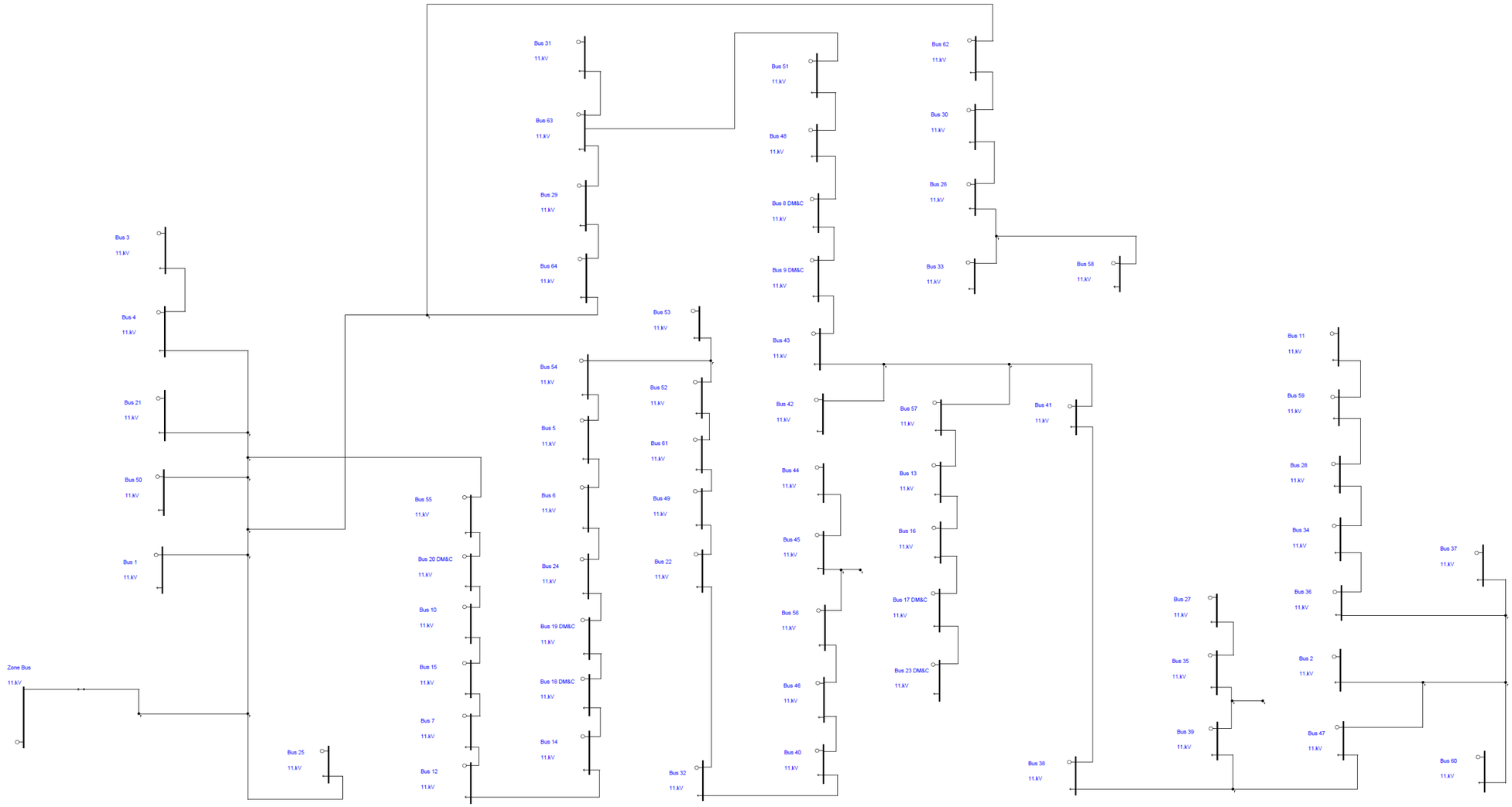

Figure 46: Unsolved 1-Line diagram of power flow model - PV EG 'in service'

Appendix F – Current and Future Levels of PV EG

TX	LOAD P (MW)	LOAD Q (MVAr)	EXISTING PV EG P (kW)	ADDITIONAL PV EG P (kW)	EXISTING PV EG P (MW)	ADDITIONAL PV EG P (MW)
64	0.099388	0.048135806	14.3	32.175	0.0143	0.032175
63	0.067155333	0.032524812	0	0	0	0
62	0.166051333	0.080422331	0	0	0	0
61	0.117496667	0.056906233	6.9	15.525	0.0069	0.015525
60	0.034095333	0.016513124	11.2	25.2	0.0112	0.0252
59	0.133732	0.064769364	13.33333333	30	0.013333333	0.03
58	0.115074	0.055732882	24	54	0.024	0.054
57	0.207277333	0.100388994	30.3	68.175	0.0303	0.068175
56	0.159664667	0.077329127	7.111111111	16	0.007111111	0.016
55	0.120400667	0.058312704	12.88888889	29	0.012888889	0.029
54	0.123266	0.059700449	23.04888889	51.86	0.023048889	0.05186
53	0.094310667	0.045676741	5	11.25	0.005	0.01125
52	0.121430667	0.058811556	10.2	22.95	0.0102	0.02295
51	0.09456	0.045797498	0	0	0	0
50	0.04792	0.023208715	45	101.25	0.045	0.10125
49	0.084634667	0.04099044	4.751111111	10.69	0.004751111	0.01069
48	0.044580667	0.021591402	2	4.5	0.002	0.0045
47	0.110021333	0.053285764	17.77777778	40	0.017777778	0.04
46	0.104016667	0.050377571	2.222222222	5	0.002222222	0.005

45	0.073842667	0.035763636	7	15.75	0.007	0.01575
44	0.094316667	0.045679647	11.3	25.425	0.0113	0.025425
43	0.01967	0.009526616	0	0	0	0
42	0.08058	0.039026675	8.2	18.45	0.0082	0.01845
41	0.066219333	0.032071487	9.6	21.6	0.0096	0.0216
40	0.08374	0.040557133	10.2	22.95	0.0102	0.02295
39	0.002089333	0.00101191	0	0	0	0
38	0.096513333	0.046743541	16.4	36.9	0.0164	0.0369
37	0.081181333	0.039317914	9.9	22.275	0.0099	0.022275
36	0.116975333	0.05665374	8.9	20.025	0.0089	0.020025
35	0.104152	0.050443116	4.5	10.125	0.0045	0.010125
34	0.124724667	0.060406913	12.96	29.16	0.01296	0.02916
33	0.037512	0.018167891	0	0	0	0
32	0.106652	0.051653921	12.7	28.575	0.0127	0.028575
31	0.116175333	0.056266282	17.77777778	40	0.017777778	0.04
30	0.033698	0.016320686	0	0	0	0
29	0.076880667	0.037235006	12.9	29.025	0.0129	0.029025
28	0.075313333	0.036475912	13	29.25	0.013	0.02925
27	0.204568	0.099076804	16.5	37.125	0.0165	0.037125
26	0.113355333	0.054900494	10.62	23.895	0.01062	0.023895
25	0.000184	8.91153E-05	0	0	0	0
24	0.00306	0.001482026	0	0	0	0
23	0.033539333	0.01624384	4.6	10.35	0.0046	0.01035
22	0.126222667	0.061132428	10.1	22.725	0.0101	0.022725

21	0.015797333	0.007650998	0	0	0	0
20	0.090369333	0.043767866	0	0	0	0
19	0.098212	0.047566243	0	0	0	0
18	0.062638	0.030336968	0	0	0	0
17	0.029814	0.014439579	4.5	10.125	0.0045	0.010125
16	0.147734	0.071550842	30	67.5	0.03	0.0675
15	0.057676667	0.027934085	0	0	0	0
14	0.110106	0.05332677	6.1	13.725	0.0061	0.013725
13	0.133128	0.064476833	15.3	34.425	0.0153	0.034425
12	0.145886	0.070655815	12.96	29.16	0.01296	0.02916
11	0.098830667	0.047865877	32.6	73.35	0.0326	0.07335
10	0.158714	0.076868699	3	6.75	0.003	0.00675
9	0.390694	0.18922174	0	0	0	0
8	0.192486	0.093225225	0	0	0	0
7	0.279006	0.135128773	3.511111111	7.9	0.003511111	0.0079
6	0.09953	0.048204579	5	11.25	0.005	0.01125
5	0.088238	0.042735614	3.866666667	8.7	0.003866667	0.0087
4	0.006307333	0.003054781	0	0	0	0
3	0.00093	0.00045042	0	0	0	0
2	0.00593	0.00287203	0	0	0	0
1	0.003347333	0.001621188	0	0	0	0
Total			544.0288889	1224.065	0.544028889	1.224065

Table 15: Existing and future predicted levels of PV EG per Tx

Appendix G – Safety Issues

The main safety issue related to the project was the installation and removal of the data loggers on the individual direct distributor feeders into installations with larger rooftop PV EG systems, the results of which were used in section 4.

A direct distributor is a dedicated low voltage feeder fed from a kiosk pad mount Tx , shown in Figure 47, that connects directly into the customers' main switchboard.

Figure 47: Kiosk Transformer

All data loggers were installed at the Tx end of the direct distributor as can be seen in Figure 48 and Figure 49.

Figure 48:: Kiosk LV board showing data logger voltage leads installed

Prior to commencing any work, a Hazard Assessment Check (HAC) was completed.
The main steps involved in carrying out a HAC are as follows:

1. Identify the hazards;
2. Assess the risk associated with the hazard;
3. Implement control measures to attempt to remove or reduce the hazard;
4. Reassess the risk after control measures are put in place.

The main hazards that were identified when installing/ removing the data loggers were:

1. Electrical – working on a live low voltage board of a kiosk Tx;
2. Driving – to get to job location;
3. Manual handling – lifting equipment in and out of the rear of the work vehicle;
4. Access – general access issues to job site, such as uneven ground, gutters, etc.

Figure 49: Direct distributor showing CT's and data logger installed

Risk was assessed using the matrix shown in figure 50 below.

Risk Matrix

LIKELIHOOD	CONSEQUENCE				
	Insignificant	Minor	Moderate	Major	Severe
Almost Certain	11	16	20	23	25
Likely	7	12	17	21	24
Possible	4	8	13	18	22
Unlikely	2	5	9	14	19
Rare	1	3	6	10	15

Hierarchy of Controls

The "Hierarchy of Controls" is a hierarchy with the most effective risk control strategy being elimination and the least effective being the provision of personal protective equipment.

Users must work down through the list. In many instances, a combination of controls will be required to reduce the risk to ALARP.

1. **Elimination** – remove the hazard.
2. **Substitution** – change process item to an item of less risk, eg, substances.
3. **Isolation** – use preventative mechanism, eg, guarding.
4. **Engineering** – use machines rather than manual labour.
5. **Administrative** – develop and implement safe work procedures, conduct training, implement a checklist.
6. **Personal Protective Equipment** – use personal protective equipment, eg, hard hats, respirators, hearing protection, insulating gloves, safety protective footwear.

Figure 50: Risk Matrix

The main hazard that was identified with regards to fitting and removing the data loggers was electrical. Following the hierarchy of controls as shown in Figure 50 above:

1. Elimination – it was not possible to eliminate the electrical hazard;
2. Substitution – it was not possible to substitute the process required;
3. Isolation – there were lexan and insulated guards on live busbars;

4. Engineering – this was not possible as there is no remote data acquisition on this piece of equipment;
5. Administrative – this is noted in the control measures as training and also would include the Safe Work Method Statement (SWMS) listed on the HAC sheet;
6. Personal Protective Equipment – this is the last resort for control measures, but it is typically unavoidable that this stage is reached when accessing live distribution network assets.

The Personal Protective Equipment (PPE) control measures used for this job can be seen in figure 51 below.

Figure 51:PPE controls associated with fitting and removing data loggers

Risk was then reassessed after control measures were implemented using the risk matrix shown in Figure 50 on the previous page.

To complete the HAC for this job, the applicable Safe Work Method Statement (SWMS) must be listed, and when completing the job all steps as listed on the HAC must be followed to ensure the task is completed safely.

The SWMS for this job were:

1. SWMS for Quality of Supply. This must be used in conjunction with the relevant works instruction (WI), which for this job this was WI for Customer Complaints – Quality of Supply;
2. SWMS for Driving Vehicle.

These were used in conjunction with several other Ausgrid documents for working safely on live assets:

1. Electrical Safety Rules (ESR) – annual refresher training conducted;
2. WI for Working on or near exposed live low voltage mains and apparatus;
3. Network Standard for Safe Electrical Working on Low Voltage Assets.

The other safety issues encountered were ergonomic issues when using different desks and chairs

Appendix H – Instruments Used in Manual Data Collection

The data logging units that were installed on the direct distributors were:

- PolyLogger II Power Systems Analysers;
- 500:1 ratio CT's.

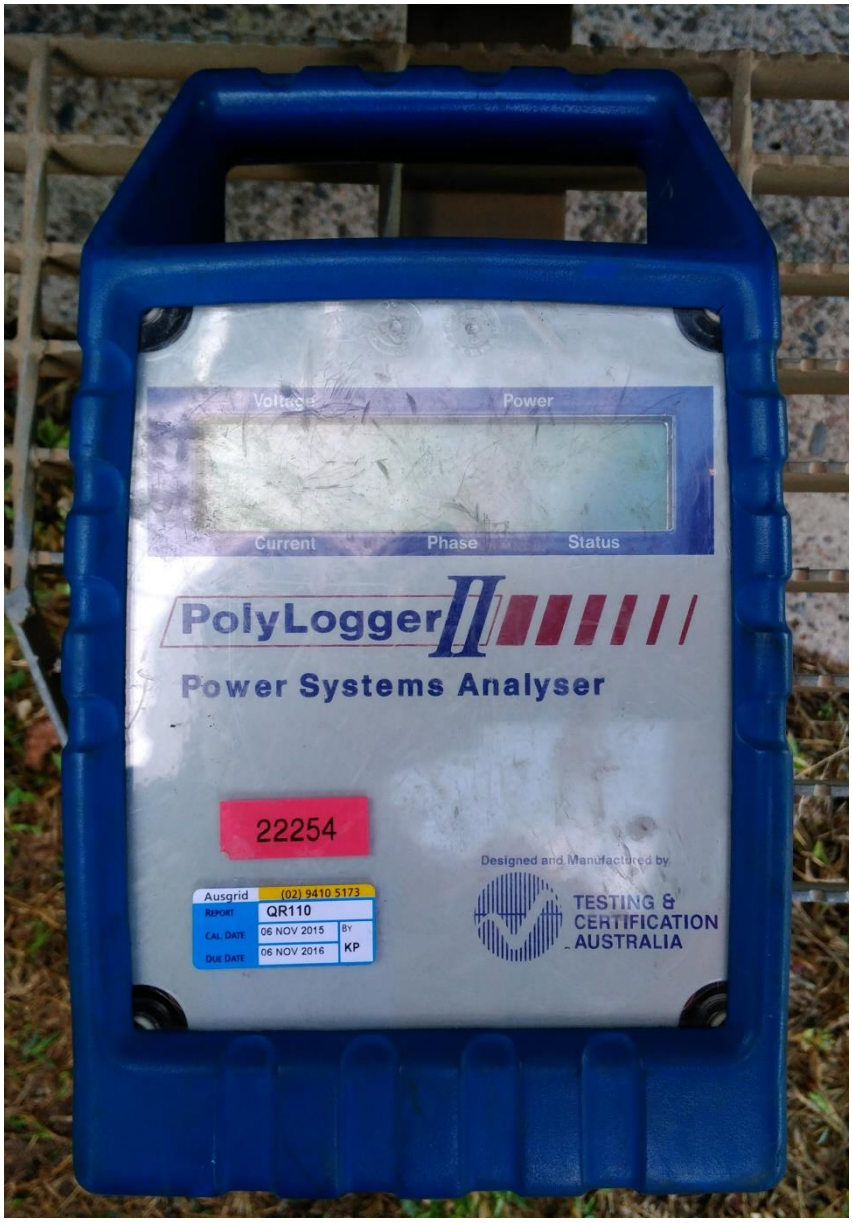

Figure 52: PolyLoggerII Power Systems Analyser

Figure 53: CT used with PolyLogger

The unit that was used to check phase angle at the zone substation was:

- Fluke 435 Power Quality Analyser.

Figure 54: Fluke 435 Power Quality Analyser

See the table below for calibration information.

Equipment type	Serial number	Calibration completed date	Calibration due date	Testing company
PolyLogger	22254	6/11/15	6/11/16	TCA
PolyLogger	28481	5/6/15	5/6/16	TCA
PolyLogger	28484	9/11/15	9/11/16	TCA
CT	29101	27/7/15	27/7/17	TCA
CT	29165	21/9/15	21/9/17	TCA
CT	29154	21/9/15	21/9/17	TCA
CT	23070	7/9/15	7/9/17	TCA
CT	23272	29/5/15	29/5/17	TCA
CT	20916	30/10/14	30/10/16	TCA
CT	29173	21/9/15	21/9/17	TCA
CT	29102	7/9/15	7/9/17	TCA
CT	25939	7/9/15	7/9/17	TCA
Fluke 435	29906	7/7/16	7/7/17	TCA

Table 16: Equipment type and calibration dates